Experimental research of wave overtopping on a breakwater with concrete armour units

J. Cui
9166061

MSc Commission
Ir. H. J. Verhagen
Prof. Dr. Ir. M. J. Stive
Dr. Ir. H. L. Fontijn
Ir. M. Klabbers

TU Delft

Delta Marine Consultants bv

Preface

This report is a presentation for a graduation research of Delft University of Technology, Faculty of Civil Engineering and Geosciences, section Coastal Engineering. The project has been carried out under guidance of Delta Marine Consultants in Gouda, The Netherlands. The subject of the research is wave overtopping for different types of concrete armour: Tetrapod units and the new Xbloc units developed by Delta Marine Consultants.

I want to thank

My graduation commission:
Ir. Henk Jan Verhagen (Delft University of Technology)
Prof. Dr. Ir. Marcel J. Stive (Delft University of Technology)
Dr. Ir. H. L. Fontijn (Delft University of Technology)
Ir. Martijn Klabbers (Delta Marine Consultants)

J. Cui
Delft, April 2004

Summary

Especially for breakwaters of intermediate height overtopping is an important value, both for the transmitted wave height in the basin behind the breakwater, as well as for the stability of the blocks on the inner slope. Rather reliable formulae exist for the determination of overtopping for normal riprap structures, as well as for classic (double layer) Tetrapod structures.

Xbloc® and Tetrapod

Recent research has shown that also Tetrapods can be applied in single layer application under certain conditions (D'ANGREMOND, ET AL [1999], VANDENBOSCH, ET AL [2002]). However, the placing density of the Tetrapods has to be larger than in a normal single layer application. The recently developed Xbloc® is applied in a single layer. Both in case of the single layer Tetrapods, as well as the single layer Xbloc (see also KLABBERS ET AL [2003]) the porosity of the top layer is more than in case of a normal riprap structure. The porosity of the Xbloc is about 50%, and the porosity of the normal riprap structure is about 40%. For Xbloc, the roughness, porosity as well as the geometry of the pores differs from a standard riprap slope. In the model tests of the Xbloc, the visual impression of the slope seemed smoother than in case of a Tetrapods layer. It is expected that the overtopping quantities over single layer Tetrapods or over Xbloc armour may deviate from well known overtopping formulae.

The overtopping formula by Van Der Meer [2002] is given as:

$$\frac{q}{\sqrt{gH_{m0}^3}} = \frac{0.067}{\sqrt{\tan\alpha}}\gamma_b\xi_0 \exp\left(-4.75\frac{R_c}{H_{m0}}\frac{1}{\xi_0\gamma_b\gamma_f\gamma_\beta\gamma_v}\right)$$

Van Der Meer makes a distinction between breaking and non-breaking wave conditions. The model tests showed that the overtopping volume increases with the increase of wave height, decrease of freeboard. The overtopping also showed an increase with the decrease of the wave steepness.

Klabbers ET AL [2003] found that wave overtopping in case of Xbloc increases with both wave height and wave length. The wave steepness could therefore not be considered as governing parameter for wave overtopping. It was however found that, the asymmetry of the incoming waves; quantified in shallow water by the Ursell parameter had a significant effect on the wave overtopping. Therefore, a new type of overtopping formula has been developed which includes the Ursell parameter.

The Xbloc overtopping formula according to KLABBERS (2003) is:

$$\frac{q}{\sqrt{gH_{mo}^3}} = \frac{1}{100}\frac{H_s * L_t^2}{d^3} * \exp\left(-3.58\frac{R_c}{H_s}\right)$$

The performed overtopping tests in this work confirmed the use of this equation for the Xbloc unit.

After comparing the test results with the Van Der Meer formula and the Xbloc formula, it seemed that the Xbloc formula showed a better fit with the test results, as can be seen in the following figures. Thus for single layer Tetrapod units and Xbloc units, the Xbloc overtopping formula is more suitable to use than the Van Der Meer formula.

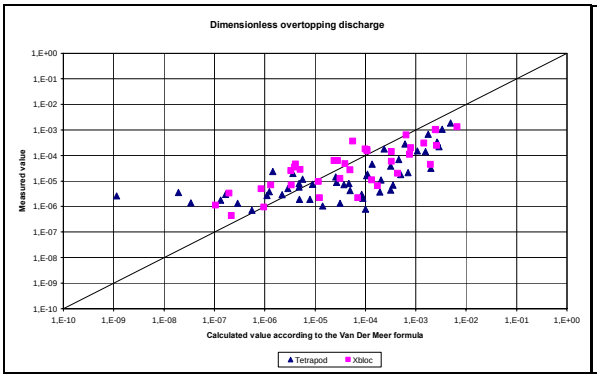

Test results compare to Van Der Meer formula.

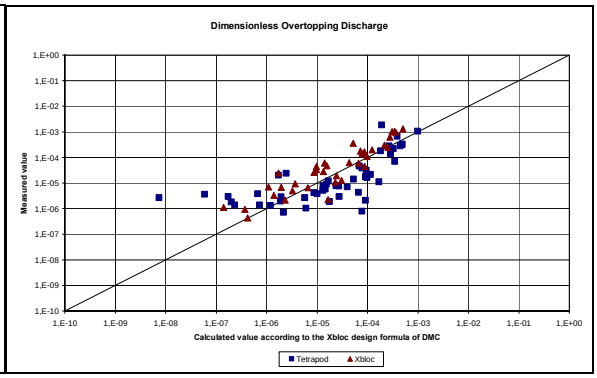

Test results compare to the Xbloc overtopping formula.

Comparison of the data from the Tetrapod tests and the Xbloc tests showed that the overtopping quantity in case of Xbloc is slightly more than for Tetrapods. But it should be noticed that the tested Tetrapods units (202g) qua weight and volume are significant larger than the tested Xbloc armour units (121g). A conclusion of the amount of overtopping between different armour units is considered only realistic if the ratio design wave height / unit diameter is in the same order for both units.

Contents

Chapter 1

Introduction

Wave overtopping has important influence on wave climate behind constructions, for example for moored ships behind breakwaters. It also has significant influence on the stability of breakwaters. Extensive study has been done by VAN DEN MEER and DE WAAL [WL 1993-2], and many other researchers. Wave overtopping data is available for smooth slopes, and for slopes with concrete armour layer units such as cubes, Dolos and double layer Tetrapod. Recently, researches of wave overtopping have been done for single armour layer Tetrapod units on breakwaters.

Based on previous test results done in WL and DHI [Klabbers 2003], data on wave overtopping is available for the Xbloc. An overtopping formula for Xbloc armoured slopes has been derived. It was found that a formula that includes the Ursell parameter gives a good fit with the experiments. In this research, use of this type of overtopping formula has been verified.

This research focused on comparing the wave overtopping data measured at the laboratory model tests of the single layer Xbloc and the single layer Tetrapod. By means of several wave flume experiments, testing various combinations of wave steepness, wave height and freeboard, different comparisons were made between the single layer Xbloc and the single layer Tetrapod. The measured wave overtopping volumes were compared with the formula of Van Der Meer. Furthermore, the experimental results of both Xbloc and Tetrapods have been compared with an overtopping formula based on the Xbloc overtopping formula.

As the size of the applied units has an important influence on the amount of overtopping, the wave conditions should be related to the unit size.

The structure of this rapport is as following. In chapter 2, the known overtopping theories and wave overtopping data will be described. The main wave flume experiments will be illustrated in chapter 3. In chapter 4, an analysis of the wave overtopping data will be made. Finally, in chapter 5, conclusions and recommendations will be given.

Chapter 2

The Known Wave Overtopping Formulas

2.1 General Wave Overtopping Formulas

Wave overtopping is a very important phenomenon for wave climate behind constructions and for the stability of the breakwaters. Much research on this subject has been done, and several formulas for predicting the quantity of wave overtopping are known.
In this chapter, some of the known formulas of wave overtopping are given in short.

2.1.1 Weggel

SAVILLE en CALDWELL (1953) researched wave overtopping volumes and wave run-up height with scaling models of different constructions.
WEGGEL (1976) analyzed these data. His tests as well as his analysis are based on regular waves. With his research, he used the following parameters:

H'_0 = wave height in deep water [m]
g = gravitational acceleration [m/s^2]
q = overtopping volume per m^1 crest length [m^2/s]
R = wave run-up height in vertical surface [m]
h = water depth before the construction [m]
h_c = construction height [m]

Weggel used these variables to construct the following dimensionless parameters:

F = $(h_c - h)/H'_0$ = dimensionless free-board [-]
F_0 = R/H'_0 = dimensionless crest height to avoid wave overtopping [-]
Q* = $q^2/g H'^3_0$ = dimensionless overtopping volume [-]

After analyzing the data, Weggel constructed the following formula using the dimensionless parameters:

$$\frac{F}{F_0} = \alpha_1 t \cdot \tanh\left[\log\frac{Q*}{Q_0*}\right] \qquad (2.1)$$

With:

α_1 = a parameter which determines the range of the tanh-curve [-]
Q_0* = dimensionless overtopping volume when the free-board is zero [-]

The parameters α_1 and Q_0* are determined by the construction form and the wave conditions. The variation of α_1 in different wave conditions is small. Thus, for smooth slope, an average value of α which only depends on the slope angle can be used.

$$\overline{\alpha_1} = 0.06 - 0.143\ln(\sin\alpha) \tag{2.2}$$

With:

α = the slope angle

Q_0* is the volume of the overtopping water when the crest of the construction is at the same level as the still water line.
Using the linear wave theory, the Q_0* can be found as following:

The volume of water in a wave above the still water level can be found:

$$V = \int_{\frac{1}{2}L}^{L} \eta dx = \int_{\frac{1}{2}L}^{L} \frac{1}{2} H \sin\left(-\frac{2\pi x}{L}\right) dx = \frac{1}{2\pi} HL \tag{2.3}$$

With:

V = volume of water in a wave above the still water level [m^3/m^1]
η = the altering of the water surface [m]
H = wave height [m]
L = wave length [m]

The quantity of the wave overtopping water is:

$$Q = \frac{V}{T} = \frac{\frac{1}{2\pi} HL}{T} \tag{2.4}$$

With:

T = wave period [s]

Filling in Q into the formula of the dimensionless overtopping volume, and L substitute by a formula of L from the linear wave theory. The formula of Q_0* becomes:

$$Q_0 * = \frac{\left[\frac{1}{(2\pi)^2}\right]^2 \left[\frac{H}{H_0'}\right]^2 \tanh^2\left[\frac{2\pi h}{L}\right]}{\frac{H_0'}{gT^2}} \tag{2.5}$$

After substitute the dimensionless variables into (2.1), the formula for wave overtopping can be found:

$$Q = \left(gQ_0^* H_0^{3\prime}\right)^{1/2} \exp\left[-\frac{0.217}{\alpha} \tanh^{-1}\left(\frac{h_c - h}{R}\right)\right] \tag{2.6}$$

$$0 < \frac{h_c - h}{R} < 1.0$$

Formula (2.6) shows the result of the wave overtopping volume per time unit and per meter crest length, for waves that have a higher wave run-up height than the free-board (h_c-h). The variable R is the wave run-up height that occurs when the front slope is so high that no wave overtopping takes place. This wave run-up height can be found from different wave run-up formulas. De formula of HUNT (1959) is a more commonly used formula for the wave run-up calculation:

$$\frac{R}{H} = \frac{\tan\alpha}{\sqrt{s}} * \gamma_f \tag{2.7}$$

With:

s = wave steepness [-]
γ_f = influence factors for the influences of the roughness [-]

2.1.2 Battjes

BATTJES (1974) has directly related the wave properties with wave overtopping in case of smooth slopes. He researched the wave run-up of irregular waves. In his research, he collected

information about the form of waves on the slope during the run-up and the run-down of a wave on the slope. He derived a relation from the hypothetic run-up and wave overtopping.

Battjes mentioned in his articles that when the wave run-up height on an infinite long slope larger is than the free-board of the same construction, the wave overtopping volume equals to the part of the run-up wave that becomes higher than the present free-board.
As you can see in the following figures:

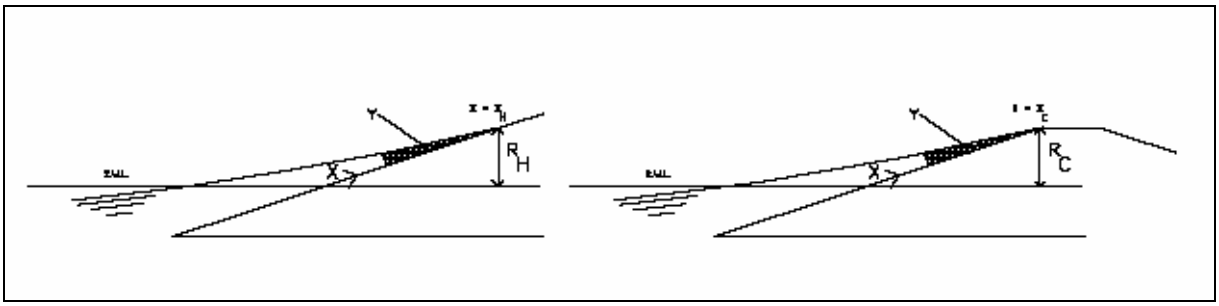

Figure 2.1 Wave overtopping according to Battjes.

Without further go into the theoretical derivation of the formula, the result of the analysis of Battjes is given in formula (2.8).

$$b = \frac{B}{HL_0\sqrt{\tan\alpha}} = 0.1\left(1 - \frac{R_c}{R}\right)^2 \qquad (2.8)$$

With:

b = dimensionless wave overtopping volume according to Battjes [-]
B = wave overtopping volume per wave per m^1 crest length [m^2]
L_o = deepwater wave length [m]
R_c = free-board [m]
R = wave run-up height [m]

The coefficient 0.1 in the formula is derived from comparing with the test results of SAVILLE and CALDWELL (1953).

2.1.3 Van Der Meer

VAN DER MEER (2002) has described two formulas for average wave overtopping in case of irregular waves. There is a separation between broken wave and non-broken wave according to the following criteria.

For broken wave: $\gamma_b \xi_{op} \leq 2$

For non-broken wave: $\gamma_b \xi_{op} > 2$

$$\xi_{op} = \frac{\tan \alpha}{\sqrt{s_{op}}} \tag{2.9}$$

γ_b = influence factors for the influences of the toe of the breakwater. [-]
ξ_{op} = breaker parameter [-]
s_{op} = wave steepness [-]

Wave overtopping can be described in two formulae linked to each other: one for breaking waves ($\gamma_b\xi_o <\approx 2$), where wave overtopping increases for increasing breaker parameter ξ_o, and one for the maximum that is achieved for non-breaking waves ($\gamma_b\xi_o >\approx 2$).

In the following figure, the breaker parameter versus the dimensionless wave overtopping discharge in logarithmic scale was shown with three different relative crest heights.

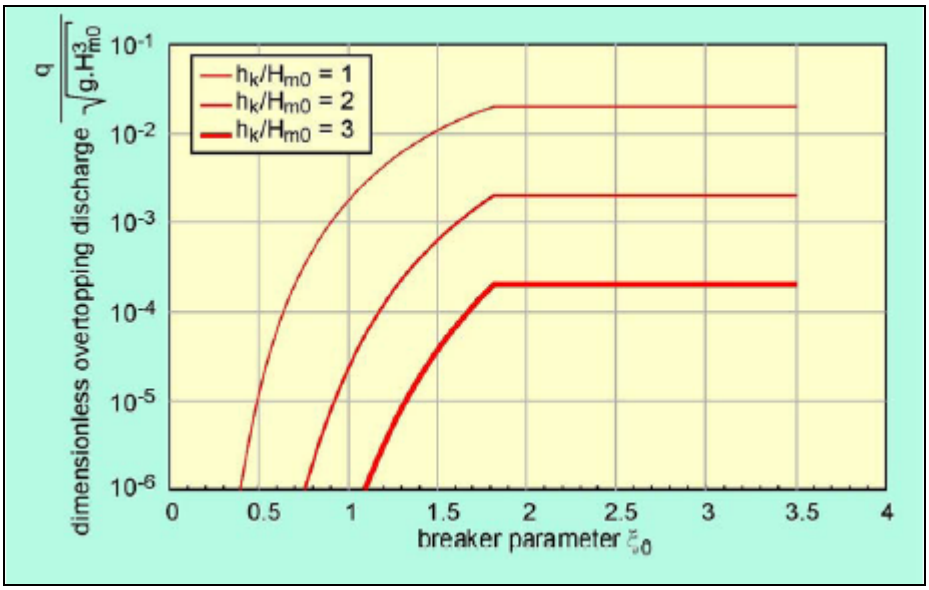

Figure 2.2 Wave overtopping as function of breaker parameter. (1:3 slope)
[Technical Rapport, Van Der Meer 2002]

The wave overtopping formulae are exponential functions with the general form:

$q = a \exp (b R_c)$

The coefficients a and b are still functions of the wave height, slope angle, breaker parameter and the influence factors. The complete formulae are:

$$\frac{q}{\sqrt{gH_{m0}^3}} = \frac{0.06}{\sqrt{\tan\alpha}} \gamma_b \xi_o \exp\left(-4.7 \frac{R_c}{H_{m0}} \frac{1}{\xi_o \gamma_b \gamma_f \gamma_\beta \gamma_v} \right) \tag{2.10}$$

and a maximum of:

$$\frac{q}{\sqrt{gH_{m0}^3}} = 0.2 \exp\left(-2.3 \frac{R_c}{H_{m0}} \frac{1}{\gamma_f \gamma_\beta} \right) \tag{2.11}$$

With:

H_{m0} = significant wave height at toe of dike [m]
ξ_o = breaker parameter [-]
s_{op} = wave steepness $s_o = \frac{2\pi H_{m0}}{g T_{m-1.0}^2}$ [-]
$T_{m-1.0}$ = spectral wave period at toe of dike [s]
g = gravitational acceleration [m/s^2]
q = wave overtopping volume per m^1 crest length [m^3/s/m^1]
α = slope angle [^{o}]
R_c = free crest height above still water line [m]
γ_b = influence factors for the influences of the toe of the breakwater [-]
γ_f = influence factors for the influences of the roughness [-]
γ_β = influence factors for the influences of the angle of the wave attack [-]
γ_v = influence factors for the influences of the foreland [-]

The dimensionless wave overtopping discharge $\frac{q}{\sqrt{gH_{m0}^3}}$ and the relative crest height $\frac{R_c}{H_{m0}}$, are both related to the breaker parameter and/or the slope of the structure. In order to take into account the influence of different conditions, the dimensionless crest height is apparently increased by dividing by the influence factors $\gamma_b \gamma_f \gamma_\beta \gamma_v$.

Both design formulae (2.10) and (2.11) are shown diagrammatically in figures 2.3 and 2.4. The dimensionless overtopping discharge on the vertical axis in figure 2.3 is give by:

$$\frac{q}{\sqrt{gH_{m0}^3}} \frac{1}{\xi_o \gamma_b}$$

and the dimensionless crest height by:

$$\frac{h_k}{H_{m0}} \frac{\sqrt{s_o}}{\tan\alpha} \frac{1}{\gamma_b \gamma_f \gamma_\beta \gamma_v}$$

In both figures the recommended lines are shown together with a mean with 5% lower and upper exceendance limits, based on measurements (see later). The formula from the Guidelines [TAW, 1989] is also shown, which agrees almost exactly with the new recommended line.

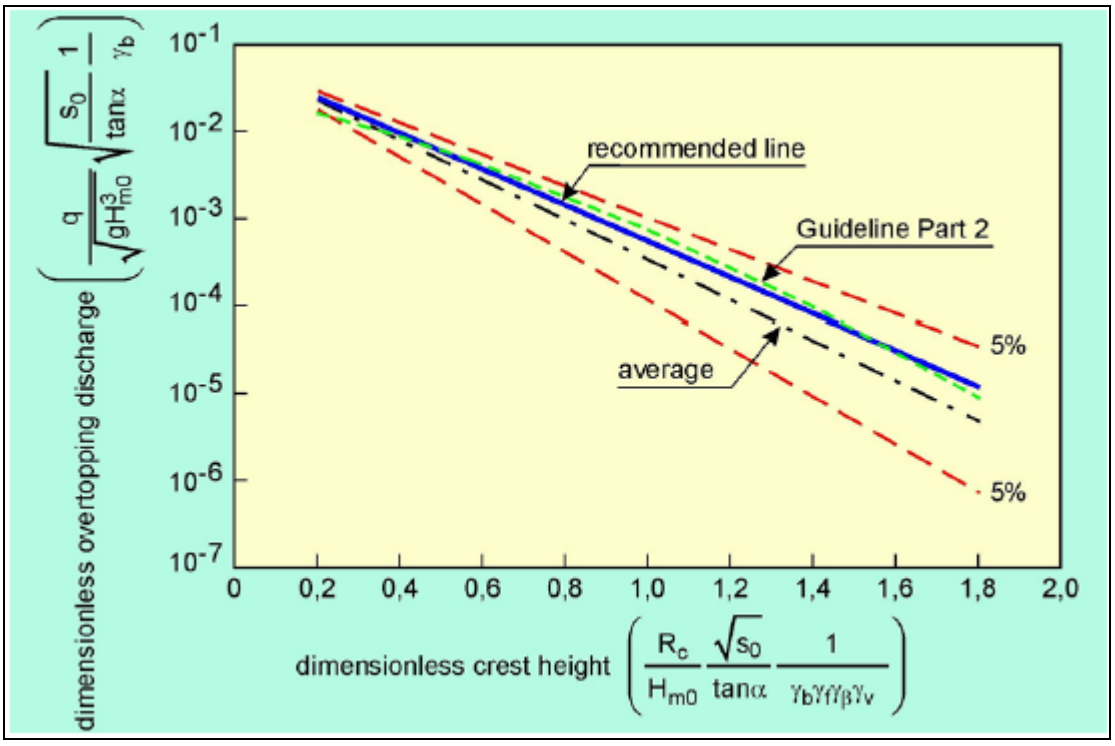

Figure 2.3 Wave overtopping with breaking waves
[Technical Rapport, Van Der Meer 2002]

Wave overtopping for non-breaking waves is no longer dependent on the breaker parameter. The formula for breaking waves (2.10) is valid up to the maximum, which is in the region of ($\gamma_b\xi_o = 2$). A check must still be made as to whether formula (2.10) exceeds the maximum of formula (2.11).

Generally it can be concluded that for wave run-up and overtopping on smooth straight slopes the differences with the Guidelines are very small. The new formulae take into account the fact that a maximum is reached for non-breaking waves. Improvement is mainly in the description of the reliability of the formulae (see later) and the better description of the influence of berm, roughness elements, angle of wave attack and vertical walls on a slope.

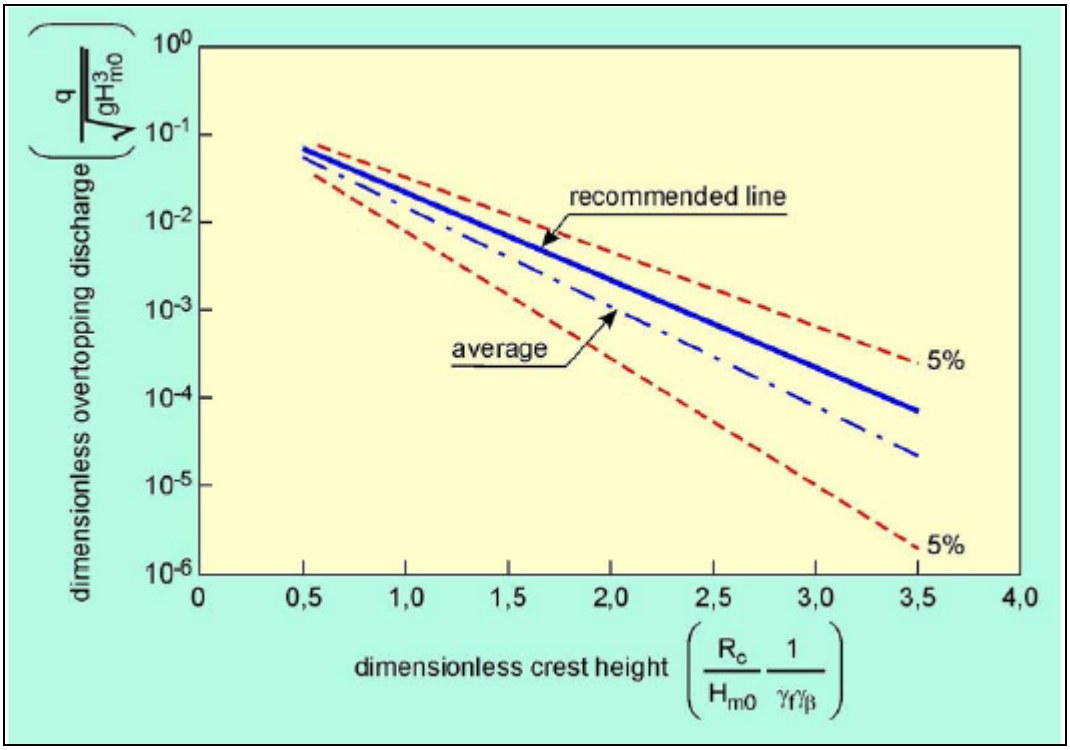

Figure 2.4 Maximum wave overtopping achieved with non-breaking waves [Technical Rapport, Van Der Meer 2002]

Figure 2.5 shows an overall view of the measured points related to breaking waves. In this figure the important parameters are given along the two axes, all existing measured points are shown with a mean and 5% lower and upper exceedance limits, and along the vertical axis the application area is also given.

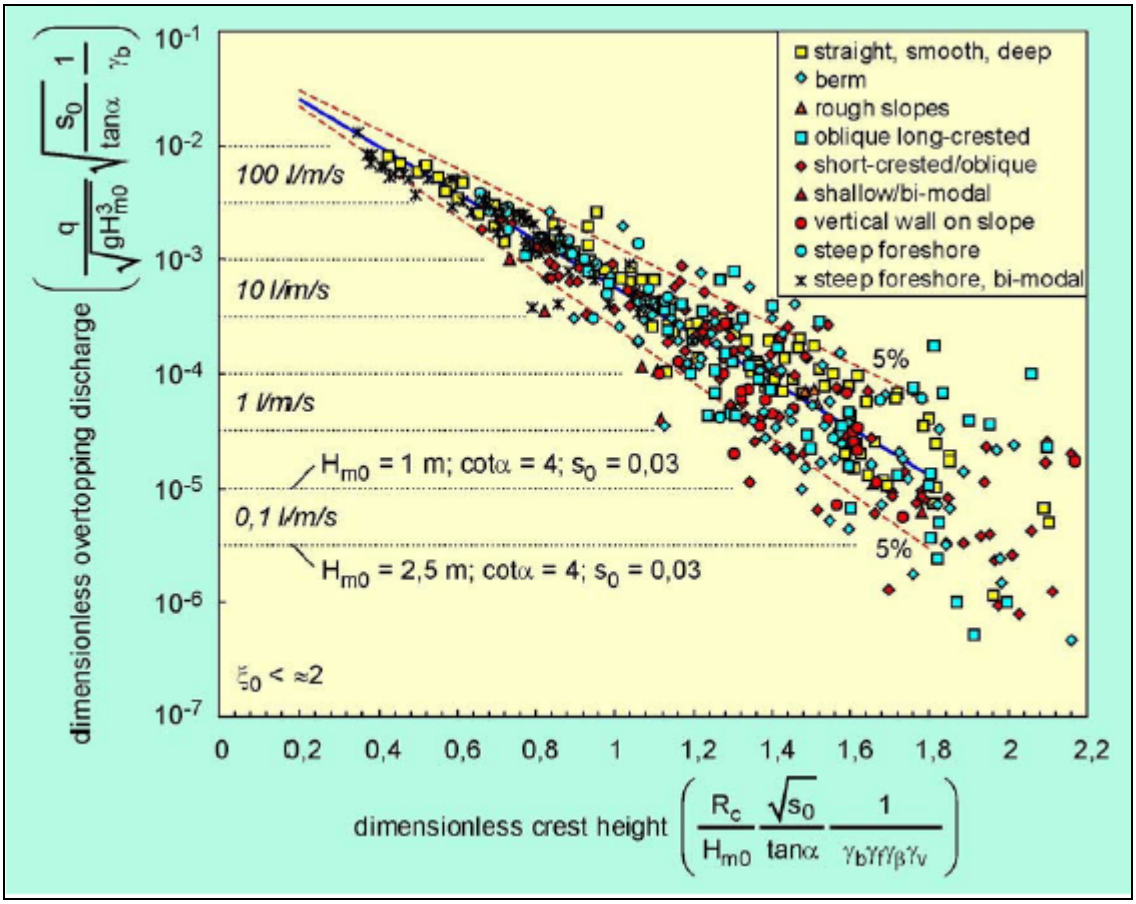

Figure 2.5 Wave overtopping data with mean and 5% under and upper exceedance limits and indication of application area; breaking waves
[Technical Rapport, Van Der Meer 2002]

The average of all observations in figures 2.5 and 2.6 can be described as:

$$\frac{q}{\sqrt{gH_{m0}^3}} = \frac{0.067}{\sqrt{\tan\alpha}}\gamma_b\xi_0 \exp\left(-4.75\frac{R_c}{H_{m0}}\frac{1}{\xi_0\gamma_b\gamma_f\gamma_\beta\gamma_v}\right) \qquad (2.12)$$

(Figure 2.4)

with maximum:

$$\frac{q}{\sqrt{gH_{m0}^3}} = 0.2\exp\left(-2.6\frac{R_c}{H_{m0}}\frac{1}{\gamma_f\gamma_\beta}\right) \qquad (2.13)$$

(Figure 2.5)

The reliability of formula (2.12) is given by taking the coefficient 4.75 as a normally distributed stochastic function with a mean of 4.75 and a standard deviation $\sigma = 0.5$. Using this standard deviation, the exceedance limits ($\mu \pm x\sigma$) can also be drawn for x plus a number of standard deviations (1.64 for the 5% exceedance limits and 1.96 for the 2.5% under and upper exceedance limits).

Figures 2.5 and 2.6 also show some wave overtopping discharges 0.1, 1, 10 and 100 l/s per m, together with an interval for each discharge. The discharges apply for a 1:4 slope and a wave steepness of $s_o = 0.03$. The uppermost line of the interval applies for a significant wave height of 1.0 m (for, e.g., river dikes) and the lowest line for a wave height of 2.5 m (for, e.g., sea dikes).

The available measured points for the maximum with non-breaking waves ($\gamma_b\xi_o >\approx 2$) are plotted in figure 2.6. The dimensionless wave overtopping discharge is now given on the vertical axis as:

$$\frac{q}{\sqrt{gH_{m0}^3}}$$

and the dimensionless crest height as:

$$\frac{h_k}{H_{m0}}\frac{1}{\gamma_f\gamma_\beta}$$

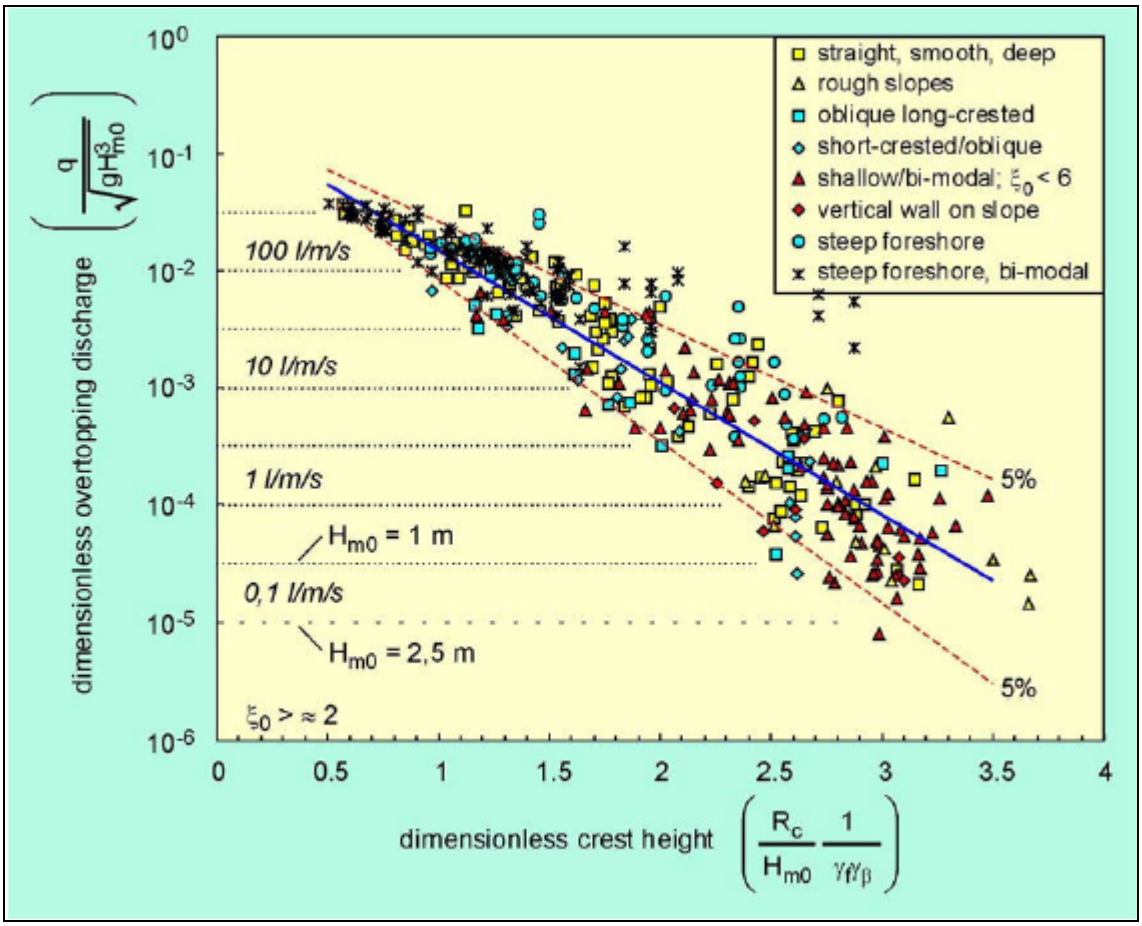

Figure 2.6 Wave overtopping data with mean and 5% under and upper exceedance limits, and indication of application area; non-breaking waves
[Technical Rapport, Van Der Meer 2002]

The reliability of formula (2.13) can be given by taking the coefficient 2.6 as a normally distributed stochastic function with a standard deviation $\sigma = 0.35$. Using this standard deviation, the 5% under and upper exceedance limits are drawn in figure 2.6. Wave overtopping discharges of 0.1, 1, 10 and 100 l/s per m are also shown on the vertical axis in figure 2.6. These intervals given apply for a wave height of $H_{m0} = 1$ m (uppermost line) and 2.5 m (lowest line) and are independent of the slope and wave steepness.

As with wave run-up, for deterministic use in practice a slightly more conservative formula should be used than for the average. The two recommended formulae for wave overtopping are formulae (2.10) and (2.11), that lie about one standard deviation higher than the average from formulae (2.12) and (2.13) (compare also figures 2.3 and 2.4). For probabilistic calculations, one can use the given estimates of the average (formulae (2.12) and (2.13) and the given standard deviation.

2.1.4 Application Areas of the Formulas

All the formulas described above are derived from analysis of the test results of scale models of breakwaters or dikes. In most cases, a relation between the test results of the wave overtopping and the variation of the parameters are given as good as possibly can. Not all the tests were uniformly setup. The variations in parameters are not in each test identical, or the values of the variation of parameters were not within de same range. Therefore, it's difficult to choose one of the formulas as a universal formula for a description of wave overtopping on breakwaters. By comparing between the conditions within which the relevant formula is derived from and the condition where the described situation is. By looking for as much similarity for both conditions as possible, a choice of a formula can be made.

In the following table, the application areas of the described wave overtopping formulas are given:

Table 2. 1 Application areas of wave overtopping formulas

Formula	Application Areas
Weggel	Smooth Slopes without superstructure, with a slope gradient of 1:1,5 -1:3 - 1:6, regular wave, roughness via parameter R
Battjes	Smooth Slopes without superstructure, with a slope gradient of 1:3 - 1:6, irregular wave, roughness via parameter R
Van Der Meer	Smooth Slopes without superstructure, with a slope gradient < 1:1, irregular wave, roughness γ_f= 0.5-1.0

2.2 Xbloc formula

According to KLABBERS (2003), a formula for wave overtopping over Xbloc armour layer units is derived from the tests done in WL and DHI.

2.2.1 General form of formula

For derivation of the Xbloc overtopping formulas the starting point was the same basic equation as discussed in 2.1.3.

According to KLABBERS (2003) the results can be described with a formula in the form of:

$$Q = a * \exp (-b * R) \qquad (2.14)$$

In which:

$Q = \frac{q}{\sqrt{gH_s^3}}$ = dimensionless discharge parameter [-]

$R = \frac{R_c}{H_s}$ = dimensionless freeboard parameter [-]

a, b = coefficients

This type of formula is similar to the Van Der Meer formulae for wave overtopping.

According to Klabbers, using this type of formula, the test results can be described by:

$$Q = 0.531 * \exp (-3.58 * R). \qquad (2.15)$$

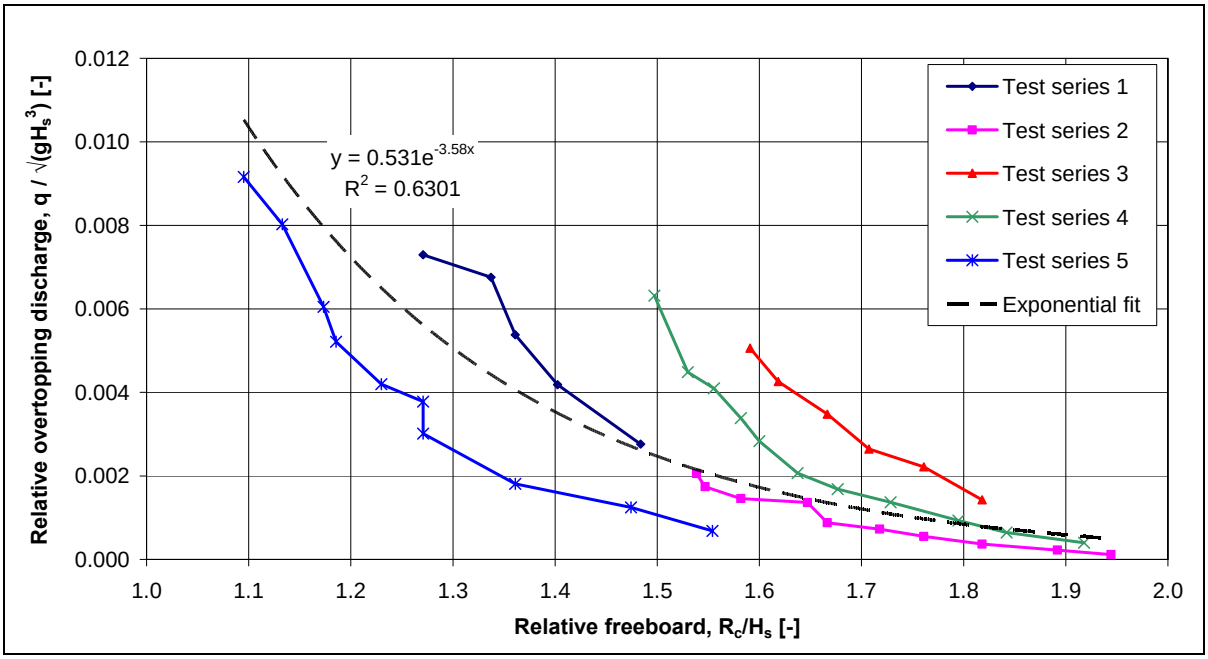

Figure 2.7 Exponential fit of overtopping curve [Klabbers, 2003]

2.2.2 Wave steepness

The formula as stated in paragraph 2.2.1 is based on the relation between freeboard, R_c, and the wave height, H_s, at the toe. Klabbers investigated to include other items in the formula to improve the fit of the overtopping formula.

Often the wave steepness [ratio wave height, wave length] is considered as an influence factor on wave overtopping. The influence of both components of the wave steepness on wave overtopping has been further analysed by Klabbers.

Figure 2.8 presents the relation between wave lengths at deep water, L_{op}, on the general overtopping formula. On the vertical axis the ratio Q / f(R) is given in which:

f(R) = 0.531 * exp (-3.58 * R) [-]

In Figure 2.9 the relation between wave height at the paddle, H_s, and the Q / f(R) ratio is presented.

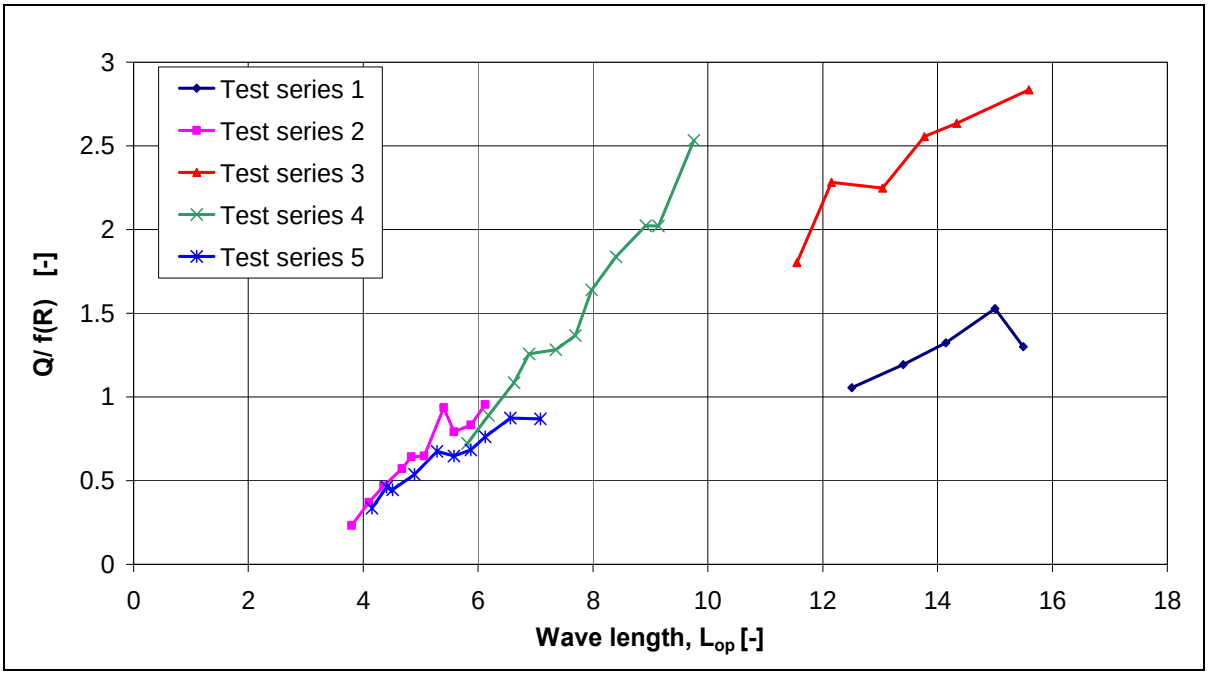

Figure 2.8 Influence of wave length on overtopping [Klabbers, 2003]

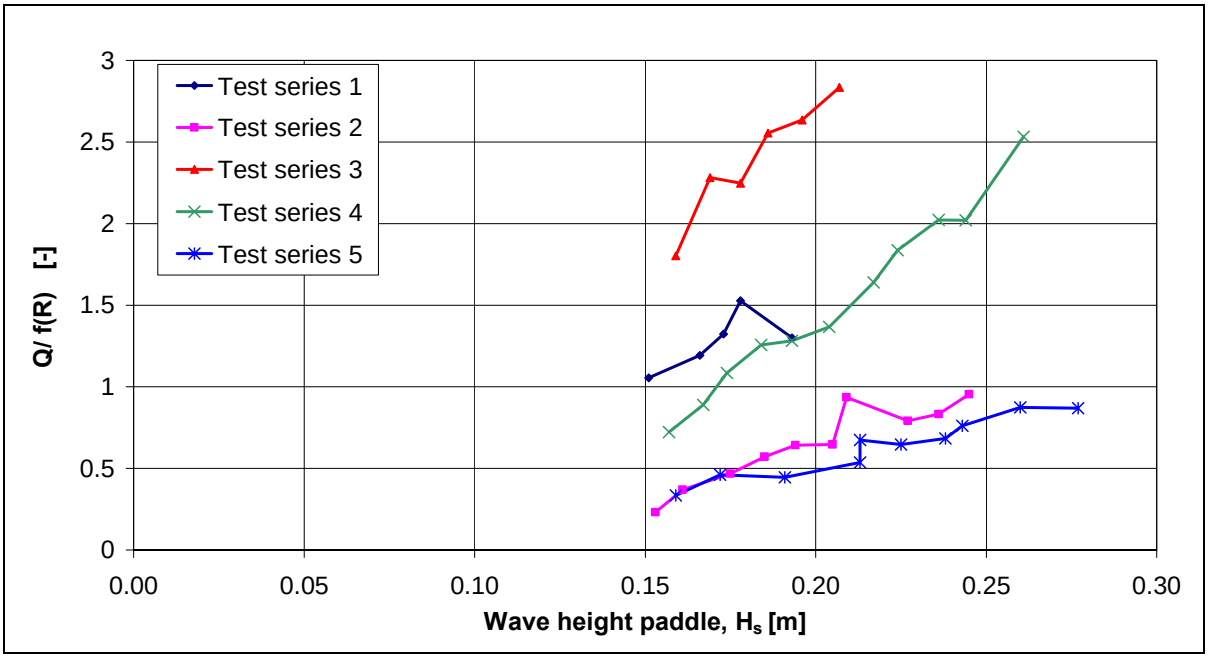

Figure 2.9 Influence of wave height on overtopping [Klabbers, 2003]

Klabbers has concluded from Figure 2.8 and Figure 2.9 that the components of the wave steepness, H_s and L_0 [or T_p] both have a similar influence on the overtopping: The amount of overtopping increases for increased values of H_s and L_0, while the wave steepness is H_s divided by L_0. It is therefore not justified to include the steepness in the overtopping formula.

2.2.3 Ursell parameter

Klabbers has presented an alternative dimensionless parameter in which both wave height and wave length are present in the multiplier is the Ursell parameter, U_r. This parameter is commonly applied to quantify non-linear effects of waves in shallow water.

$$U_r = \frac{H_s * L_t^2}{d^3} \qquad (2.16)$$

In which:

H_s = significant wave height at toe [m]
$L_{t,p}$ = local wave length at toe, based on T_p [m]
d = local water depth at toe [m]

Figure 2.10 presents the relation between Ursell parameter, U_r, on the general overtopping formula. On the vertical axis the ratio Q / f(R) is given, similar to paragraph 2.2.2.

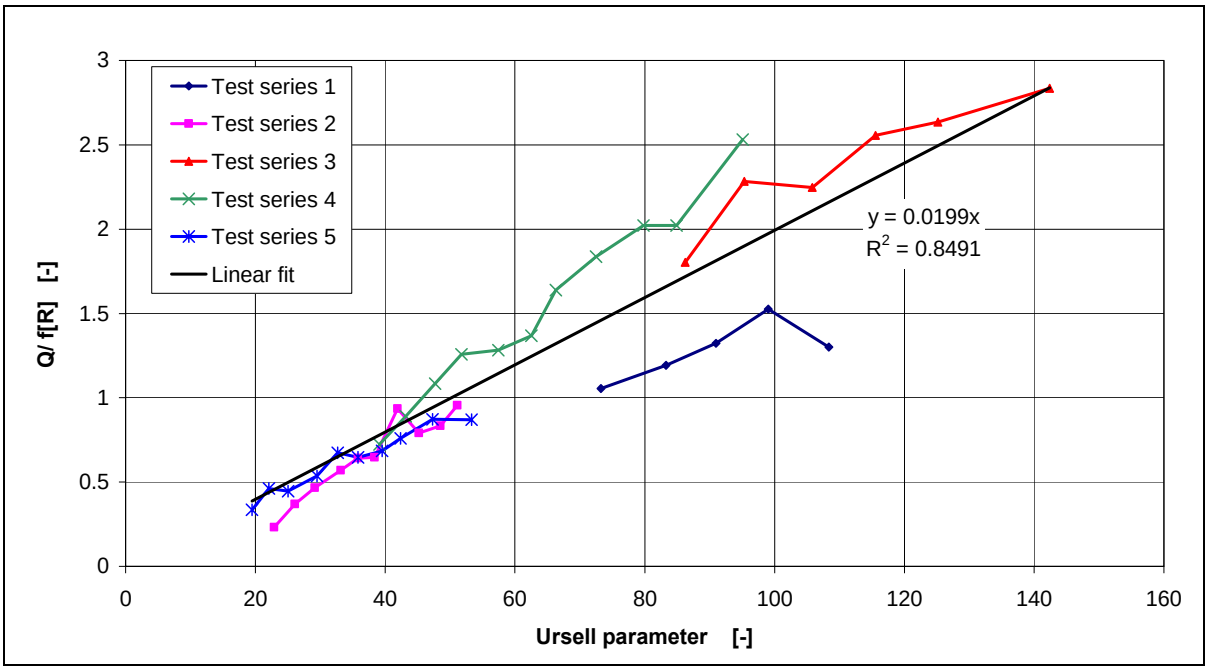

Figure 2.10 Influence of Ursell parameter on overtopping [Klabbers, 2003]

Klabbers found that an increased value of U_r will result in increased values of Q: The asymmetry of the wave profile [η_{crest}/H_s] is increasing with increasing U_r [which will increase the overtopping rate]. Thus it is recommended to include the Ursell parameter in the overtopping formula.

2.2.4 Recommended overtopping formula for overtopping Xbloc

According to Klabbers, the overtopping formula with Ursell parameter included will be as follows:

$Q = (1/100)\, U_r \exp(-3.58\, R)$ (2.17)

In which:

$Q = \frac{q}{\sqrt{gH_s^3}}$ = dimensionless discharge parameter [-]

$R = \frac{R_c}{H_s}$ = dimensionless freeboard parameter [-]

q = average overtopping rate [m^3/s per m width]
U_r = Ursell parameter [$U_r = H_s * L_t^2 / d^3$] [-]
g = gravitational acceleration [m/s^2]
R_c = freeboard [= crest level – still water level] [m]
H_s = incident wave height near the toe [m]

Figure 2.11 presents overtopping formula as well as the relative overtopping volumes measured in the WL test series.

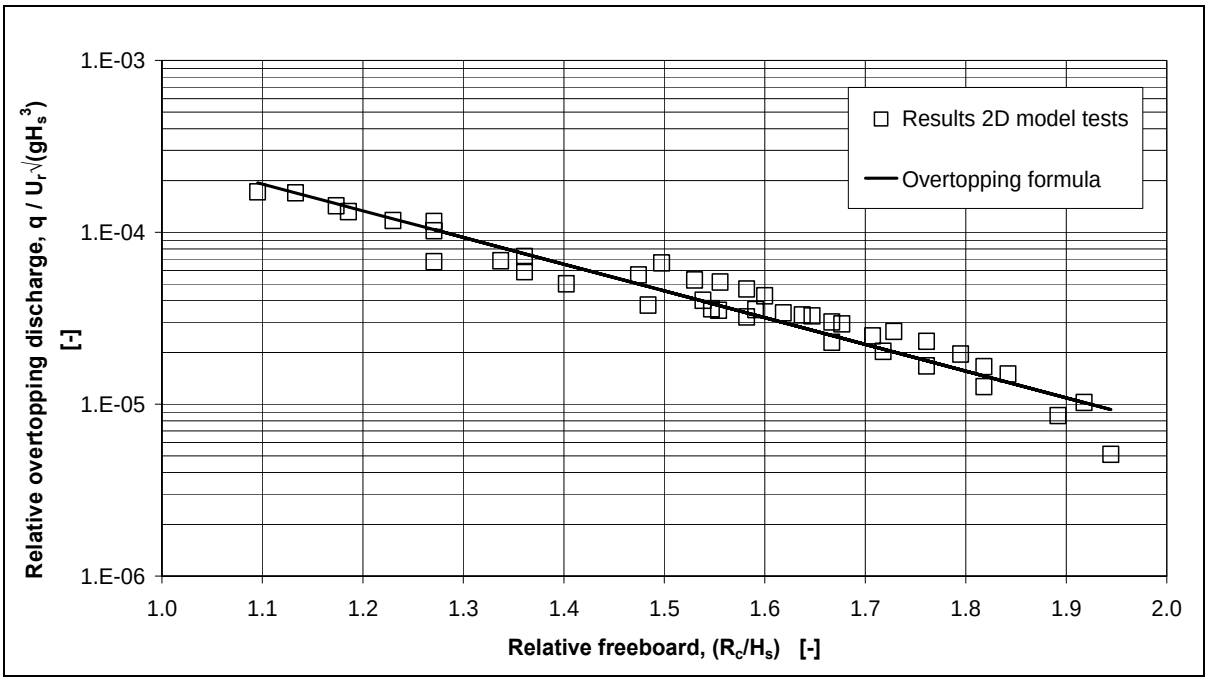

Figure 2.11 Fit of formula for overtopping discharge [Klabbers, 2003]

The standard deviation of the difference between calculated and measured values of overtopping discharges is 2.1 E-04. The uncertainty of the overtopping formula, given by the ratio standard deviation / mean calculated overtopping discharge, is 29.4%.
In this research, the standard deviation also will be determined.

Chapter 3

Wave flume experiments

This chapter deals with the set-up of the model tests. First, the scaling of the model is discussed. The different environmental and structural parameters, as mentioned in the previous chapter and their relevance to the model set-up will be treated in the following paragraphs. The model set-up and the test program conclude this chapter.

3.1 Scaling

A proper representation of reality by means of scale modelling is based on similarity between prototype and model. In fluid mechanics, similarity generally includes three basic classifications:

- Geometric similarity
- Kinematical similarity
- Dynamic similarity

When all geometric dimensions of the model are related to the corresponding dimensions of the prototype by a constant scale factor, the model is geometrically similar:

$$K = \frac{x_M}{x_P} = \frac{y_M}{y_P} = \frac{z_M}{z_P} \tag{3.1}$$

The science of kinematics studies the space-time relationship. Kinematical similarity consequently signifies similarity of motion. If the velocities at corresponding points on the model and prototype are in the same direction and differ by a constant scale factor, the model is regarded as kinematical similar to the prototype.

In addition to the requirements for kinematical similarity, the model and prototype forces must be in a constant ratio to be considered dynamic similar. Complete similarity is obtained if all relevant dimensionless parameters[1] have the same corresponding values for model and prototype:

$$\pi_P = \pi_M = f(\pi_1, \pi_2, ..., \pi_r) \tag{3.2}$$

In which the π's are a complete set of dimensionless products.

[1] Dimensionless groups are formally found through non-dimensionalizing conservation equations. An informal approach is the use of Buckingham Pi Theorem (e.g. LANGHAAR, 1951)

Two common dimensionless parameters in free-surface flow are the Reynolds number and the Froude number. The Reynolds number represents the inertia of the flow related to its viscosity. To obtain similarity the Reynolds number for both the model and prototype must be equal:

$$\mathrm{Re} = \left(\frac{Vh}{\upsilon}\right)_P = \left(\frac{Vh}{\upsilon}\right)_M \tag{3.3}$$

With:

$K_V = V_M / V_P$,
$K_h = h_M / h_P$,
$K_\upsilon = \upsilon_M / \upsilon_P = 1$
(Modelling is done with water),

Last equation can be written as:

$$K_V = \frac{1}{K_h} \tag{3.4}$$

The Froude number represents the inertia of the flow related to the gravity. Again, to achieve similarity the Froude number must be equal in model and prototype:

$$Fr = \left(\frac{V^2}{gh}\right)_P = \left(\frac{V^2}{gh}\right)_M \tag{3.5}$$

With:

$K_V = V_M / V_P$,
$K_h = h_M / h_P$,
$K_g = 1$
(Gravity remains the same),

Last equation can be written as:

$$K_V = \sqrt{K_h} \tag{3.6}$$

The same principle can be applied on the celerity of waves. According to the linear wave theory, the celerity of a wave can be described as:

$$c = \sqrt{\frac{gL}{2\pi}\tanh\left(\frac{2\pi h}{L}\right)} \tag{3.7}$$

With:

$K_c = c_M / c_P$,
$K_L = L_M / L_P$,
$K_h = h_M / h_P$,

In addition, where the argument of the hyperbolic tangent in model and prototype are the same because of geometric similarity, last equation changes:

$$K_c = \sqrt{K_L} = \sqrt{K_h} \tag{3.8}$$

With c = L/T, the Froude time scale between prototype and model becomes:

$$K_t = \sqrt{K_h} \tag{3.9}$$

Equation (3.4) shows that, if a small-scale model is tested in the same fluid as the prototype, the preservation of Reynolds number requires the stream velocity for the model to be greater than for the prototype. On the other hand, according to equation (3.6), the preservation of Froude's number requires the opposite condition. In free-surface flow, gravity is considered dominant over viscosity and therefore the wave flume experiments are Froude scaled. A deviation between Reynolds number in the model and prototype is consequently inevitable. This non-similitude of Reynolds number lead to scale effects.

In the model, the top and secondary layers were scaled with a constant length-scale factor between prototype and scale model to represent the stability of these layers correctly. According to VAN GENT (1995), applying this scale factor to the top of the structure results in an acceptable representation of the non-linear friction for porous media flow.[2] However, this scale factor is not applicable to scale the linear friction. Since this friction term is usually dominant in the small-scale core of the model, the use of the same scale factor would lead to a too high friction in the model. This discrepancy can be partly solved by scaling the core material by a different factor, which leads to more course core material. This can be achieved by scaling the core according to a method described by BURCHARTH ET AL. (1999).[3]

[2] See paragraph (3.2.2) for an explanation of the linear and non-linear friction as found in the Forchheimer equation.
[3] See paragraph (3.2.2) for a more detailed explanation of this core scaling procedure.

HUDSON (1959) claimed that viscous effects could be neglected in the model if the Reynolds numbers in the pores of a breakwater are above 3×10^4. Literature that is more recent even suggests a value as low as 1×10^4 to discount for these effects (e.g. VAN DER MEER, 1988b).

3.2 Scope of the present study

Because of limitations in time and resources, not all involved parameters were examined. A selection in both environmental and structural parameters was made, mainly based on the relevance to engineering practice.

3.2.1 Environmental parameters

The wave height and period are obvious parameters to include. The wave period is often written as a wavelength and when related to the wave height, results in the wave steepness:

$$s_{m0} = \frac{2\pi H_s}{g T_{m0}^2} \tag{3.10}$$

During each experiment, the wave height was gradually increased. Three different values of the dimensionless wave steepness were investigated, namely a (deep-water) steepness of s_{m0} = 0.02, 0.04 and 0.06. The subscript $_0$ indicates deepwater values. In general, the steepness of wind-generated waves is between 0.02 and 0.06. By investigating these three steepness, this frequently occurring range is covered. IRIBARREN (1950) related the slope angle of the structure to the wave steepness:

$$\xi = \frac{\tan\alpha}{\sqrt{2\pi H_s / g T_{m0}^2}} \tag{3.11}$$

BATTJES (1974) described possible breaker types as a function of this parameter and called it the surf similarity parameter. The parameter tells whether a wave will break and how the wave will break. For different values of ξ, waves brake in different ways. Battjes distinguished the following breaker types: surging, collapsing, plunging and spilling.
In engineering practice, when an armour layer is constructed of artificial concrete units, a slope angle more gentle than cot α = 1.5 is rare. Because of this fact, the influence of the slope angle on the overtopping of the structure will not be treated further. Therefore, the surf similarity is of lesser importance in this research and overtopping is related to the wave steepness instead.

Irregular waves

An irregular wave field is best described with a variance density spectrum. The spectrum provides a statistical description of the fluctuating wave height caused by wind. As was applied by Van Den Bos and De Jong, for this research, also a JONSWAP spectrum is applied:

$$E(f) = \alpha g^2 (2\pi)^{-4} f^{-5} \exp\left\{ -\frac{5}{4}\left(\frac{f}{f_{peak}} \right)^{-4} \right\} \cdot \gamma^{\exp\left\{ -\frac{1}{2}\left(\frac{f - f_{peak}}{\sigma - f_{peak}} \right)^2 \right\}} \quad (3.15)$$

The JONSWAP spectra result in a good description of wind generated wave fields in the North Sea. This spectrum is also commonly used in wave flume experiments (e.g. VAN DEN BOSCH, 2001), making the laboratory data accessible for comparison. The mean values of the shape parameters γ, σ_a and σ_b of the JONSWAP observations were $\gamma = 3.3$, $\sigma_a = 0.07$ and $\sigma_b = 0.09$.

Storm duration

VAN DER MEER (1988a) reanalyzed results of THOMPSON and SHUTTLER (1975) to show the importance of the storm duration on the stability of a breakwater. He demonstrated that the relation between the number of waves (N) and the damage (S) could be described by:

$$f(S) = \frac{S(N)}{S(5000)} = 1.3\left[1 - e^{-3\times10^{-4} N} \right] \quad (3.19)$$

When only the most important region is considered (N < 7000 - 10000) a different relation can be established:

$$S = 0.014\sqrt{N} \quad (3.20)$$

Because of a limitation in time, the total number of generated waves in all tests was set at approximately 1000. This is consistent with the tests done by VAN DEN BOSCH (2001). The assumption is made that after 1000 waves, the JONSWAP-spectrum has been fully developed.

Water depth and angle of wave attack

Freeboard has influence of the amount of overtopping water. Therefore with the height of the structure was fixed, the water depth of the scale model varies from h = 0.60m to 0.70m.

The wave flume can only generate wave attack perpendicular to the breakwater. However, for this kind of research, wave attack under other angles is not relevant. Thus, it is suitable to do this research in the wave flume, and the angle of wave attack will not be considered in this research.

3.2.2 Structural parameters Core material

VAN DER MEER (1988a) demonstrated that the permeability of the structure has significant influence on its stability. Froude scaling the material may lead to relatively large viscous forces corresponding with small Reynolds numbers. JENSEN and KLINTING (1983) pointed

out that correct scaling requires similar flow fields in the prototype and the model. Similar flow fields are obtained if the hydraulic gradients I in geometric similar points are the same:

$$I_P = I_M \tag{3.21}$$

Furthermore, they provided a method to calculate scale distortion for core and secondary material to achieve this requirement. The distortion is calculated from the Reynolds number at maximum pore velocity. However, because the flux in the core varies in time and space, BURCHARTH ET AL. (1999) proposed the usage of a time and space averaged pore velocity for the calculation of Reynolds number. An estimation of I in one-dimensional cases can be made by means of the extended Forchheimer equation:

$$I = aU + b|U|U + c\frac{\delta U}{\delta t} \tag{3.22}$$

In which U is a characteristic pore velocity and a, b and c are dimensional coefficients. The first term can be regarded as the laminar contribution and the second term as the contribution of turbulence. The last term represents the inertia. According to BURCHARTH (1995) the last term in equation (3.22) can be disregarded when scaling porous flow in breakwater cores. VAN GENT (1995) demonstrated the relative small importance of the inertia term in oscillatory flow tests, thereby validating Burcharth's assumption. The dimensional friction coefficients are denoted as
(VAN GENT, 1995):

$$a = \alpha\frac{(1-n)^2}{n^3}\frac{\upsilon}{gD_{n50}^2} \tag{3.23}$$

$$b = \beta\frac{(1-n)}{n^3}\frac{1}{gD_{n50}} \tag{3.24}$$

With:

$$\beta = \beta_c\left(1+\frac{7.5}{KC}\right)$$

The non-dimensional α and β_c are empirical determined coefficients dependent on parameters like grading, shape, aspect ratio and orientation of the stones. VAN GENT (1995) states that values of 1000 and 1.1 can be used for α and β_c, respectively. KC stands for the Keulegan-Carpenter number and represents the ratio between the amplitude of the water particle oscillations and the diameter of the core rubble mound.

$$KC = \frac{\hat{U}T}{nD_{n50}} \tag{3.25}$$

Û is the amplitude of the velocity and T the oscillation or wave period.

To determine the horizontal pressure gradient in the core, it can be seen as a function of harmonic oscillating pore pressure (BURCHARTH ET AL., 1999):

$$p(x,t) = (0.55\rho_w g H_s) e^{\delta\left(\frac{2\pi}{L'}\right)x} \cos\left(\frac{2\pi}{L'}x + \frac{2\pi}{T_P}t\right) \tag{3.26}$$

$$I_x = \frac{1}{\rho_w g}\frac{dp(x,t)}{dx} \tag{3.27}$$

Where L' represents the wavelength in the core. The wave length in the core is found as the ratio between the length of the incident wave and a coefficient that accounts for seepage length as a result of the deviation of the flow path caused by the grains, L' = L/$\sqrt{D}$. LE MEHAUTE (1957) gives the empirical coefficient a value of 1.4 for quarry rock material. 6 is the dimensionless damping coefficient, characterized by:

$$\delta = 0.0141\frac{n^{1/2}L_p^2}{H_s b} \tag{3.28}$$

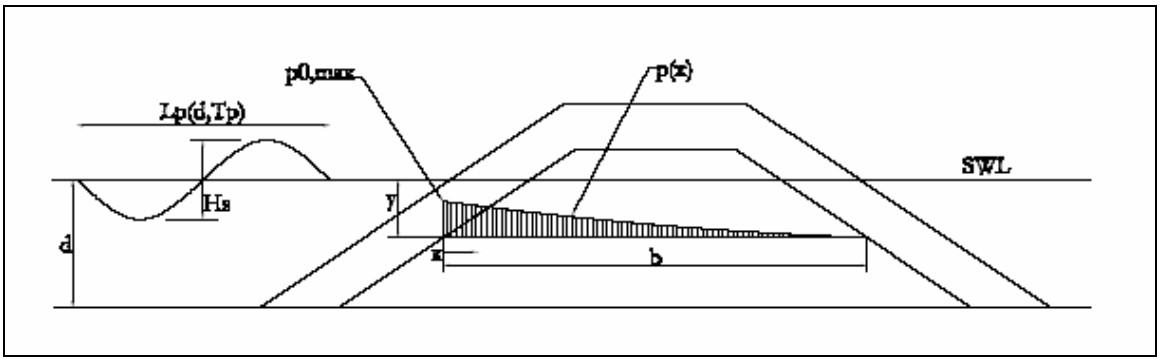

Figure 3.1 Horizontal distribution of the pore pressure amplitudes induced by irregular waves

Burcharth suggested that the diameter of the core material in models is chosen in such a way that the Froude scale law hold for a characteristic pore velocity. This method can be used in order to make a good approximation of the occurring Reynolds number in the core. The flux velocity is calculated by means of equations (3.22) and (3.27). These flux velocities are averaged with respect to time (one wave period) in 6 characteristic points (see table (3.4)). This is followed by space averaging these velocities in these points, and thus obtaining the characteristic pore velocity in the structure.

To apply the Burcharth method of scaling, first the model of Van Den Bosch is re-scaled to prototype dimensions. These dimensions were used to determine the characteristic pore velocity in the core of this prototype design. Froude scaling this pore velocity by means of the above-described method resulted in the dimensions of the model core material as used in the wave flume experiments.

Re-scaling this model to prototype with K = 1/25 gives the characteristic dimensions as found in table (3.1).
The prototype with a W_s/W_a ratio of approximately 1/27 and a W_c/W_s ratio of 1/5 represents a realistic design of a breakwater.

Table 3. 1 Re-scaling of the model to prototype with K = 1/25

	Armour layer	Secondary layer	Core
W_{50}^M	206 g	7.3 g	1.6 g
D_{n50}^M	44 mm	14 mm	8.4 mm
W_{50}^P	3100 kg	115 kg	25 kg
D_{n50}^P	1075 mm	350 mm	210 mm

Relevant parameters were established to calculate the characteristic pore velocity in this prototype. The maximum velocity Û that occurred in the characteristic points was used to determine the KC-number.

Following VAN GENT's (1995) recommendation of $\alpha = 1000$ and $\beta_c = 1.1$ along with equations (3.23), (3.24), (3.25) and a usage of a (median) sea-state of $H_S^P = H_s^M$ /K = 4.0m (with corresponding T_p = 8.01s) led to the use of the following parameters:

Table 3. 2 Parameters used to calculate the characteristic pore velocity in the prototype

	D_{n50} (mm)	n	Û (m/s)	KC	α	β	a (s/m)	b (s^2/m^2)
Prototype	210	0.4	0.115	10.96	1000	1.9	0.013	8.65

The above-described parameters, along with equation (3.22) and (3.27) were used to calculate the time averaged pore velocity in all six characteristic points (see table (3.4)). The characteristic pore velocity in the prototype thus becomes $\overline{U}_P$ = 0.102m/s. Burcharth suggested that the diameter of the core material in models is chosen in such a way that the Froude scale law holds for this characteristic pore velocity. Accordingly, the characteristic pore velocity in the model should be $\overline{U}_M = \overline{U}_P / \sqrt{K}$ = 0.020m/s. This criterion is met by setting the diameter of the core material in the model at D_{n50} = 18mm and using the parameters listed in table (3.3). The length scale for the core material now becomes D_{n50}^M / D_{n50}^P = 1/12 and $I_M = I_P$ = 0.084, opposite to Van Den Bosch's model with D_{n50}^M / D_{n50}^P = 1/25 and $I_M = 0.094 \neq I_P$.

Table 3. 3 Parameters used to calculate the characteristic pore velocity in the model

	D_{n50} (mm)	n	Û (m/s)	KC	α	β	a (s/m)	b (s^2/m^2)
Model	18	0.4	0.032	7.12	1000	2.3	1.77	122

The characteristic pore velocity in the model leads to a Reynolds number O(500). This Reynolds number is below the critical value of Re = 1 x 10^4 and therefore viscous scale effects are inevitable. Although Burcharth's method of scaling leads to a better representation of reality, still it is far from perfect. A more suitable model could be made if the size of the core material varied according to the local flow conditions. By averaging in time and space these local conditions are lost, leading to a model structure that is too permeable at the sides of the core and too impermeable in its centre. A better solution lies in the stratification of the material along the complete width of the core, i.e. increase the size of the core material towards the centre of the core. Part of this solution was met by the introduction of an intermediate layer between the core and the secondary layer. This layer had a thickness of 5.0cm and a nominal diameter of D_n = 15.2mm. Using the same procedure as described earlier, an intermediate layer with a nominal diameter of D_{n50} = 15.2mm (see table 3.5) calculates a time-averaged pore velocity in x = 0 of 0.054m/s. Again, $\overline{U}_M \approx \overline{U}_P / \sqrt{K}$.

Secondary material

The dimensions of the secondary material are often determined by a rule of thumb recommended by VAN DER MEER (1993) that states:

$$W_s \approx \left(\frac{1}{25} - \frac{1}{15} \right) \times W_a \tag{3.29}$$

Table 3. 4 Time-averaged pore velocity at six different locations

y (m)	0.0			4.0		
b (m)	20.25			32.25		
x (m)	0	b/4	b/2	0	b/4	b/2
U (m/s)	0.126	0.100	0.086	0.110	0.100	0.089

Table 3. 5 Parameters used to calculate the characteristic pore velocity in the transition layer at x=0.

	D_{n50} (mm)	α	β	$\overline{U}$ (m/s)
Prototype	350	1000	4.0	0.28
Model	15.2	1000	4.2	0.054

With a Tetrapod mass of W_{50} = 206 grams and a median mass of W_{50} = 7.3 grams for the secondary layer, VAN DEN BOSCH (2001) already chose relatively light material for the underlayer. He observed excessive washout of secondary layer material, which seriously

undermined armour layer stability. The first tests, however, did not agree with his observations. An explanation was sought in the different core scaling procedures between the current scale model and the model used by Van Den Bosch. This led to extra experiments with geotextile placed between secondary layer and core to approach the permeability of Van Den Bosch's structure.[4] Nevertheless, the outcome resulted the initial test program -in which the weight of rock material of the secondary layer gradually increased after each series- to be altered. Instead, the weight decreased after every series. Consequently, the material Van Den Bosch used formed a starting point of secondary layer rock weight that was examined. The following weight classes of secondary layer material formed the basis of this research.

Table 3. 6 Weight classes of the secondary layer as used in the wave flume experiments

Description	W_{50} (g)	D_{n50} (mm)	W_a/W_s
Large	6.5	13.6	31
Mid	4.3	11.3	47
Small	1.7	8.6	119

Changing the grading of the material is time intensive. Therefore, the grading was not varied in the test series. VAN DER MEER ET AL. (1996) already conducted experiments to gain insight in the influence of rock shape and grading on stability of low-crested structures. From analysis of their laboratory-data followed the conclusion that material properties of rock, such as shape and grading, appear to be of little influence on the stability of the armour layer. A careful assumption that this statement is also applicable for the secondary layer, justifies the choice of not varying the grading.

Literature (e.g. CUR, 1995; SPM, 1984) recommends a layer thickness of $2 \times D_{n50}$. However, the effect of the layer-thickness on the stability of the secondary layer was excluded by means of a fixed layer thickness for all three series. By excluding the effect of the layer-thickness, the overall comparability of the different layers is improved. A secondary layer thickness of 4.0cm was chosen. When compared to CUR's guideline, this thickness of the secondary layer is considerable. Primarily, this substantial thickness was realized to minimize the effect of large additional friction forces between the rough texture of the core and the upper part ($2 \times D_{n50}$) of the secondary layer. Burcharth's method to determine the Reynolds number in the core also served to make an estimation of this number in the secondary layer. With the nominal diameter ranging from 13.6mm to 8.6mm, the Reynolds number showed O(1000). With the Reynolds number in this range, the flow can be considered transitional between laminar and turbulent. As with the core, viscous scale effects are present and should be taken into consideration when model data is translated back to prototype.

[4] A more thorough discussion on the differences in outcome as well as the additional experiments can be found in paragraph (4.1).

3.3 Model Set-Up

3.3.1 Model dimensions

The physical model tests are performed in the Fluid-Mechanics Laboratory of the Faculty of Civil Engineering and Geosciences.

The wave flume has a length of 40 meter, a width of 0.80 meter and a height of 0.85 meter. A foreshore with a 1:30 slope is constructed over a length of 6.60 meter and started at 24.80 meter from the wave board. The distance between the toe of the structure and the wave board is 31.40 meter.

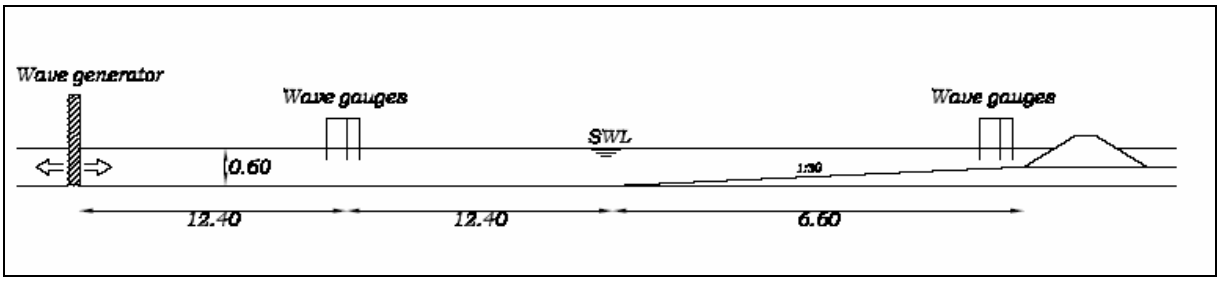

Figure 3.2 Setup of the wave flume

To exclude wave set-up caused by excess pressures in the structure, the inner slope is constructed of rubble mound of a homogenous gradation of D_{n50} = 18 mm and D_{85}/D_{15} = 1.3 to insure permeability. The inner slope also has an angle of cot α = 1.5.

Table 3. 7 Main dimensions of the model

Description	Parameter	Value
Length wave flume	L_{fl}	40.00 m
Width wave flume	B	0.80 m
Height wave flume	h_{fl}	0.85 m
Length wave board to structure	L_{ws}	31.40 m
Length foreshore	L_{fs}	6.60 m
Slope angle foreshore	cot β	30

3.3.2 Test Program

In the test program, several combinations of wave steepness and freeboard of the crest height are used. For the armour layer, a comparative experimental research between a single layer of Tetrapod and a single layer of Xbloc are carried out.

The total number of generated waves in all tests is approximately 1000.
Other parameters are:

- The secondary layer: D_{n50} = 25 mm;
- Grading of the secondary material: D_{85}/D_{15} = 1.3;

3.3.2.1 Packing Density

The packing density of the Tetrapod armour layer is n_v = 0.3.
According to the following formula, the total number of units in a considered area can be calculated.

$$N_a = n_L \cdot A \cdot k_t \cdot (1 - n_v) \cdot D_{n50}^{-2} \qquad (3.30)$$

With:

N_a = total number of units in area considered [-];
n_L = number of layers making up the total thickness of armour [-];
A = area considered [m^2];
k_t = layer thickness coefficient [-];
n_v = fictitious porosity [-]; $n_v = 1 - \frac{\rho_b}{\rho_r}$
ρ_b = bulk density as laid;
ρ_r = density of rock

For the Tetrapod model is the nominal diameter of the unit D_{n50} = 0.043 m.

The placement density of the Tetrapod is to be calculated using:

$$\frac{N_a}{A} = n_L \cdot k_t \cdot (1 - n_v) \cdot D_{n50}^{-2} \qquad (3.31)$$

With:

n_L = 1; k_t = 1.04; n_v = 0.3; D_{n50} = 0.043 m;

$$\frac{N_a}{A} = 1 \cdot 1.04 \cdot (1 - 0.3) \cdot 0.043^{-2} = 394$$

So the placement density of the Tetrapod is 394 units per m^2.

The placement density of the Xbloc [Reedijk ET AL 2003] is $1.19/D^2$ [units/m^2]. With D is the unit height, D = 1.44*D_n. The D of the model unit is 5.4 cm, which means that the placement density of the Xbloc for the model unit is 408 units per m^2.

3.3.2.2 Wave Steepness

There are three different deep-water wave steepness used in this research. In table 3.2 the wave steepness S_{0m} and wave height H_s [m] at the wave machine are presented with the resulting wave periods T_m [s] as used.

Table 3. 8 Combinations of Hs and Tm as used in this research

S_{0m} \ H_s	0.10	0.12	0.14
0.02	1.79	1.96	2.12
0.04	1.27	1.39	1.50
0.06	1.03	1.13	1.22

Each test series in principle consisted of 3 test-runs with increasing wave height and increasing wave period to obtain the same wave steepness at deep water.

3.3.2.3 Stability

A calculation is done for the stability of the Tetrapod and Xbloc.
Tetrapod [D'Angremond 2000]:

$$\frac{H_s}{\Delta D_n} = \left(3.75 \frac{N_{od}^{0.5}}{N^{0.25}} + 0.85 \right) * s_{om}^{-0.2} \qquad (3.32)$$

With:

$N_{od} = 0.5$,
$N = 1000$,
$S_{om} = 0.06$,
$D_n = 0.043$ m,
$\Delta = (\rho_a - \rho)/\rho = (2400-1000)/1000 = 1.4$,
The maximal allowable $H_s = 0.14$ m.

Formula for Xbloc [Klabbers 2003] is:

$$\frac{H_s}{\Delta D_n} = \sqrt[3]{K_D \cot \alpha} \qquad (3.33)$$

With:

$\text{Cot}\alpha = 1.5$
$K_d = 16$

D_n = 0.054/1.44=0.0375 m,
$\Delta = (\rho_a-\rho)/\rho$ = (2300-1000)/1000=1.3,
The maximal allowable H_s = 0.14 m.

3.3.2.4 Crest Height

The crest height of the breakwater is taken as 1.6 times the maximal allowable H_s calculated for the stability of Tetrapod and Xbloc, plus the height of the design water depth. In this case, the extreme wave height H_s is 0.14 m and the water depth is 0.6 m. Therefore, the crest height is 1.6*0.14+0.6 = 0.824 m. The crest height in the test was chosen to be 0.85 m above the wave flume bottom.

3.3.2.5 Dimension of the Water Collector Bin

According to the wave-overtopping formula of VAN DER MEER (2002), the quantity of water as a result of wave overtopping can be calculated.

$$\frac{q}{\sqrt{gH_{mo}^3}} = 0.2 \cdot \exp\left(-2.3 \frac{R_c}{H_{mo}} \frac{1}{\gamma_f \cdot \gamma_\beta}\right) \tag{3.34}$$

With:

q = average wave overtopping discharge [m^3/m/s]
g = gravitational acceleration [m/s^2]
H_{mo} = significant wave height at the toe of the breakwater [m]
R_c = free crest height above the still water line [m]
γ_f = influence factors for the influences of the roughness [-]
γ_β = influence factors for the influences of the angle of the wave attack [-]

For H_{mo} = 0.14 m, R_c = 0.25 m, γ_f = 0.7, γ_β = 1 and g = 9.81 m/s^2, q can be found:

$$\frac{q}{\sqrt{9.81 \cdot 0.14^3}} = 0.2 \cdot \exp\left(-2.3 \cdot \frac{0.25}{0.14} \cdot \frac{1}{0.7 \cdot 1}\right)$$

q = 9.288*10^{-5} m^3/m/s

Note here that γ_f = 0.7 is chosen for one layer of random rubble stone. For the analysis of the obtained data, this factor will be further studied.

The width of the breakwater is 0.80 m. Each test is carried out for 20 minutes. Therefore the total quantity of water as a result of wave overtopping is:

$9.288*10^{-5}$ $m^3/m/s$ * 0.80 m * 20*60 s = 0.089 m^3.

According to the Xbloc overtopping formula, q can also be calculated as:

$$\frac{q}{\sqrt{gH_{mo}^3}} = \frac{1}{100} U_r * \exp\left(-3.58 \frac{R_c}{H_s}\right) \tag{3.35}$$

With:

q = average overtopping rate [m^3/s per m width],
U_r = Ursell parameter $U_r = \frac{H_s * L_t^2}{d^3}$ [-],
g = gravitational acceleration [m/s^2],
R_c = freeboard = crest level – still water level [m],
H_s = incident wave height near the toe [m]

The calculated q is $5.61*10^{-5}$ $m^3/m/s$. And V_{water} = 0.054 m^3.

Based on the calculated volume of water according to the Van Der Meer formula, the required dimension of a water collector bin can be determined. A water collector bin with a volume lager than 0.089 m^3 is required.
A collector bin of 0.80 m width, 0.50 m height and 0.40 m length (volume is 0.16 m^3) is needed for collecting the wave overtopping water.

3.3.2.6 Test Series

The parameters variation in the tests series are:

- Wave steepness in deep water: s_{0m} = 0.02, 0.04 and 0.06;
- Free crest height above the quite water line: R_c = 0.15, 0.20, 0.225 and 0.25 m

The series of tests can be seen in the following table:

Table 3. 9 Test series

Series	h [m]	S_{0m}	Armour Units	R_c
A	0.10, 0.12, 0.14	0.02, 0.04, 0.06	Tetrapod	0.15, 0.20, 0.225, 0.25
B	0.10, 0.12, 0.14	0.02, 0.04, 0.06	Xbloc	0.15, 0.20, 0.225, 0.25

In order to investigate the reliability of the test results, several of the above tests were repeated for 3 times.

3.3.2.7 Description of the main construction

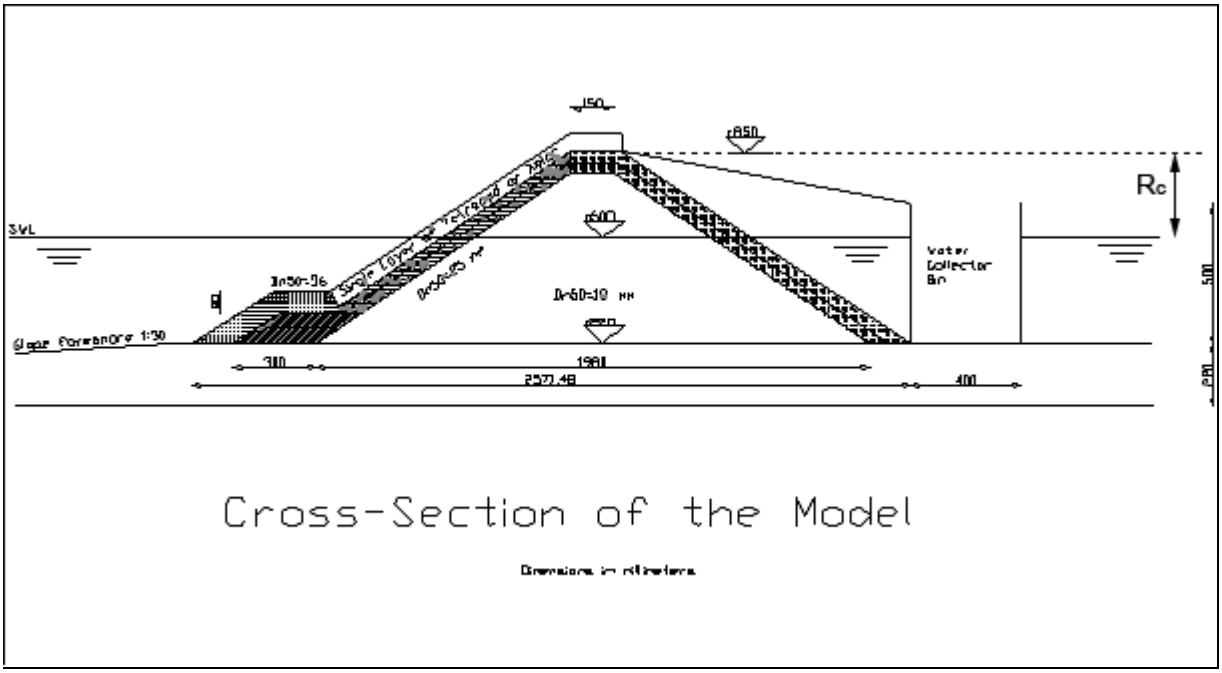

Figure 3.3 Cross section of the model

The main construction parameters are:

Table 3. 10 Structural Parameters

Description	Parameters	Value
Still water line	h_0	0.60 m
Height of the crest	h_{cr}	0.83 m
Width of the crest	w_{cr}	0.15 m
Slope angle of the structure	cot α	1.5
Volume water collector	V_{col}	0.16 m^3
Width of the collector bin	W_{cb}	0.80 m
Height of the collector bin	h_{cb}	0.50 m
Length of the collector bin	l_{cb}	0.40 m
Density of water	ρ_w	1000 kg/m^3

3.3.3 Instrumentation

Wave gauges are positioned at deep water (halfway between the wave board and the structure of the breakwater) and before the toe of the structure. By positioning the wave gauges at these two locations, the wave propagating towards the structure can be separated from the reflected wave.
Wave gauge is also put on top of the crest, this way, the percentage of the overtopping wave can also be determined.

3.3.4 Procedures of the measurements

The procedures of the measurements during the tests are as following:

1. The beginning water level in the water collector bin was noted.
2. The water level in the wave flume was controlled and justified.
3. Wave gauges were controlled for distance between each other and the depth under water level.
4. Wave height meters were calibrated.
5. A new data file was started using computer to register the measured wave height.
6. The right program file with relevant wave height and steepness was chosen.
7. The computer program, which drives wave board to generate waves, was started.
8. On the end of the test, the wave height registration was stopped, and the wave board was stopped.
9. The ending water level in the water collector bin was noted.
10. The water collector bin was emptied

Chapter 4

Analysis of the Wave Flume Experiments

In this chapter, the results of the wave flume experiments were described and analyzed. During the tests, the wave heights were registered by a computer which was linked to several wave height meters. The wave overtopping was apart registered by measuring the difference between the beginning water level and the ending water level in the water collector bin.

4.1 Processing the Measured Data

The wave characters are processed using a program called “refreg”, which is a standard program for analyzing wave data’s from the Fluid Mechanics Laboratory of Civil Engineering. This program used a so called two point measurements to determine the following wave characters:

- Incident wave height
- Reflected wave height
- Reflection coefficient
- Wave period
- Wave length
- Wave steepness

Together with the registered beginning and ending water level in the water collector bin, the wave overtopping volume and the discharge over the crest can be calculated according to the following formulas.

$$V = \left(h_{end} - h_{begin}\right) A \tag{4.1}$$

$$q = \frac{V}{tB} \tag{4.2}$$

With:

A = bottom area of the water collector bin [m^2]
V = wave overtopping volume [m^3]
h_{end} = ending water level in the water collector bin [m]
h_{begin} = beginning water level in the water collector bin [m]
q = discharge over the crest per m^1 width [$m^3/s/m^1$]
t = test duration time [s]
B = width of the wave flume [m]

In Appendix A is all the wave parameters and the calculated overtopping volume and discharge shown for each test.

4.2 Overtopping Discharge

In order to compare the results of overtopping discharge with Tetrapod and Xbloc, the test results are also given in one graph. (See figure 4.1 till figure 4.8)

The overtopping discharge of Xbloc and Tetrapod are mostly in the same order, but usually the Xbloc overtopping is somewhat more. As can be seen in the following figures with freeboard = 0.25m, 0.225m, 0.20m and 0.15m. In all the figures, the wave height is the incident wave height at deep water.

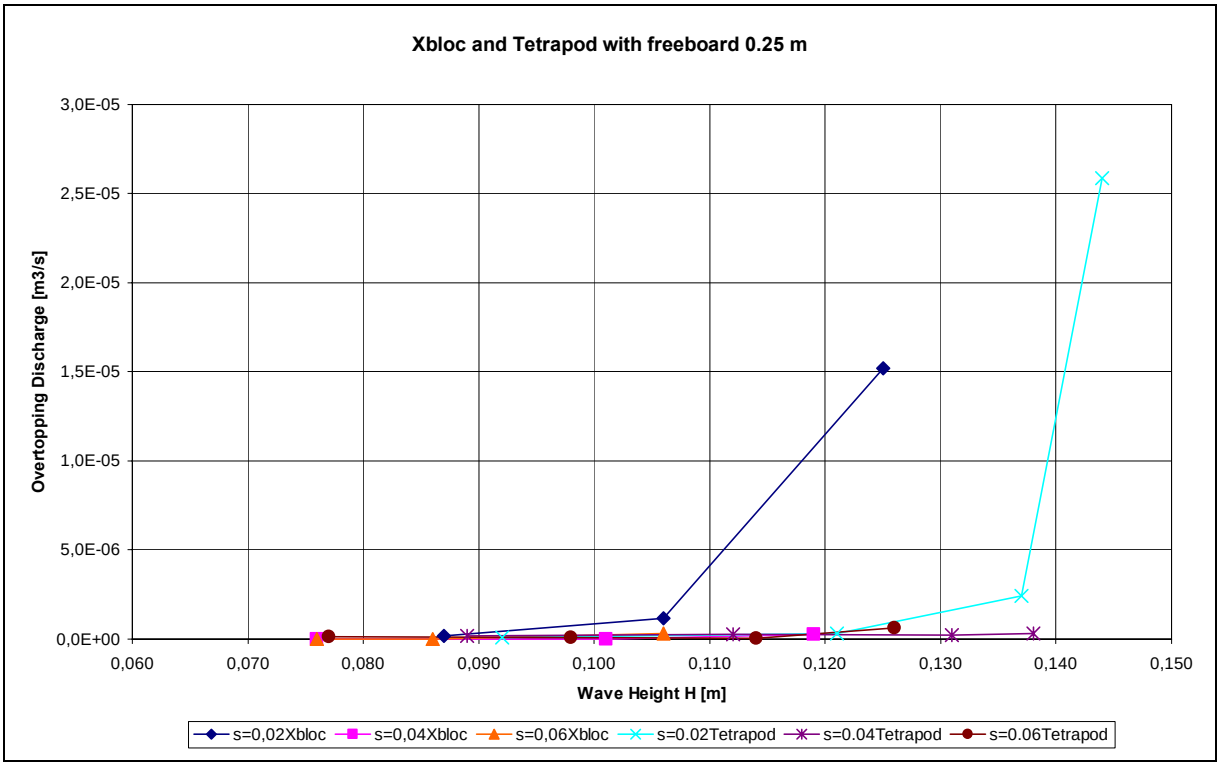

Figure 4.1 Overtopping for Xbloc and Tetrapod with freeboard = 0.25 m. (normal scale)

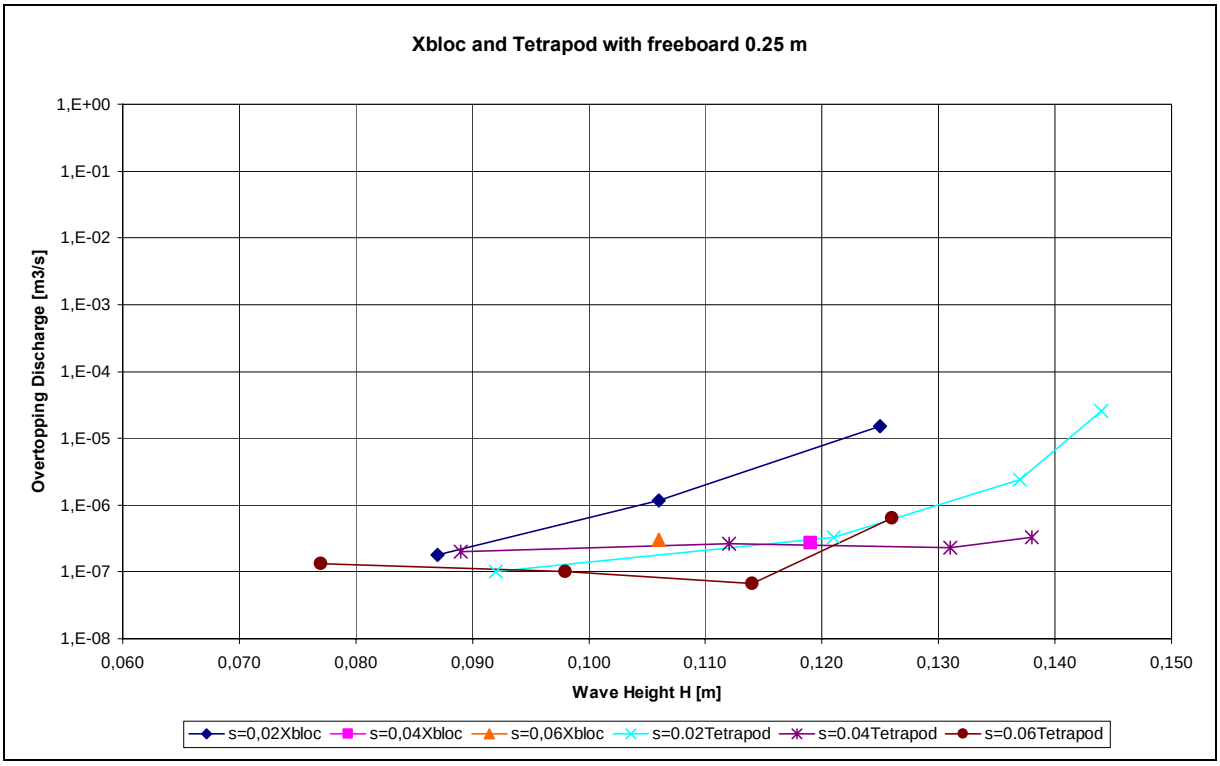

Figure 4.2 Overtopping for Xbloc and Tetrapod with freeboard = 0.25 m. (logarithmic scale)

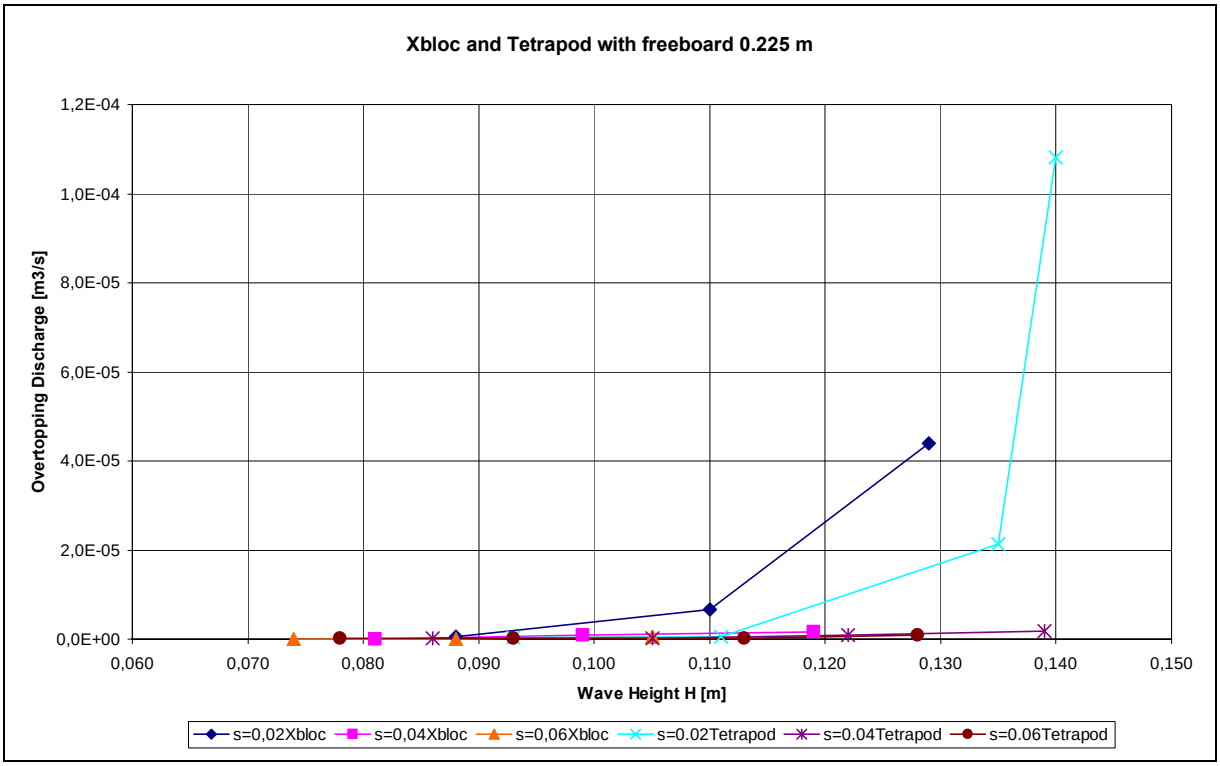

Figure 4.3 Overtopping for Xbloc and Tetrapod with freeboard = 0.225 m. (normal scale)

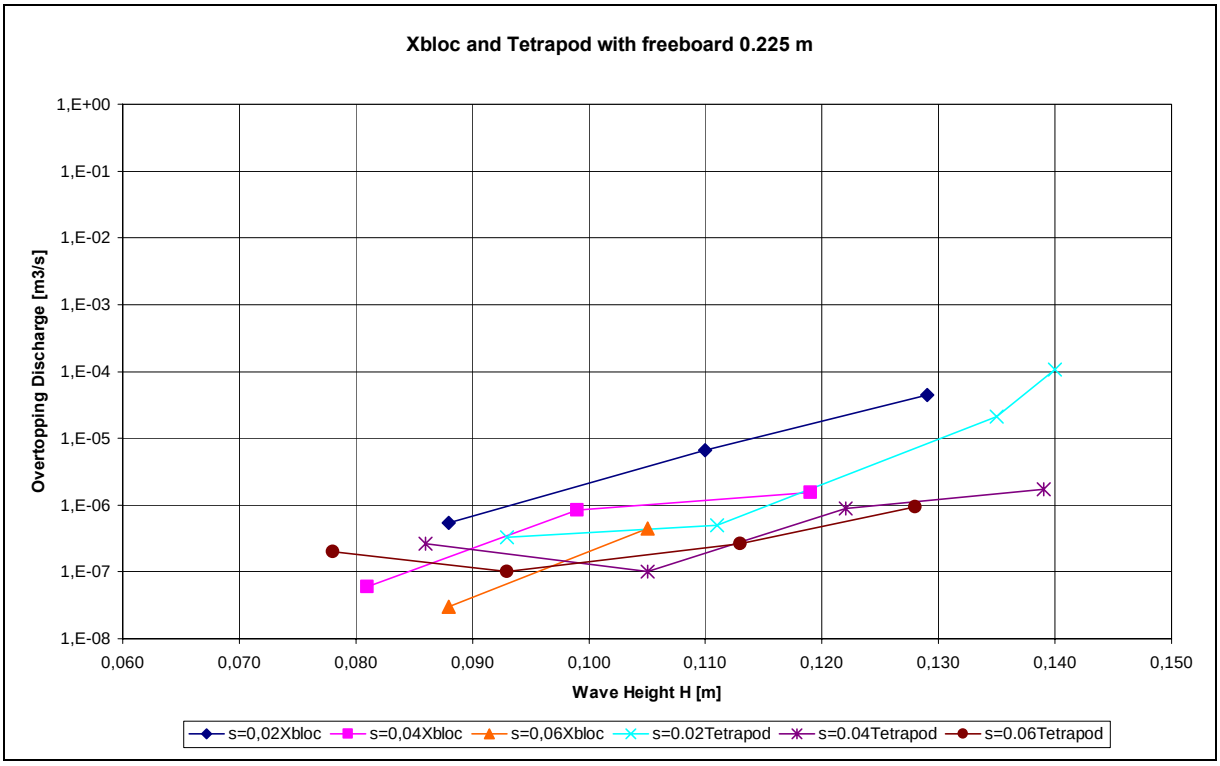

Figure 4.4 Overtopping for Xbloc and Tetrapod with freeboard = 0.225 m. (logarithmic scale)

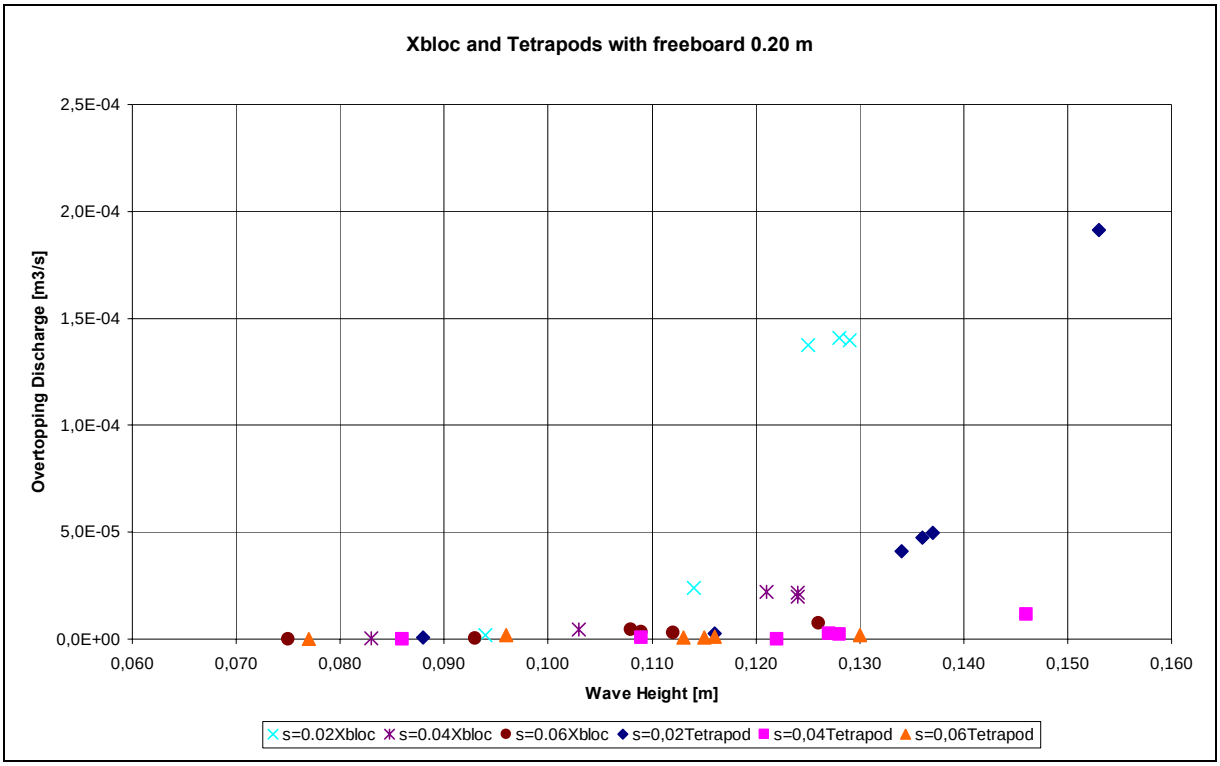

Figure 4.5 Overtopping for Xbloc and Tetrapod with freeboard = 0.20 m. (normal scale)

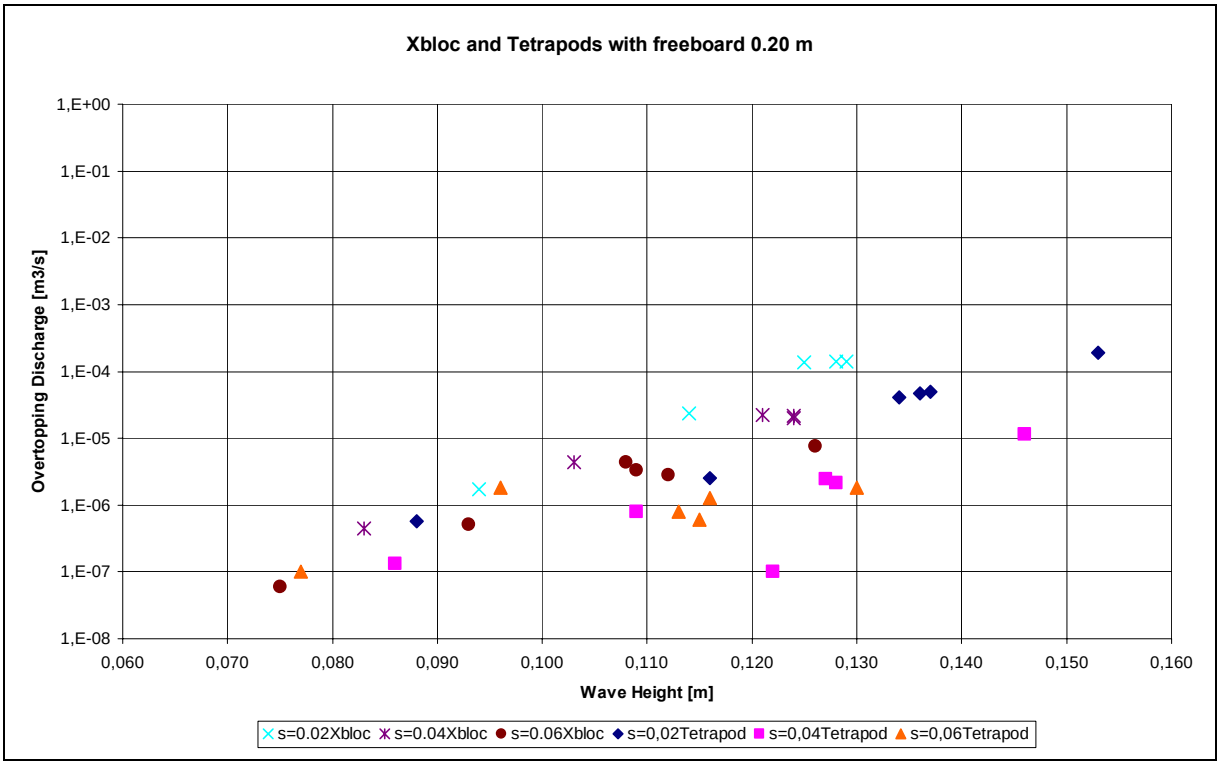

Figure 4.6 Overtopping for Xbloc and Tetrapod with freeboard = 0.20 m. (logarithmic scale)

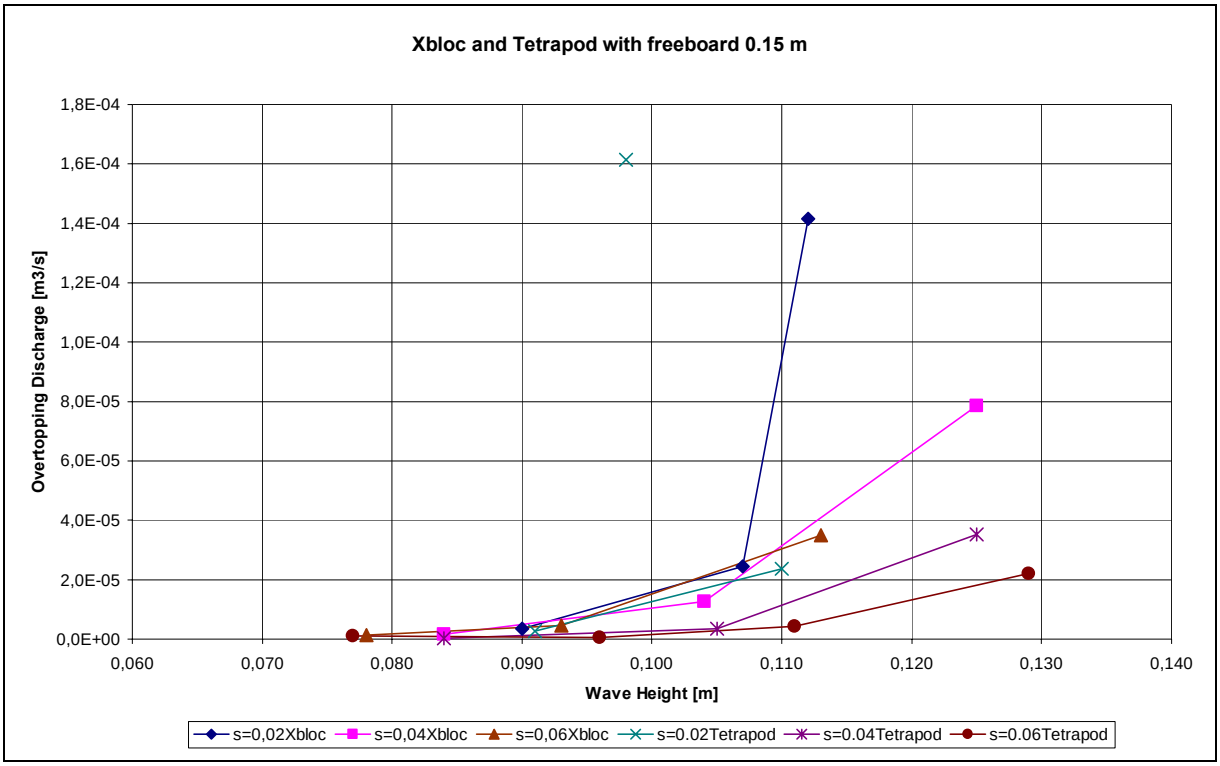

Figure 4.7 Overtopping for Xbloc and Tetrapod with freeboard = 0.15 m. (normal scale)

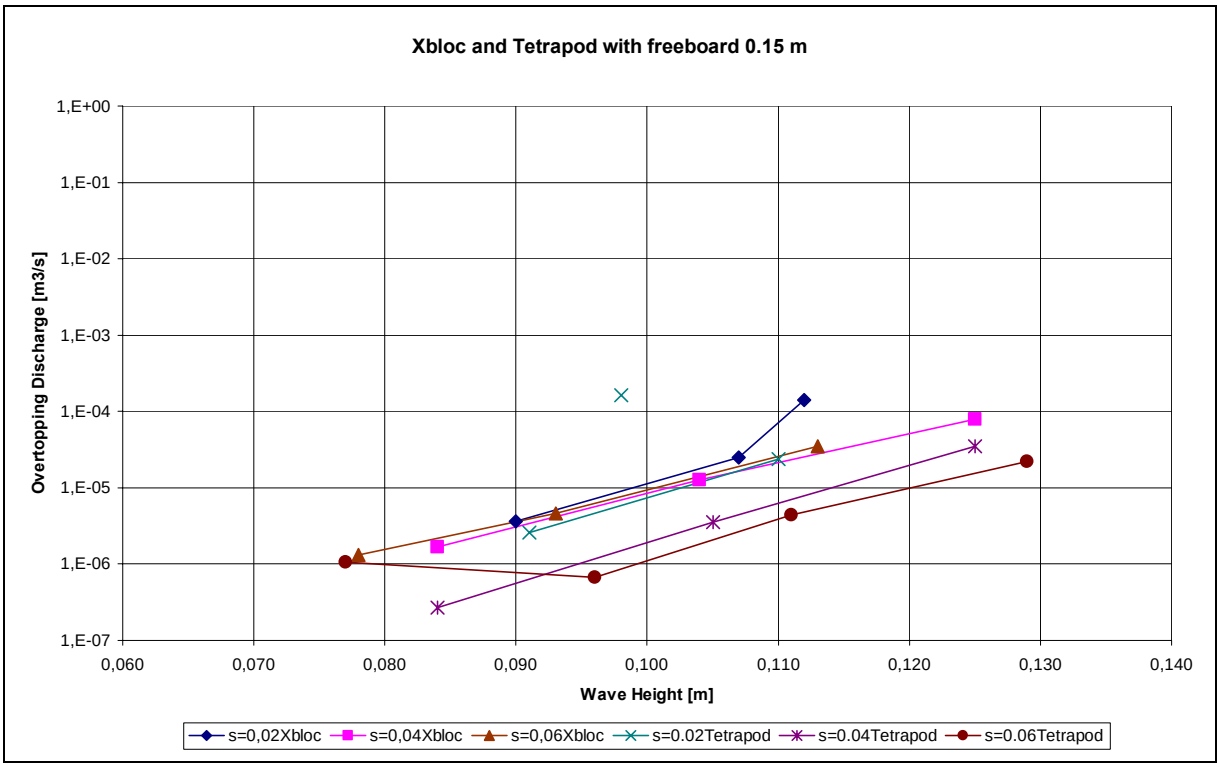

Figure 4.8 Overtopping for Xbloc and Tetrapod with freeboard = 0.15 m. (logarithmic scale)

As shown in figures 4.1 till 4.8, for both Xbloc and Tetrapod, the overtopping discharge increased with the increasing of the wave height.

Note that there is one exceptional point. Which is the case for Tetrapod with freeboard = 0.15 m. As shown in figure 4.7 and figure 4.8. This exceptional point occurred at steepness s = 0.02, at a wave height of 0.098 m. The reason for this exception is not known. An assumption of this exceptional point is that this was caused by a measurement failure.

As shown in the figures 4.1 till 4.8, in all cases, the most overtopping discharge occurs when the wave steepness s = 0.02. This applies for Tetrapod as well as Xbloc.

4.3 Dimensionless Presentation

4.3.1 Reflection Coefficient as Function of Breaker Parameter

In order to compare the Xbloc with Tetrapod, the reflection coefficient of both concrete armour units as function of the breaker parameter were given in one graphic.

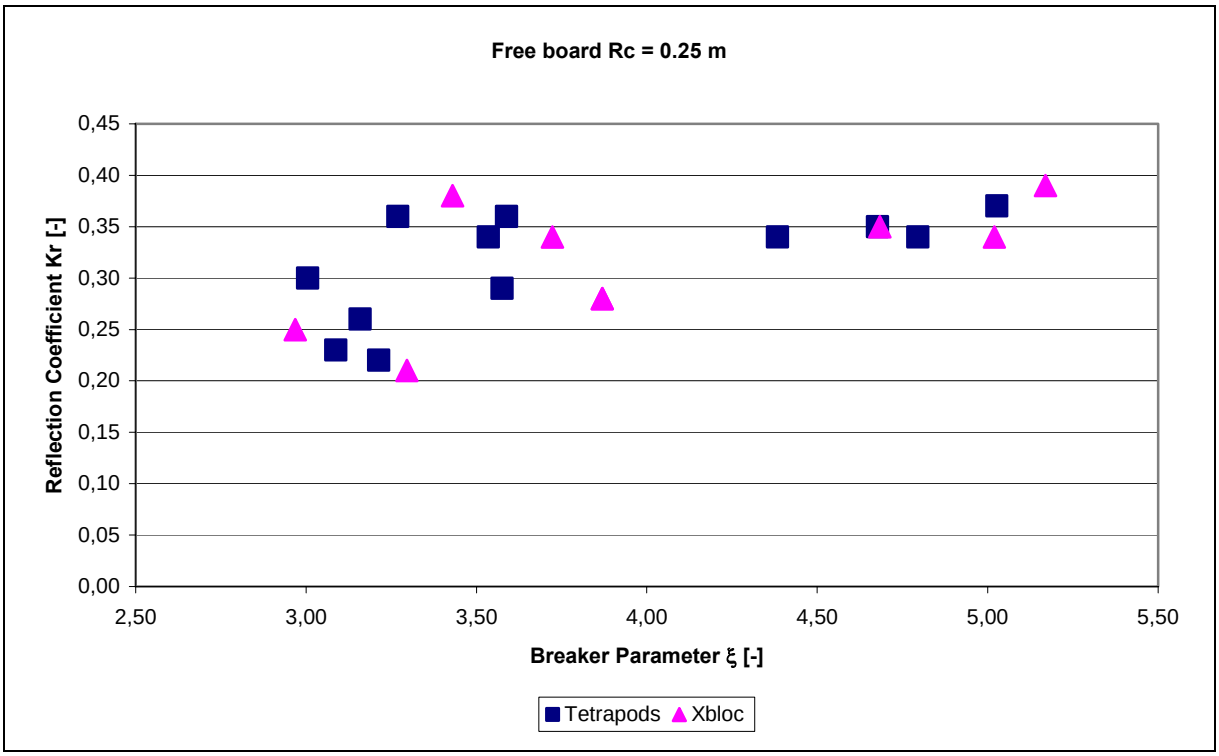

Figure 4.9 Reflection coefficient as function of breaker parameter, R_c = 0.25m.

It was shown in figure 4.9, that the reflection coefficients as function of breaker parameter for both Xbloc as well as Tetrapod are quite in the same order, although the Xbloc model is slightly smaller than the Tetrapod model. (The nominal diameter of the Xbloc model is 3.75 cm, and the nominal diameter of the Tetrapod model is 4.3 cm.)

4.3.2 Wave Overtopping as Function of Breaker Parameter

In order to compare the wave overtopping with different freeboard and wave height, a dimensionless wave overtopping discharge $Q' = \frac{q}{\sqrt{gH_{m0}^3}}$, was introduced and plotted in a graphic on the vertical logarithmic axis, against the breaker parameter ξ_o on the horizontal axis.

As shown in the following two figures.

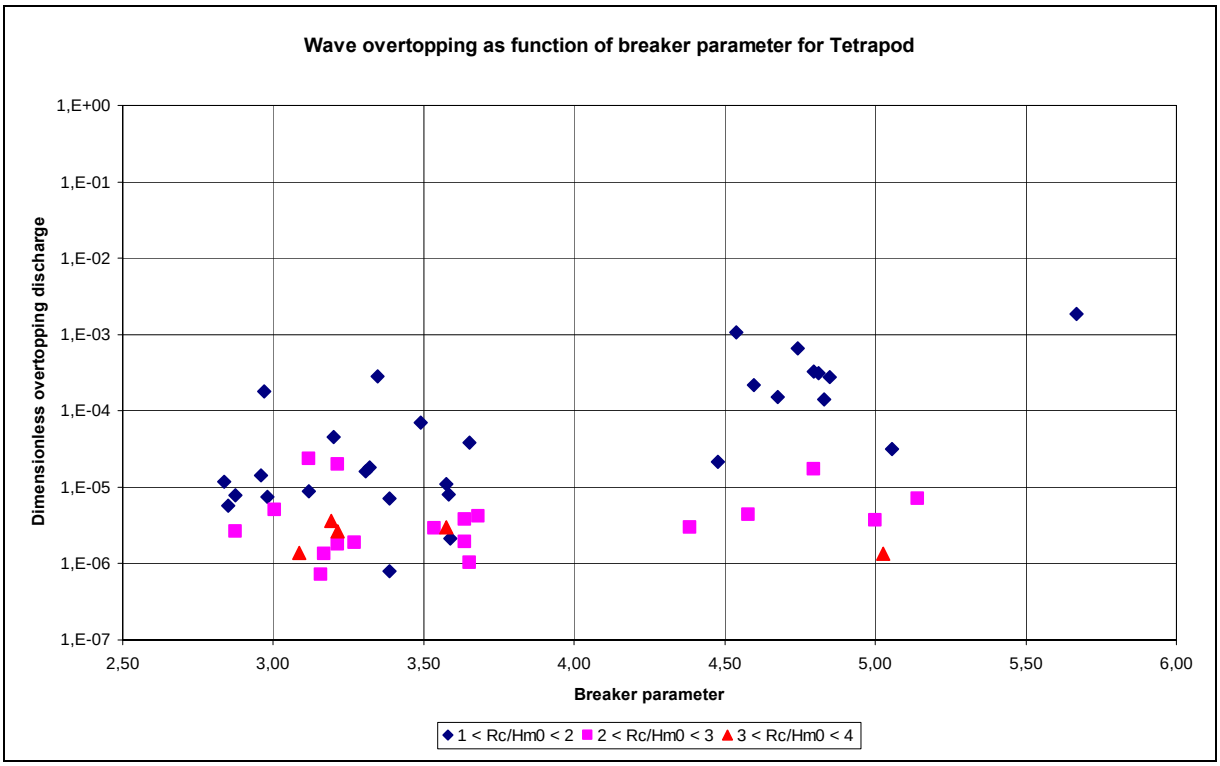

Figure 4.10 Wave overtopping as function of breaker parameter for Tetrapod.

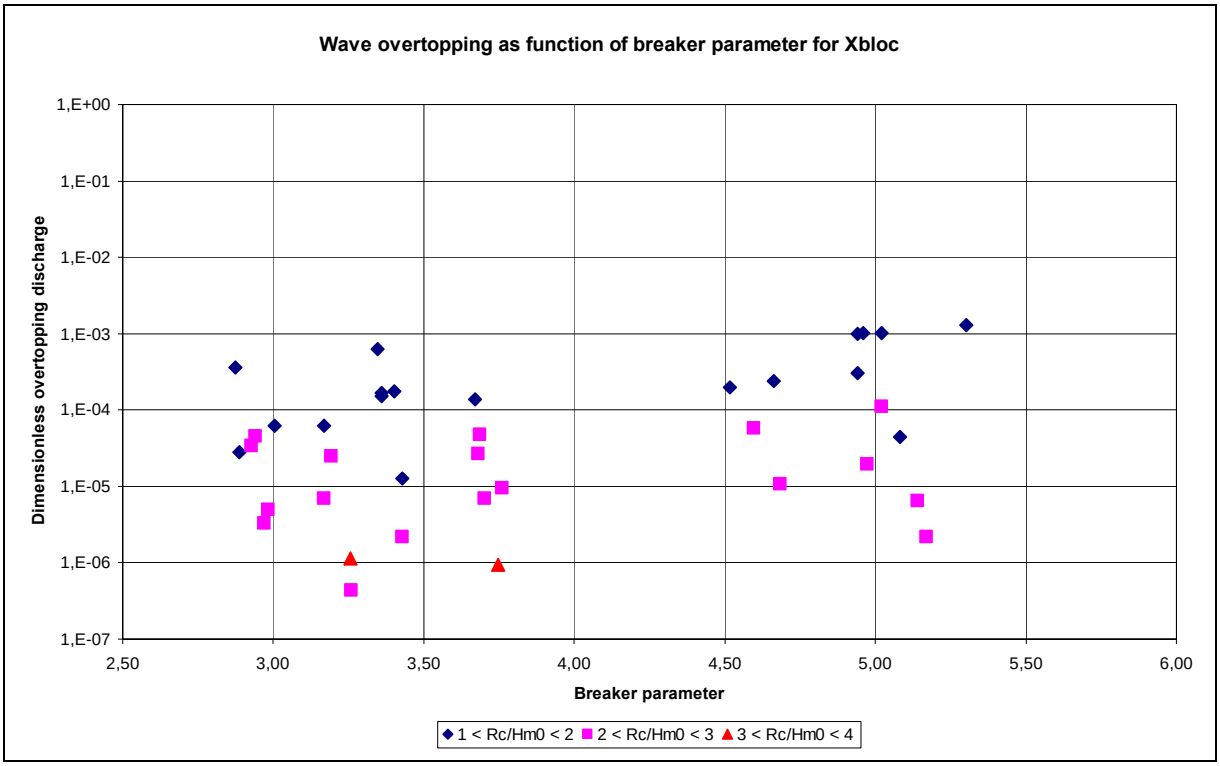

Figure 4.11 Wave overtopping as function of breaker parameter for Xbloc.

Figure 4.10 and figure 4.11 show the test results of the dimensionless overtopping as function of the breaker parameter. In the figures, the values of the dimensionless height R_c/H_{mo} were given as three series. Namely: $1<R_c/H_{mo}<2$; $2<R_c/H_{mo}<3$; $3<R_c/H_{mo}<4$. In order to compare the test results with the known formula of Van Der Meer, the parameters of the tests were calculated with the Van Der Meer formula.

According to the Van Der Meer formula:

$$\frac{q}{\sqrt{gH_{m0}^3}} = \frac{0.067}{\sqrt{\tan\alpha}}\gamma_b\xi_0 \exp\left(-4.75\frac{R_c}{H_{m0}}\frac{1}{\xi_0\gamma_b\gamma_f\gamma_\beta\gamma_v}\right) \qquad (4.3)$$

In this case, the parameters are decided as following:

$\tan\alpha = 1.5$ (given situation at the model test)
$\gamma_b = 1$ (no toe at the breakwater)
ξ_0 = variable according to the data obtained from the test.
R_c/H_{m0} = variable according to the data obtained from the test.
$\gamma_\beta = 1$ (wave attack perpendicular to the breakwater)
$\gamma_v = 1$ (there is no foreland effect)
γ_f = not known for the Tetrapod and Xbloc at this model test (roughness factor).

4.3.3 Determination of roughness factor γ_f

Because γ_f is not known for the Tetrapod and Xbloc in this test, the value of the γ_f should be estimated.
Note that γ_f is defined as the roughness factor. However, γ_f does not only depend on the roughness of the material, it also depends on the porosity of the material. Thus, although γ_f is named as the roughness factor, it is actually a fit-factor.
In the following paragraphs, the value of γ_f = 0.7, 0.5, 0.3 and 0.2 are respectively calculated according to the Van Der Meer formula. The calculated values are compared with the test results.

γ_f = 0.7

With an estimation of γ_f = 0.7, the wave overtopping as function of breaker parameter obtained from the formula (2.12) was shown in the following figures.

In order to compare the wave overtopping as function of breaker parameter according to Van Der Meer with the test results, in the following two figures, the test results were shown in the same graphic with the Van Der Meer lines.

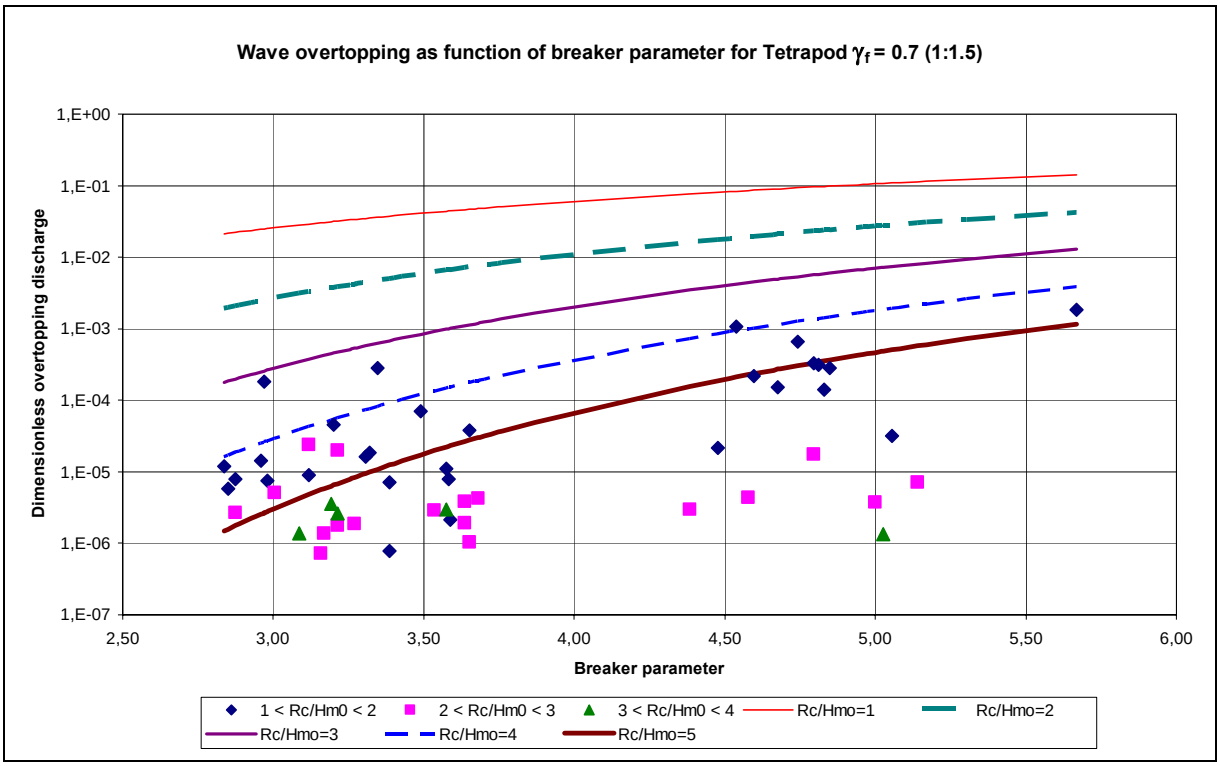

Figure 4.12 Wave overtopping as function of breaker parameter for Tetrapod, compare with Van Der Meer. (1:1.15)

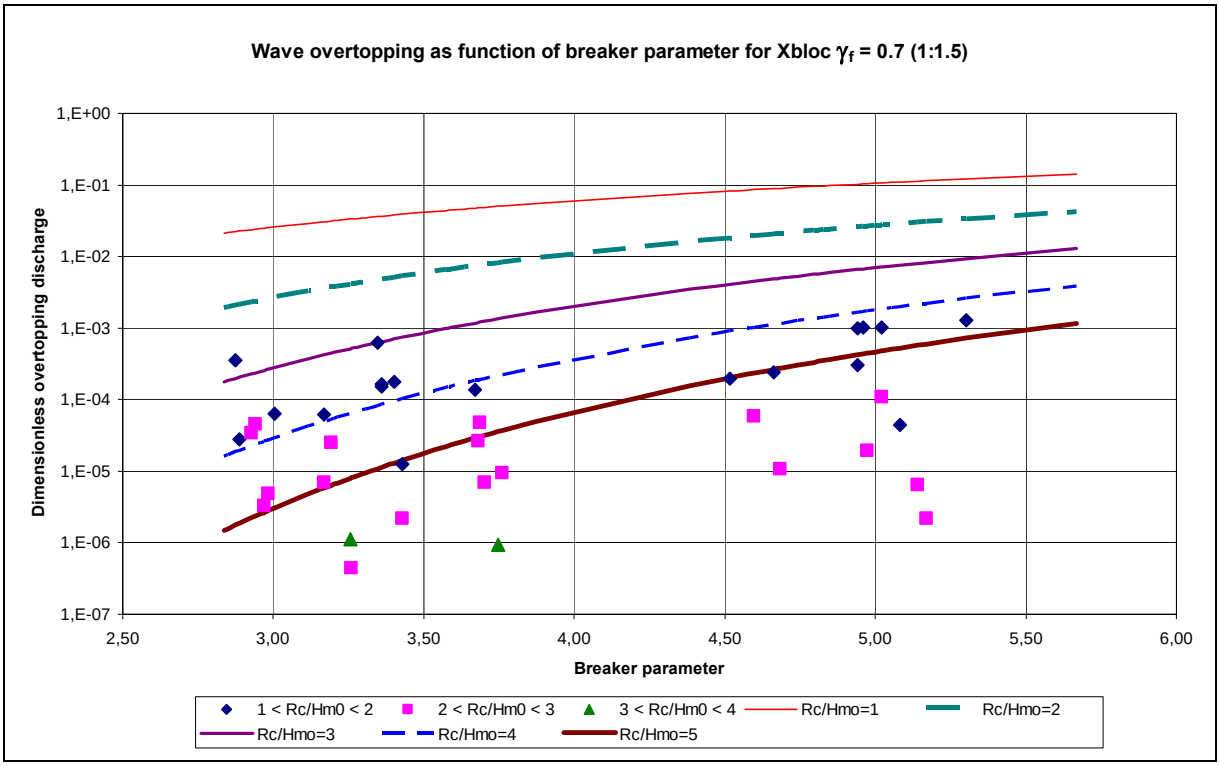

Figure 4.13 Wave overtopping as function of breaker parameter for Xbloc, compare with Van Der Meer. (1:1.15)

As was shown in Figure 4.12 and Figure 4.13, the estimation of $\gamma_f = 0.7$ does not give a good fit for comparing the test results with the lines calculated according to Van Der Meer formulas.

$\gamma_f = 0.5$

With an estimation of $\gamma_f = 0.5$, is the graphic according to Van Der Meer different as shown in the following figures.

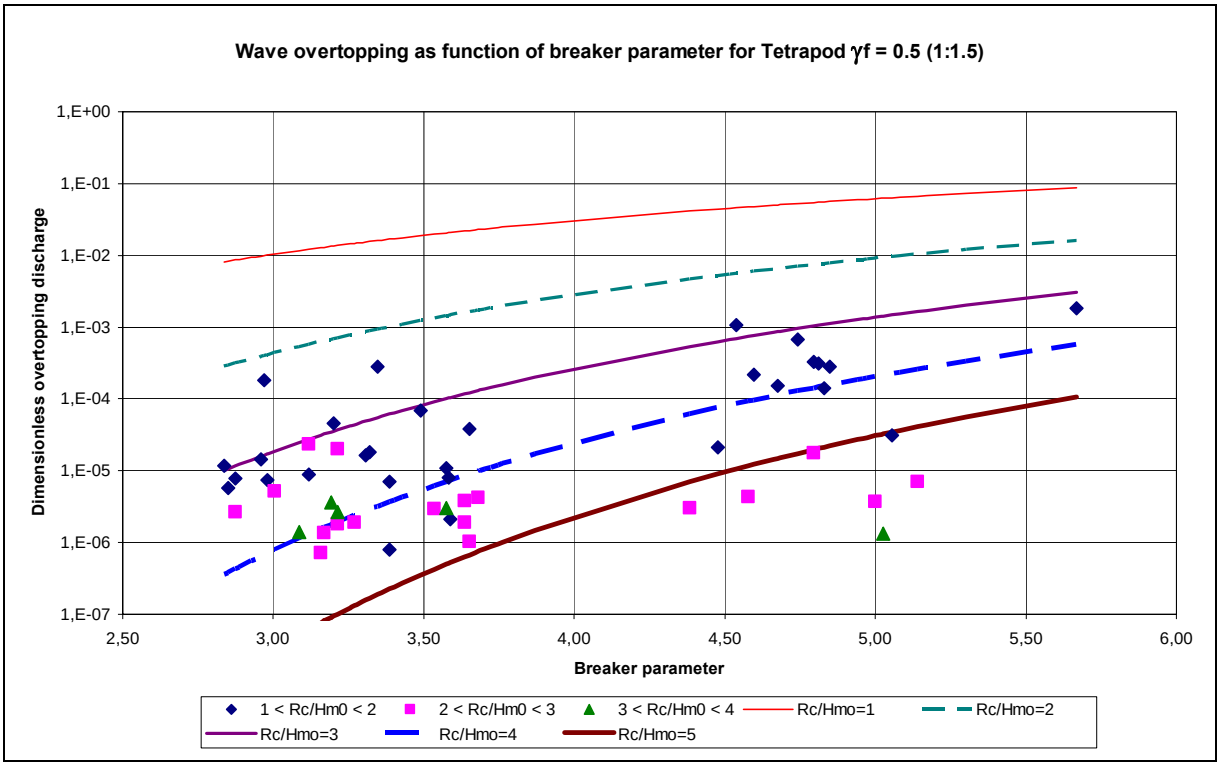

Figure 4.14 Wave overtopping as function of breaker parameter for Tetrapod, compare with Van Der Meer. (1:1.15)

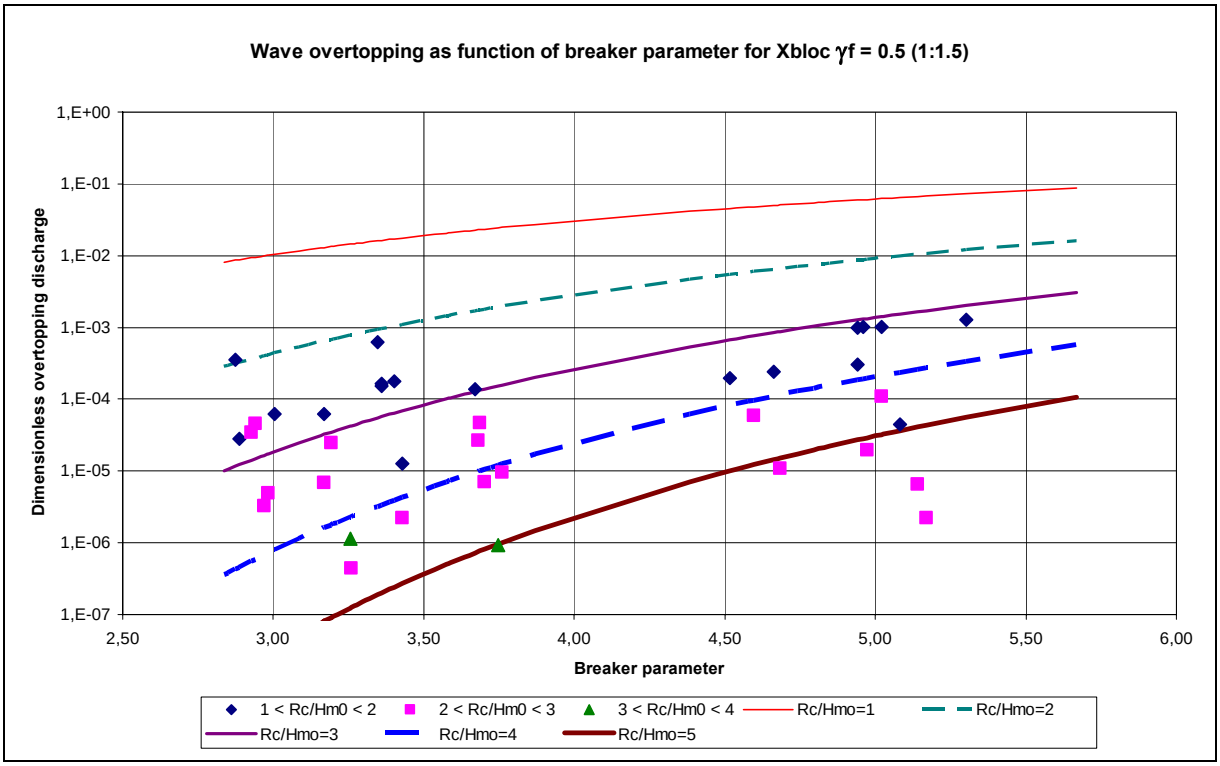

Figure 4.15 Wave overtopping as function of breaker parameter for Xbloc, compare with Van Der Meer. (1:1.15)

As was shown in Figure 4.14 and Figure 4.15, the estimation of $\gamma_f = 0.5$, now gives a better fit for comparing the test results with the lines calculated according to the Van Der Meer formulas.

$\gamma_f = 0.3$

Now estimate $\gamma_f = 0.3$. The graphic according to the Van Der Meer formula is shown in the following figures.

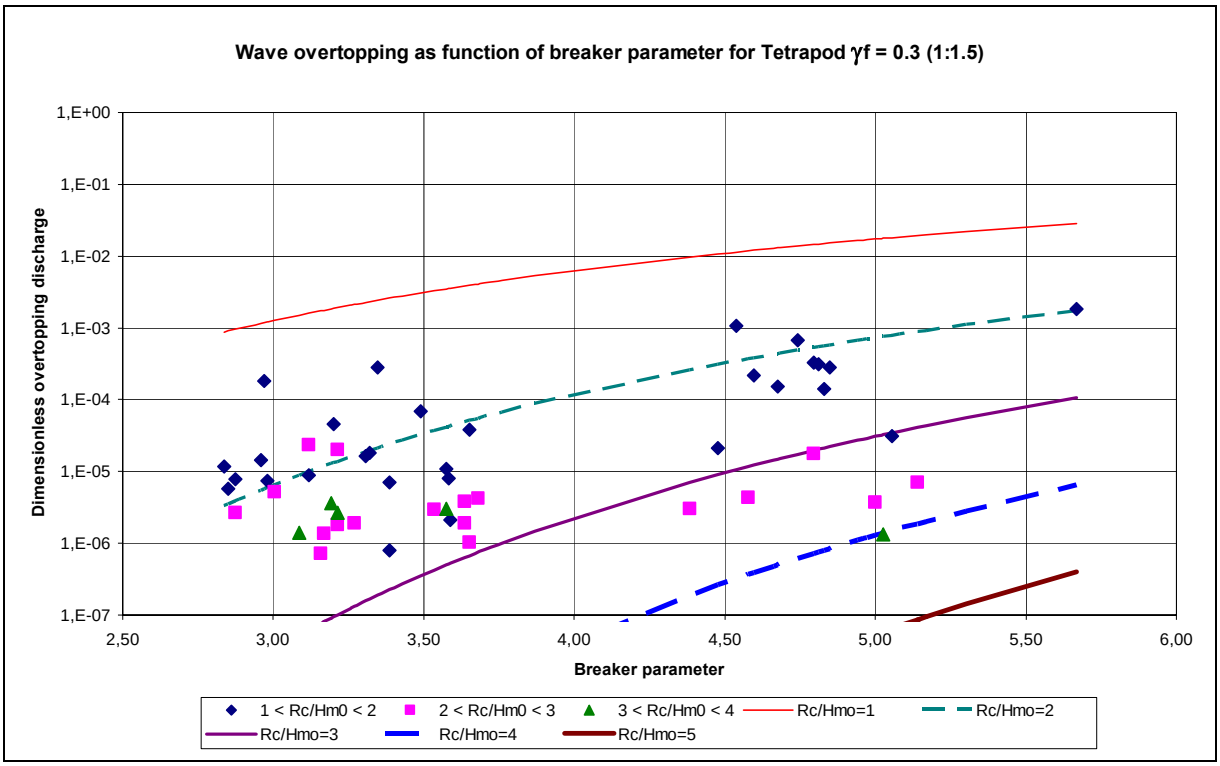

Figure 4.16 Wave overtopping as function of breaker parameter for Tetrapod, compare with Van Der Meer. (1:1.15)

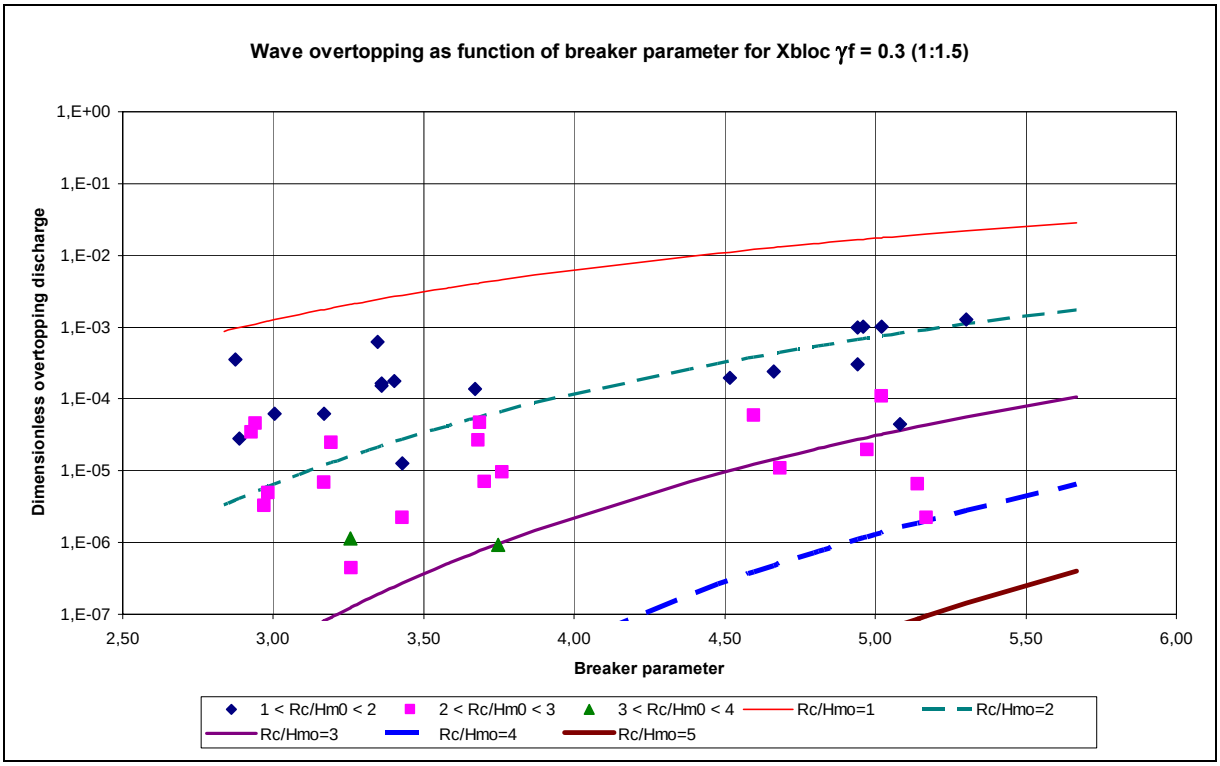

Figure 4.17 Wave overtopping as function of breaker parameter for Xbloc, compare with Van Der Meer. (1:1.15)

As were shown in Figure 4.19 and Figure 4.20, an estimation of $\gamma_f = 0.3$ gives a good fit for comparing the test results with the lines calculated according to the Van Der Meer formulas.

$\gamma_f = 0.2$

Now estimate $\gamma_f = 0.2$. The graphic according to the Van Der Meer formula is shown in the following figures.

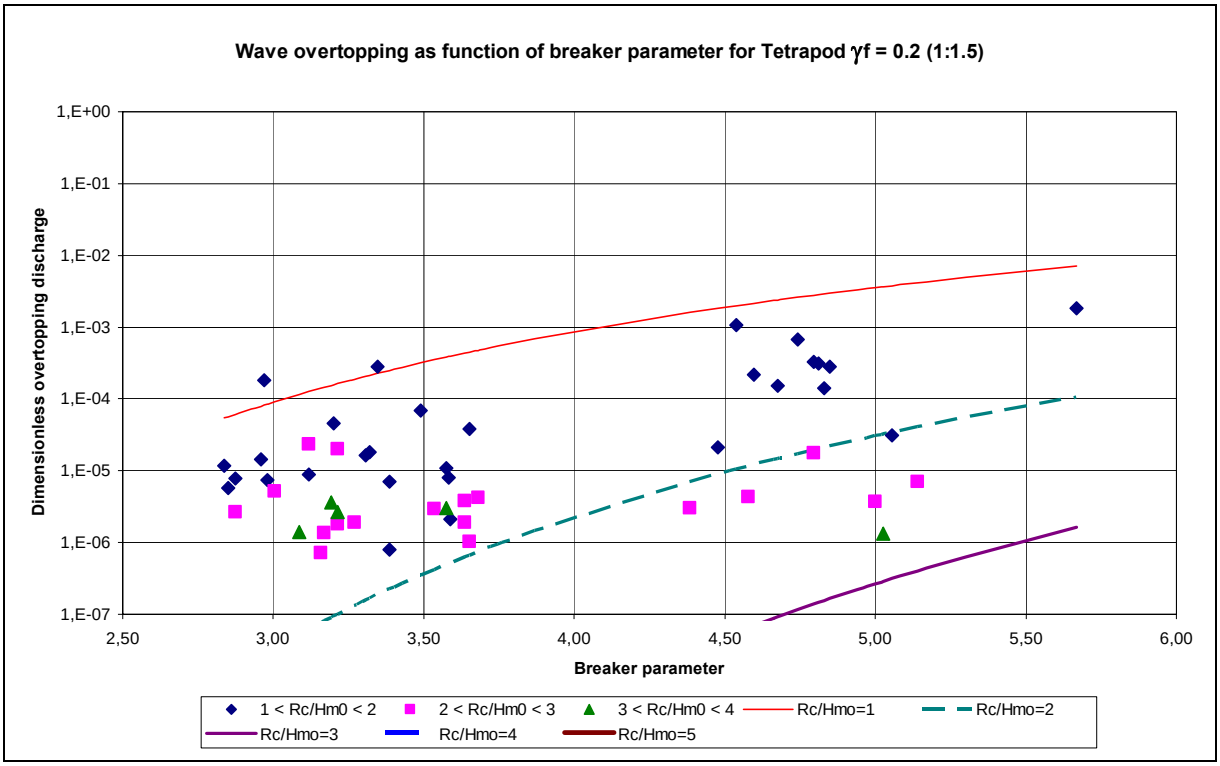

Figure 4.18 Wave overtopping as function of breaker parameter for Tetrapod, compare with Van Der Meer. (1:1.15)

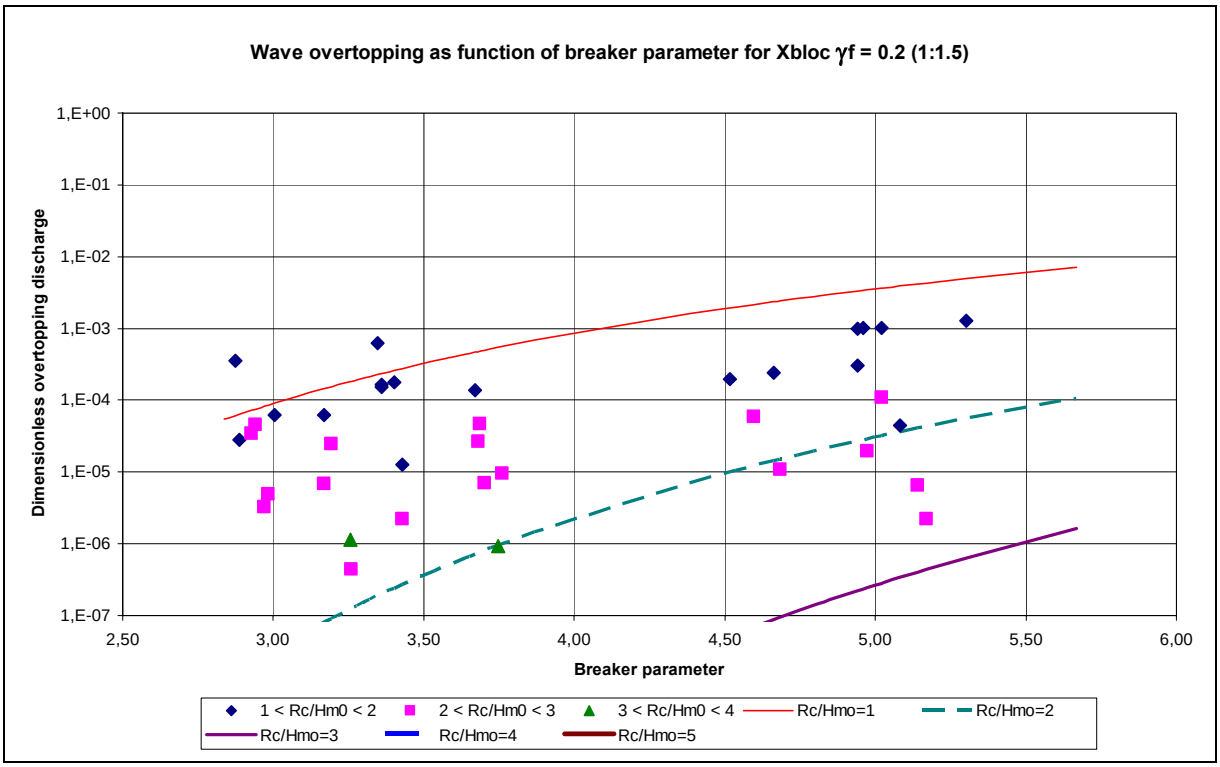

Figure 4.19 Wave overtopping as function of breaker parameter for Xbloc, compare with Van Der Meer. (1:1.15)

As shown in figure 4.18 and figure 4.19, an estimation of $\gamma_f = 0.2$ does not gives a good fit for comparing the test results with the lines calculated according to the Van Der Meer formulas.

Thus, an estimation of $\gamma_f = 0.3$ gives the best fit for comparing the test results with the lines calculated according to the Van Der Meer formulas.

According to the literature, the lowest γ_f for broken stones is 0.55. But the roughness factor γ_f that was determined in this case is 0.3, thus lower than the lowest roughness factor in standard cases. As was explained earlier in the chapter, the roughness factor depends not only on the roughness of the material, but also on the porosity of the material. For this model test, the single layer Tetrapod and Xbloc units have a high porosity than the normal riprap structure. This has influence over the roughness factor.

4.3.4 Dimensionless Wave Overtopping

In order to compare the wave overtopping discharge versus crest height for all the tests with both Tetrapods and Xbloc, a dimensionless overtopping discharge and a dimensionless crest height were introduced.

$$Q^* = \frac{q}{\sqrt{gH_{m0}^3}} \tag{4.4a}$$

$$h^* = \frac{R_c}{H_{m0}} \tag{4.4b}$$

With:

Q^* = dimensionless overtopping discharge [-]
h^* = dimensionless crest height [-]
H_{m0} = significant wave height at toe [m]
g = gravitational acceleration [m/s^2]
q = wave overtopping volume per m^1 crest length [$m^3/s/m^1$]
R_c = free crest height above still water line [m]

In the tests, the parameters are decided as following:

$\tan \alpha = 1.5$ (given situation at the model test)
$\gamma_b = 1$ (no toe at the breakwater)
q = variable according to the data obtained from the test.
ξ_0 = variable according to the data obtained from the test.
s_0 = variable according to the data obtained from the test.
R_c/H_{m0} = variable according to the data obtained from the test.
$\gamma_\beta = 1$ (wave attack perpendicular to the breakwater)

$\gamma_v = 1$ (there is no foreland effect)
$\gamma_f = 0.3$ (as was estimated)

The test results of wave overtopping were given in the following figure.

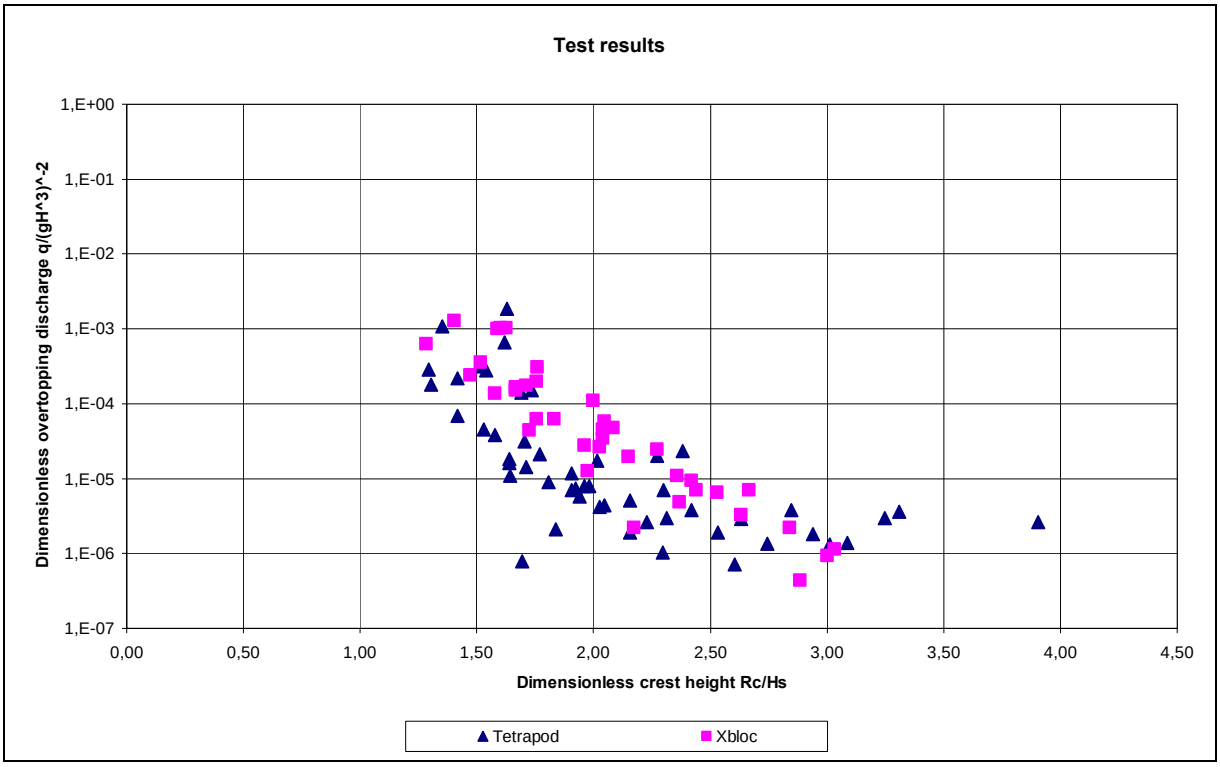

Figure 4.20 Wave overtopping data for comparing Tetrapod and Xbloc, breaking waves

It was shown in figure 4.20, that the dimensionless discharge of Tetrapod and Xbloc are almost in the same domain. Xbloc has a slightly higher discharge than the Tetrapods.

In the following paragraph, the test results were compared with the known wave overtopping formula of Van Der Meer, and the known formula for Xbloc.

The test results of the Tetrapod in the dimensionless overtopping discharge versus dimensionless crest height graphic (figure 4.19) show a turning point at the dimensionless crest height $R_c/H_s = 2.94$. When the dimensionless crest height is lower than 2.94, the dimensionless overtopping discharge decreases with the increase of the dimensionless crest height. When the dimensionless crest height is higher than 2.94, the dimensionless overtopping discharge does not show any decrease with the increase of the dimensionless crest height, but stays almost constant.

4.3.5 Comparing Test Results with Known formulas

4.3.5.1 Van Der Meer Formula

The design form of the Van Der Meer Formula is:

$$Q^*_{VDM} = \frac{q}{\sqrt{gH_{m0}^3}} = \frac{0.067}{\sqrt{\tan\alpha}}\gamma_b\xi_o \exp\left(-4.75\frac{R_c}{H_{m0}}\frac{1}{\xi_o\gamma_b\gamma_f\gamma_\beta\gamma_v}\right) \quad (4.5)$$

When fill the values of the R_c/H_{m0} from the test results into the Van Der Meer formula (4.5), Q^*_{VDM} can be determined.

In this case, the parameters are decided as following:

$\tan\alpha = 1.5$ (given situation at the model test)
$\gamma_b = 1$ (no toe at the breakwater)
ξ_0 = variable according to the data obtained from the test.
s_0 = variable according to the data obtained from the test.
R_c/H_{m0} = variable according to the data obtained from the test.
$\gamma_\beta = 1$ (wave attack perpendicular to the breakwater)
$\gamma_v = 1$ (there is no foreland effect)
$\gamma_f = 0.3$ (as was estimated)

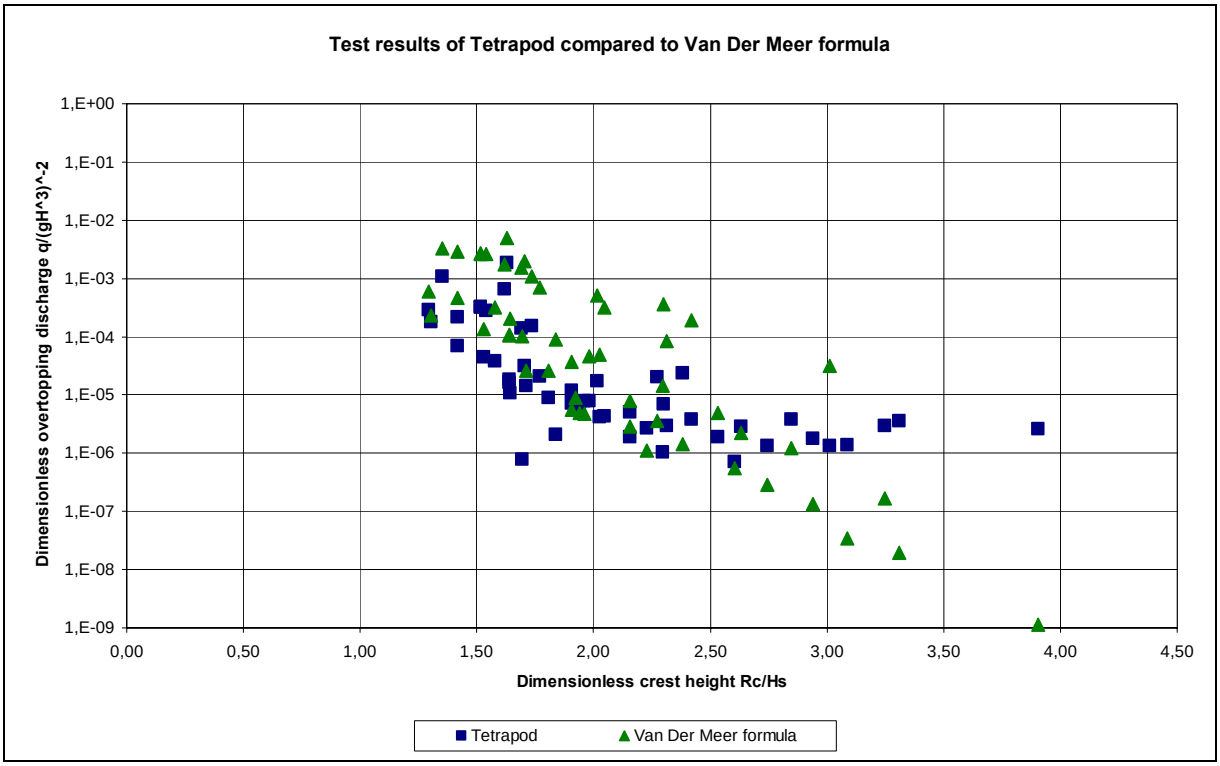

Figure 4.21 Test results of Tetrapod compared to the Van Der Meer formula.

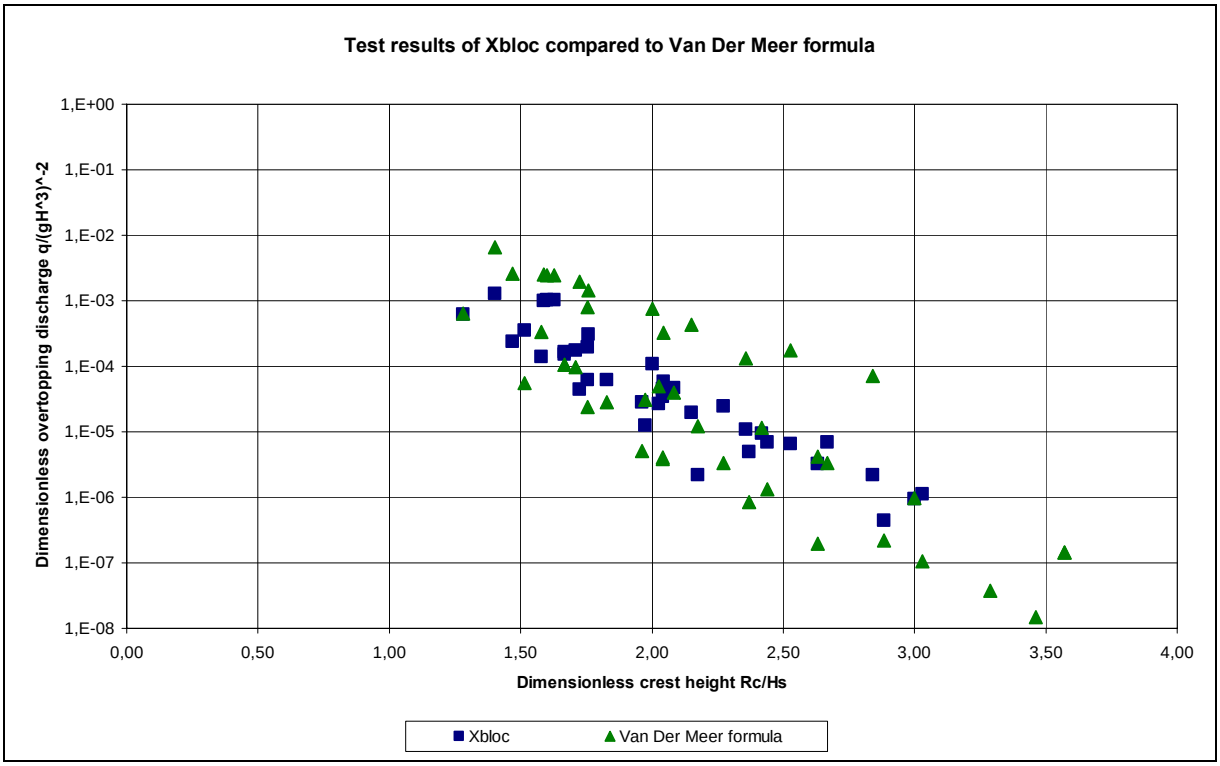

Figure 4.22 Test results of Xbloc compared to the Van Der Meer formula.

It was shown in Figure 4.21 and Figure 4.22 that the Van Der Meer formula gives a good estimation of the test results. It is also to see, that the Van Der Meer formula does not give a

perfect match for the test results. Especially for Tetrapod, with higher value of the dimensionless wave height, the underrating is large.

In the following figure, the test results versus the results calculated according to the Van Der Meer formula were given in one graph.

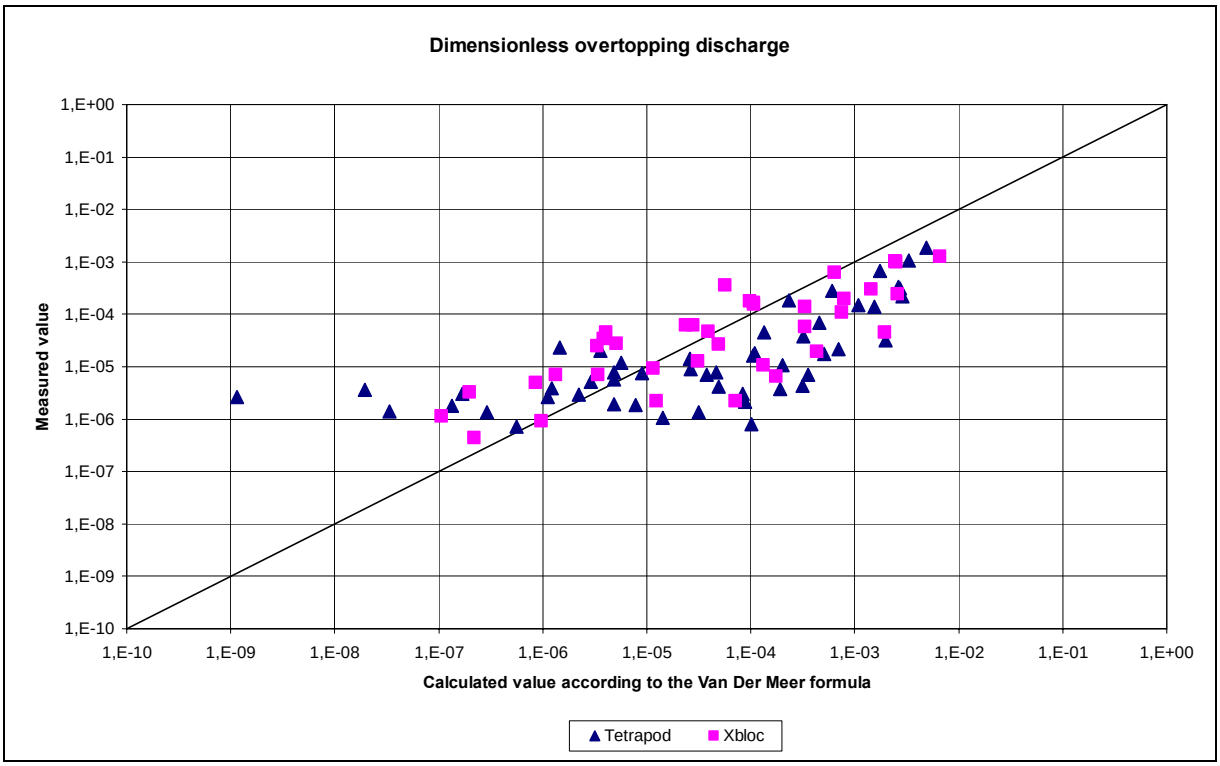

Figure 4.23 Test results compare to Van Der Meer formula.

As shown in figure 4.23, compared to the Van Der Meer formula the test results are lower than expected based on the formula. This means that the Van Der Meer formula gives a slight overestimation of the test results.

4.3.5.2 Xbloc Overtopping Formula

The Xbloc overtopping formula according to KLABBERS (2003) is:

$$Q = (1/100)\, U_r \exp(-3.58\, R) \qquad (4.6)$$

With:

$$Q = \frac{q}{\sqrt{gH_s^3}}$$

$$R = \frac{R_c}{H_s}$$

$$U_r = \frac{H_s * L_t^2}{d^3}$$

Filling in into (4.6) gives:

$$\frac{q}{\sqrt{gH_{mo}^3}} = \frac{1}{100}\frac{H_s * L_t^2}{d^3} * \exp\left(-3.58\frac{R_c}{H_s}\right) \qquad (4.7)$$

When filling in the values of the test results into (4.7), the $Q^*_{Klabbers}$ can be found.

In order to evaluate the Xbloc overtopping formula, not only the test results of Xbloc, but also that of Tetrapod were compared to the Xbloc formula. The results were shown in the following two graphs.

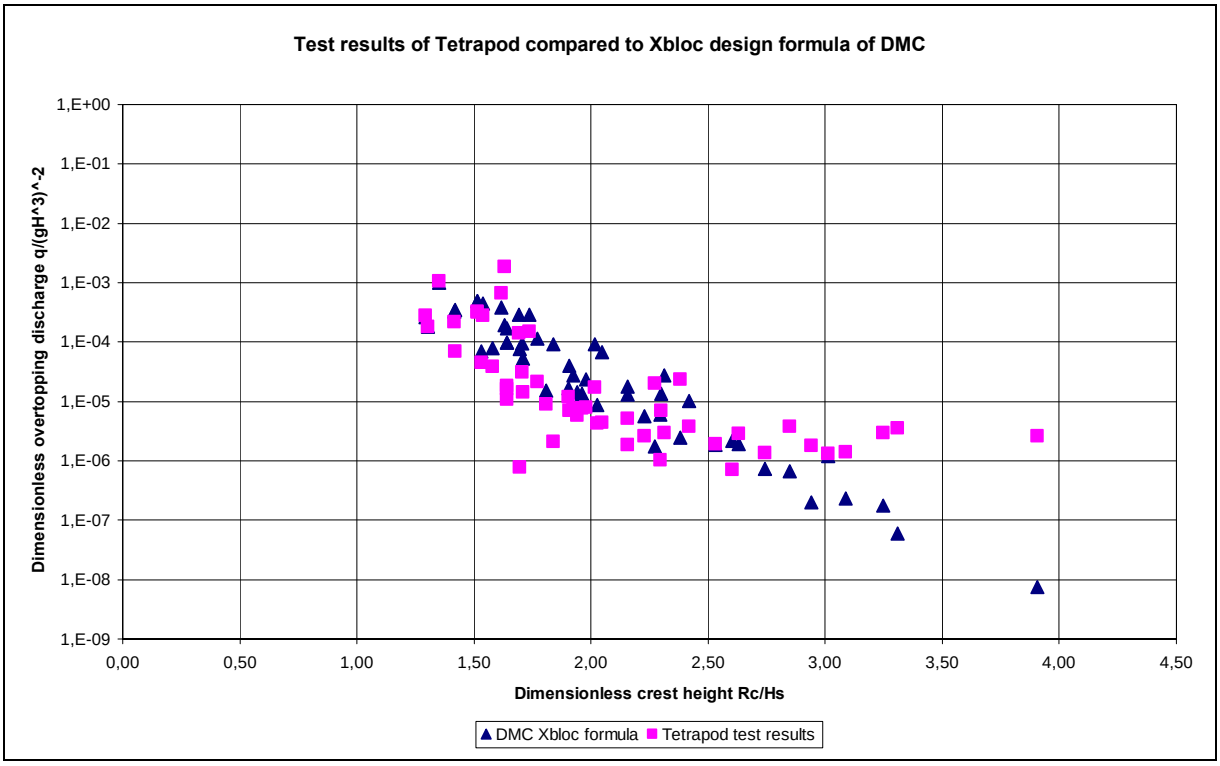

Figure 4.24 Test results compare to the Xbloc overtopping formula.

As can be seen in the above figure 4.24, the Xbloc overtopping formula also gives a good estimation of the Tetrapod test results for the dimensionless crest height Rc/Hs < 2.50.

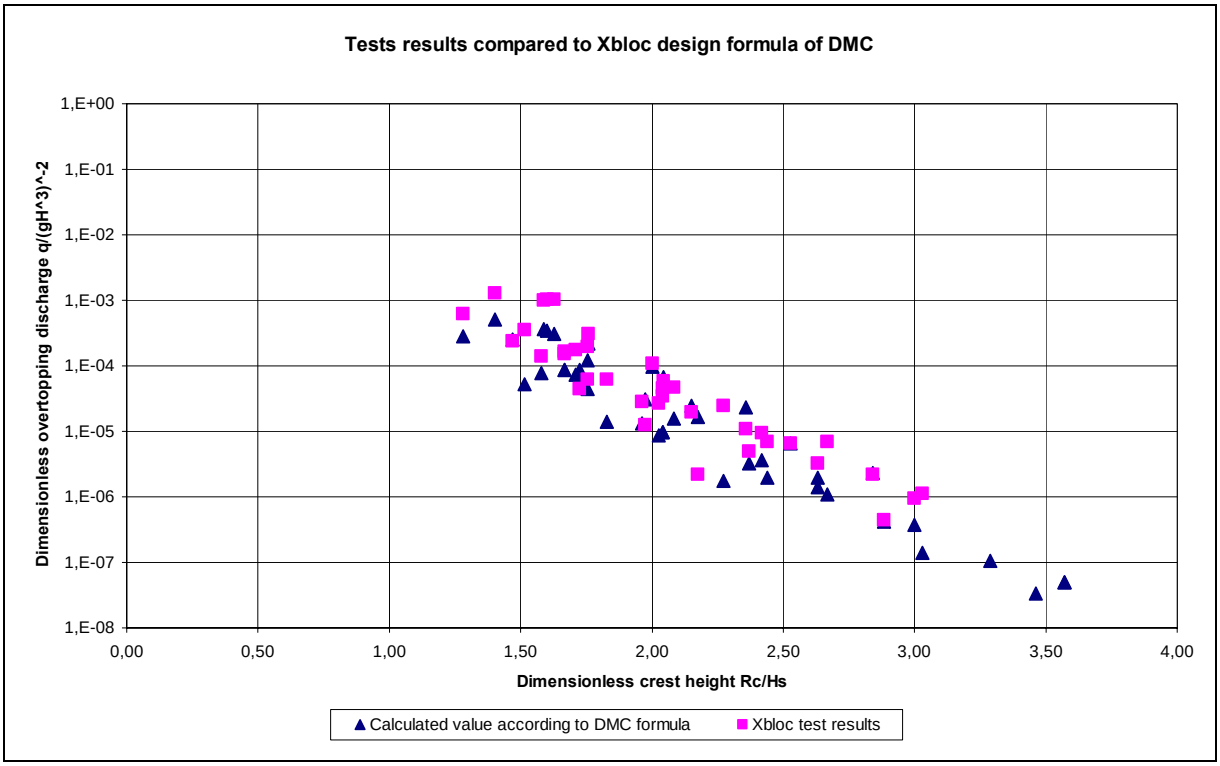

Figure 4.25 Test results compare to the Xbloc overtopping formula.

As was shown in figure 4.25, values of the dimensionless overtopping discharge obtained from the Xbloc overtopping formula have a good match with the test results. This means that for estimation of wave overtopping on the Xbloc armour units, the Xbloc overtopping formula is a better fit than the Van Der Meer formula.

In the following figure, the test results of Tetrapod versus the results calculated according to the Xbloc overtopping formula were given in one graphic.

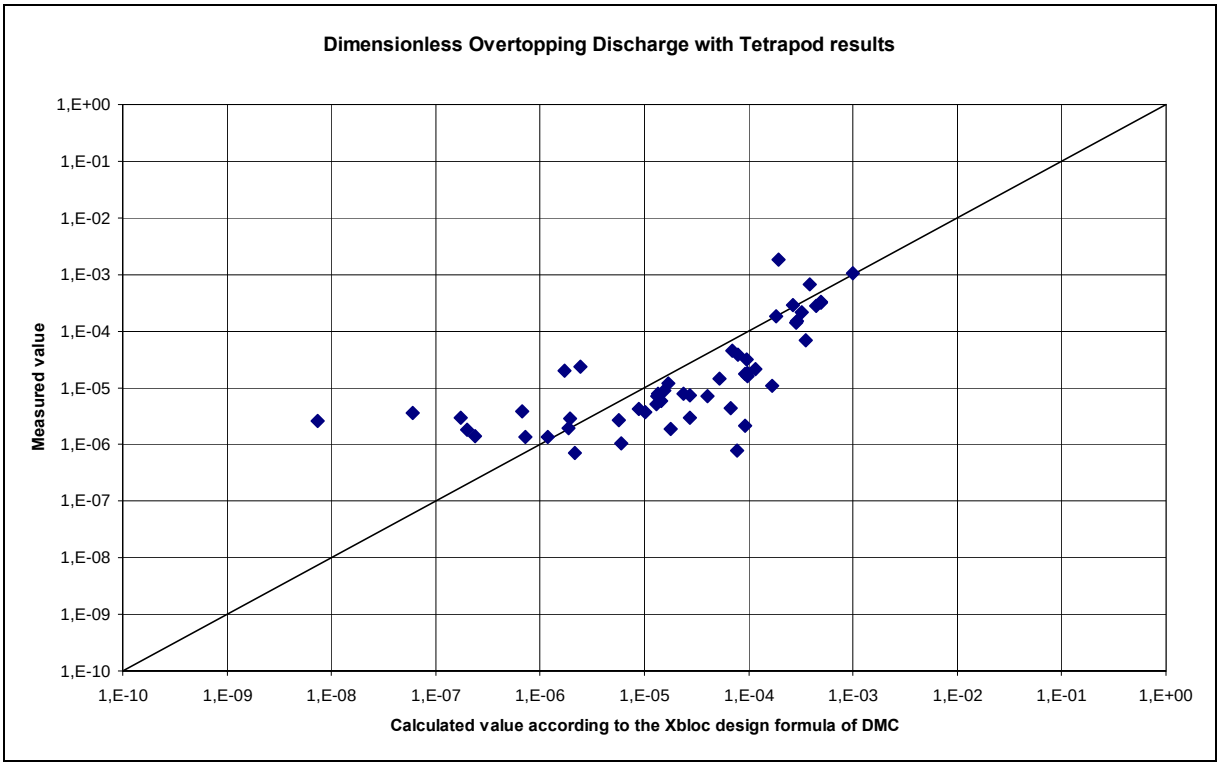

Figure 4.26 Test results compare to the Xbloc overtopping formula.

The above figure 4.26 shows that compared to the Xbloc overtopping formula, the test results of Tetrapod shows a wider spreading.

In the following figure, the test results of Xbloc versus the results calculated according to the Xbloc overtopping formula were given in one graphic.

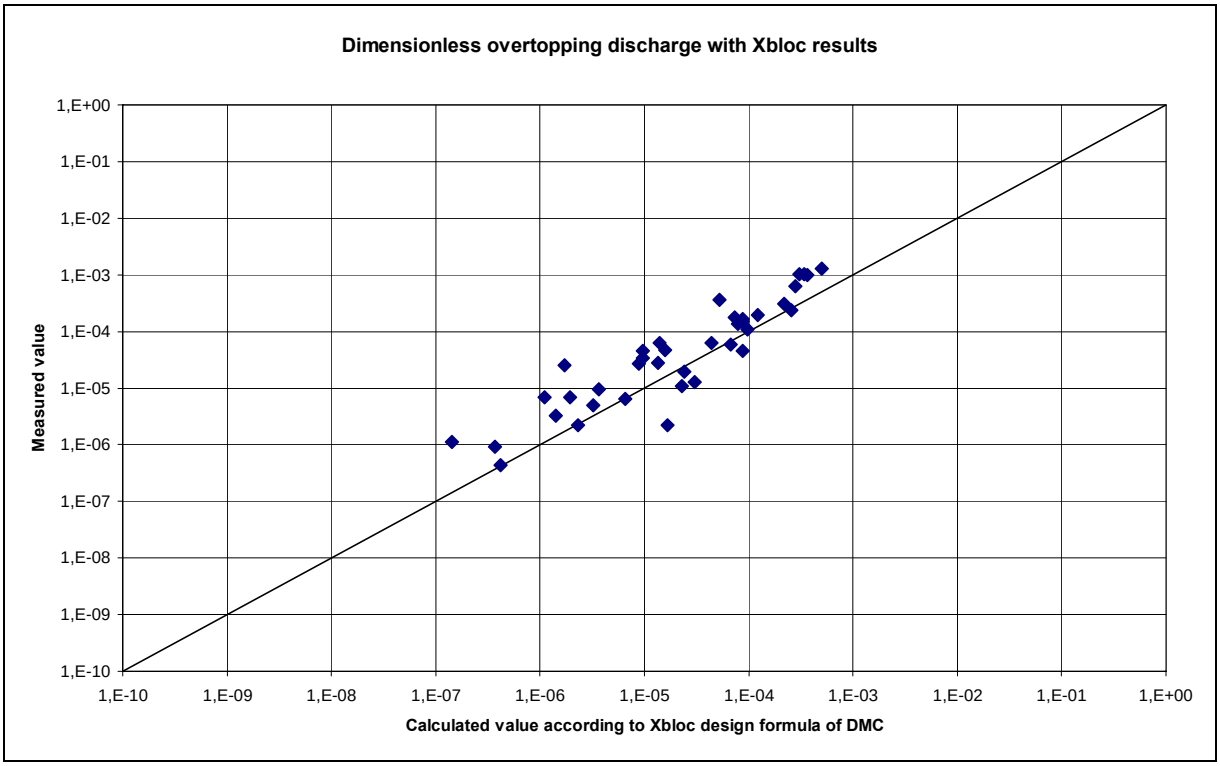

Figure 4.27 Test results compare to the Xbloc overtopping formula.

Figure 4.27 also shows that compare to the Xbloc overtopping formula, the test results gives a good match. This means that the Xbloc overtopping formula gives a correct estimation of the test results.

Note that in the test series, the freeboard Rc was defined as the distance between the still water line and the bottom of the Xbloc units. While in the WL tests of Klabbers (2003) Rc was defined as the distance between the still water line and the top of the Xbloc units. This difference in the definition of the freeboard does not cause much difference in the dimensionless overtopping discharge, as can be seen in Figure 4.27.

In the following figure is the test results of both Tetrapod and Xbloc compared to the Xbloc formula.

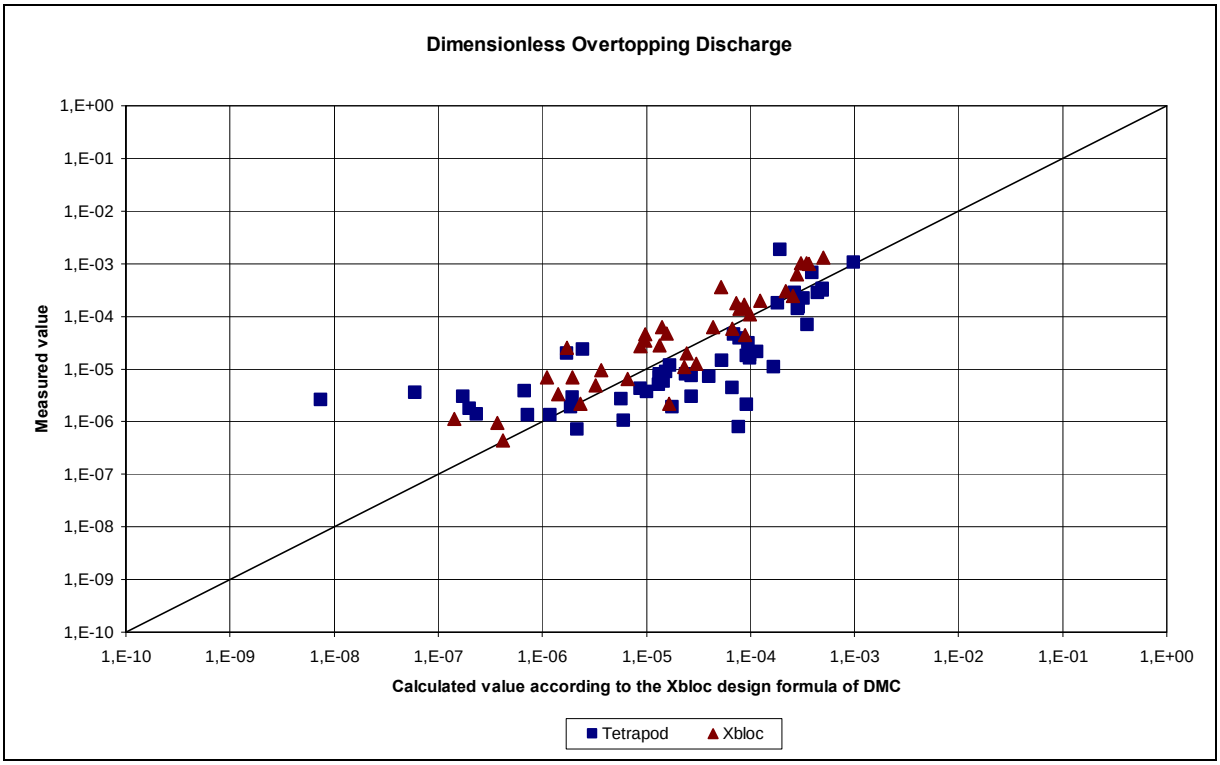

Figure 4.28 Test results compare to the Xbloc overtopping formula.

As was shown in figure 4.28, the Xbloc overtopping formula gives a slightly better estimation of the test results than the Van Der Meer formula.

4.3.5.3 Regression

In order to have an idea of the reliability of the test results compared to the Xbloc overtopping formula. A regression line for the test results compared to the Xbloc overtopping formula was given in the following figure.

The regression coefficients were calculated using Excel. The intersection is 8.02E-4, and the variable coefficient is -2.88E-4.

In formula form:

$y = -2.88E\text{-}4\ x + 8.02E\text{-}4$

In this graphic, the reliability lines for both the lower 95% and the higher 95% were shown together with the regression line.

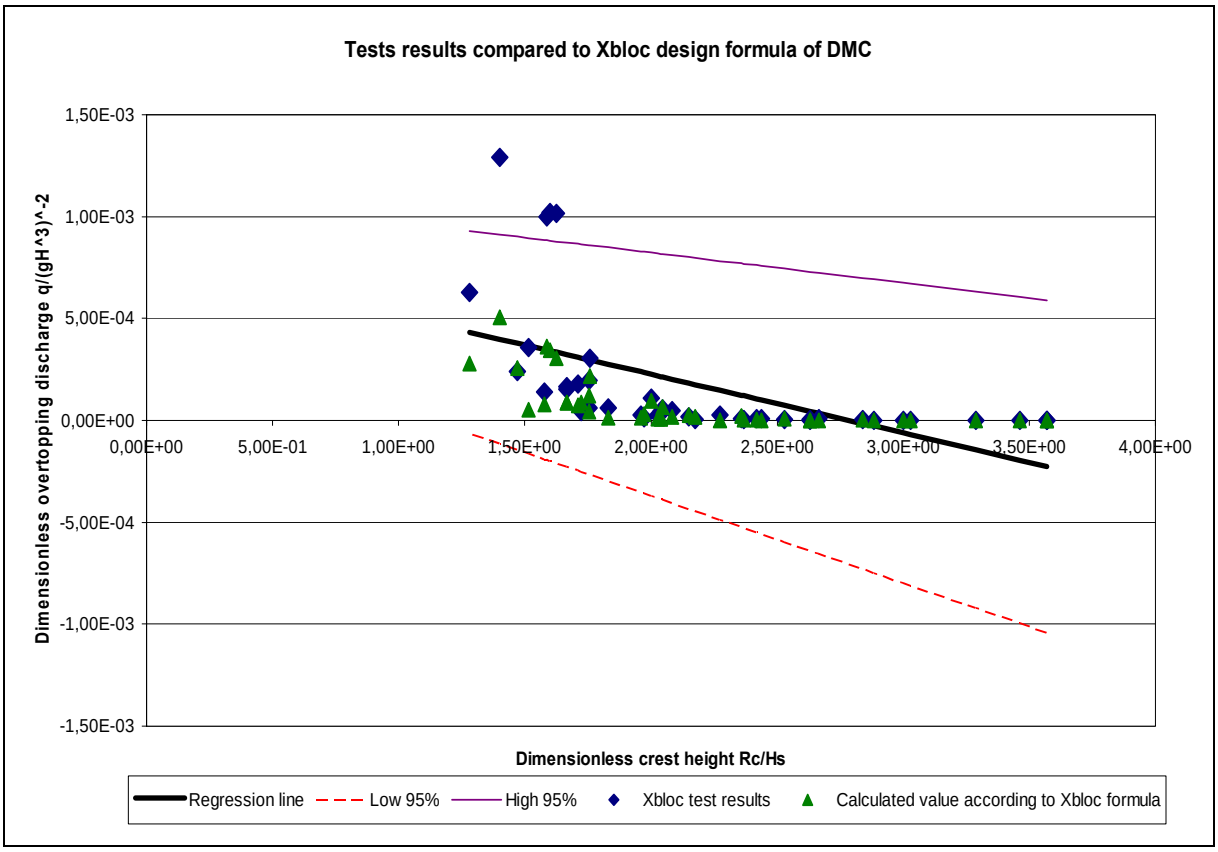

Figure 4.29 Regression line in linear scale

Chapter 5

Conclusion and Recommendation

In this chapter, conclusions derived from the experimental research, are presented. The conclusions cover the two areas of interest; the single armour layer of Tetrapod and Xbloc. Next, recommendations are given for further research.

5.1 Conclusion

- The experiments demonstrate that an increase in wave height results an increase in overtopping discharge, as was expected.

- The experiments demonstrate that a decrease in freeboard results an increase in overtopping discharge, as was expected.

- The experiments demonstrate that a decrease in wave steepness results an increase in overtopping discharge, which was not expected.

- An estimation of $\gamma_f = 0.3$ gives a good fit for comparing the test results with the values calculated according to the Van Der Meer formulas. According to the literature, the lowest γ_f for broken stones is 0.55. But the roughness factor γ_f that was determined in this case is 0.3, thus lower than the lowest roughness factor in standard cases. An explanation is that for this test, the single layer Tetrapod and Xbloc units have a high porosity. This has influence over the roughness factor.

- The test results showed that the measured overtopping volume of the Tetrapod and Xbloc are smaller than that was calculated according to the Van Der Meer formula. That means that in this case, the Van Der Meer formula gives a slightly overestimation of the measured volume. In this case, the high porosity of the Tetrapod and Xbloc units has also influence over the overtopping, thus result in smaller value of overtopping than was estimated by the formula.

- The test results show that the Xbloc gives slightly more overtopping discharge than the Tetrapod. But it should be noticed that the tested Tetrapods units (202g) qua dimension and weight, are significant larger than the tested Xbloc armour units (121g). A conclusion of the amount of overtopping between different armour units is considered only realistic if the ratio design wave height / unit diameter is in the same order.

- The Xbloc overtopping formula gives a good fit for the Xbloc test results. This is a better formula to estimate wave overtopping discharge with Xbloc armour units than the Van Der Meer formula. The test results obtained from the test series gave independently a verification of the Xbloc overtopping formula.

- After comparing the test results of the Tetrapod, it shows that the Xbloc overtopping formula gives a slightly better estimation as the Van Der Meer formula. Thus, the Xbloc overtopping formula is also a good formula for estimation of the test results of single layer Tetrapod units.

5.2 Recommendation

- In this experimental research, only limited condition for the wave overtopping was researched. Namely, the incident wave attack is perpendicular to the breakwater. The influences of a toe at the breakwater, angle of wave attack and foreland effect are not considered in this research. Further researches which include these factors are recommended.

- Other packing densities of the Xbloc and the packing densities of the sub layer were not under the consideration of this research. Also, for further researches of breakwater with Xbloc armour layer, the influence of the crest width could be considered.

References

Anderson, O.H., Juhl, J. and Sloth, P., (1992) Rear Side Stability of Berm Breakwaters, Proceedings of the Twenty-third International Coastal Engineering Conference, American Society of Civil Engineers, pp. 1020-1771, New York, USA.

Battjes, J.A. (1974) Computation of set-up, long shore currents, run-up and overtopping due to wind generated waves , Delft University of Technology, Delft, The Netherlands

Battjes, J. A., (2000) Collegehandleiding CTWA4320 Korte Golven, Technische Universiteit Delft, Faculteit Civiele Techniek en Geowetenschappen, Delft, The Netherlands

Bhageloe, G.S. (1998) Breakwaters with a single layer, MSc Thesis, Delft University of Technology, Delft, The Netherlands

Broderick, L.L. (1984) Riprap stability versus monochromatic and irregular waves, Conf. on coastal structures

Bruun, P., (1985) Design and construction of mounds for breakwaters and coastal protection, Elsevier Science Publishers B.V, Amsterdam, The Netherlands.

Burcharth, H.F., Andersen, O.H. (1995) On the one-dimensional steady and unsteady porous flow equations, Coastal Engineering 24, Elsevier

Burcharth, H.F., Liu, Z., Troch, P. (1999) Scaling of core material in rubble mound breakwater model tests, Proceedings of COPEDEC V, Cape Town, South Africa

CUR (1993) Filters in de waterbouw, CUR Publication 161, Gouda, The Netherlands

CUR (1995) Manual on the use of rock in hydraulic engineering, CUR Publication 169, Gouda, The Netherlands

D'Angremond, K., Van Roode, F.C. (2000) Breakwaters and closure dams. Bed bank and shore protection 2, Delft University of Technology, Delft, The Netherlands

D'Angremond, K., Berendsen, E., G.S., Bhageloe, G.S., Van Gent, M.R.A., Van Der Meer, J.W. (1999) Breakwaters with a single armour layer, 5th COPEDEC, Capetown, South Africa

De Jong, R.J. (1996) Stability of Tetrapods at front, crest and rear of a low-crested breakwater, MSc Thesis, Delft University of Technology, Delft, The Netherlands

De Jong, W. (2002) Experimental research on the stability of the armour and secondary layer in a single layered Tetrapod breakwater, MSc Thesis, Delft University of Technology, Delft, The Netherlands

De Rouck, J., Van Der Meer, J.W., Allsop, N.W.H., Franco, L., Verhaeghe, H. (2002) Wave overtopping at coastal structures: development of a database towards up-graded prediction methods, 28th ICCE, Cardiff, UK.

Gent, M.R.A. van, (1995) Communications on Hydraulic and Geotechnical Engineering, Wave Interaction with Permeable Coastal Structures, Faculty of Civil Engineering, Delft University of Technology, Delft, The Netherlands

Hasselman, K. ET AL. (1973) Measurement of wind-wave growth and swell during the Joint North Sea Wave Project (JONSWAP), Deutches Hydrographisches Institut, Hamburg, Germany

Herbich, J. B., (1990) Handbook of Coastal and Ocean Engineering Volume 1, Wave Phenomena and Coastal Structures, Gulf Publishing Company, Houston, USA.

Hudson, R.Y. (1958) Design of quarry stone cover layer for rubble mound breakwater, WES, Research Report No 2.2, Vicksburg, USA

Hudson, R.Y. (1959) Laboratory investigations of rubble mound breakwaters, WES Report, Vicksburg, USA

Hughes, S.A. (1993) Physical Models and Laboratory Techniques in Coastal Engineering, World Scientific Publishing Co. Pte. Ltd., Singapore

Hunt, I. A., (1959) Design of Seawalls and Breakwaters, Journal of the Waterways and Harbour Division, American Society of Civil Engineers, Vol. 85, WW3 pp. 123-152

Iribarren, R. (1950) Generalizacion de la formula para el calculo de los diques de escollera y comprobacion de sus coefficientes, Revista de Obras Publicas, Madrid, Spain

Iribarren, R. (1954) Other verifications of the formula calculating breakwater embankments, PIANC, Bull. No 39

Jensen, O.J., Klinting, P. (1983) Evaluation of scale effects in hydraulic models by analysis of laminar and turbulent flows , Coastal Engineering 7

Jobson J.D. (1991) Applied Multivariate Data Analysis, Volume-I, Springer-Verlag, New York, USA Langhaar, B. (1951). Dimensional Analysis and Theory of Models, New York, USA

Juhl, J., Sloth, P., (1994) Wave Overtopping of Breakwaters under Oblique Waves, Proceedings of the Twenty-Fourth International Coastal Engineering Conference, American Society of Civil Engineers, p. 1183-1196, New York, USA.

Juul Jensen, O., (1984) A monograph on rubble mound breakwaters, Danish Hydraulic Institute, Hørsholm, Denmark.

Klabbers, M., Muttray, M.O., Reedijk, J.S. (2003) Xbloc armour unit development, Hydraulic performance of Xbloc armour units – 2-D model tests at WL Delft, Delta Marine Consultants, Gouda, The Netherlands

Kudale, M.D.,Kobayashi, N., (1997) Hydraulic Stability Analyses of Leeside Slopes of Overtopped Breakwaters, Proceedings of the Twenty-fifth International Coastal Engineering Conference, American Society of Civil Engineers, pp. 1721-1734, New York, USA.

Le M´ehaut´e, H.L. (1957) Perm´eabilit´e des digues en enrochement aux ondes de gravit´e p´eriodique, Houille Blanche 6

Postma, G.M. (1989) Wave reflection from rock slopes under random wave attack, MSc Thesis, Delft University of Technology, Delft, The Netherlands

Price, W.A. (1979) Static stability of rubble mound breakwaters, Dock and harbour authority. Vol. LX

Reedijk, B., Klabbers, M., Van Den Berg, A., Hakenberg, R., (2003) Development of the Xbloc Breakwater Armour Unit, Delta Marine Consultants, Gouda, The Netherlands

Saville, Jr., T., Caldwell, J.M., (1953) Experimental Study of Wave Overtopping on Shore Structures, Proceedings, Minnesota International Hydraulics Convention, Minneapolis, Minnesota, USA

Schiereck, G.J. (1998) Introduction to bed, bank and shore protection, Delft University of Technology, Delft, The Netherlands

Schijf, J.B., (1972) Golfoploop en golfoverslag, Technische Adviescommissie voor de Waterkeringen, 's-Gravenhage, The Netherlands

SPM (1984) Shore Protection Manual Coastal Engineering Research Center, Washington

Steenaard, J. (2002) Verdeling van overslaand water over een golfbreker, MSc Thesis, Delft University of Technology, Delft, The Netherlands

Thompson, D.M., Shuttler, R.M. (1975) Riprap design for wind wave attack. A laboratory study in random waves, HRS, Report EX 707, Wallingford, UK

Van den Bosch, A.F.M. (2001) Influence of the density of placement on the stability of armour layers on breakwaters, MSc Thesis, Delft University of Technology, Delft, The Netherlands

Van Gent, M.R.A. (1995) Wave interaction with permeable coastal structures, PhD Thesis, Delft University of Technology, Delft, The Netherlands

Van Gent, M.R.A., Spaan, G.B.H., Plate, S.E., Berendsen, E.,Van der Meer, J.W. and d'Angremond, K. (1999) Single-layer rubble mound breakwaters, Proc. International Conference Coastal Structures, Santander, Spain

Van Gent, M.R.A., Kuiper, C. (2000) Single-layer rubble mound breakwaters with high density concrete cubes, WL|Delft Hydraulics, Project H3675, Delft, The Netherlands

Van Den Bosch, A., D'angremond, K., Verhagen, H.J., Olthof, J. (2002) Influence of the density of placement on the stability of armour units on breakwaters. 28th ICEE, Cardiff, UK.

Van Der Meer, J.W. (1988a) Rock Slopes and Gravel Beaches under Wave attack, PhD Thesis, Delft University of Technology, Delft, The Netherlands

Van Der Meer, J.W. (1988b) Stability of Cubes, Tetrapods and Accropodes, Proceedings of the Conference Breakwater '88, Thomas Telford, London, UK

Van Der Meer, J.W. (1993) Conceptual design of rubble mound breakwaters, WL|Delft Hydraulics, Delft, The Netherlands

Van Der Meer, J.W., Tutuarima, W.H., Burger, G. (1996) Influence of rock shape and grading on stability of low-crested structures, Proceedings of the International Conference on Coastal Engineering, Orlando, USA

Van Der Meer, J.W., (2000) Technisch Rapport Golfoploop en Golfoverslag bij Dijken. Rapport A-99.32, Technische Adviescommissie voor de Waterkeringen, Delft, The Netherlands.

Van Der Meer, J.W., (2002) Technisch Rapport Golfoploop en Golfoverslag bij Dijken, Technische Adviescommissie voor de Waterkeringen, Delft, The Netherlands

Weggel, R. J., (1976) Wave overtopping equation, Fifteenth Coastal Engineering Conference, pp. 2737-2755, American Society of Civil Engineers, New York, USA.

List of Symbols

γ_β = influence factors for the influences of the angle of the wave attack [-]
γ_b = influence factors for the influences of the toe of the breakwater [-]
γ_f = influence factors for the influences of the roughness [-]
γ_v = influence factors for the influences of the foreland [-]
Δ = Relative density [-]
b = dimensionless wave overtopping volume according to Battjes [-]
B = wave overtopping volume per wave per m^1 crest length [m^2]
d = local water depth at toe [m]
D_{15} = Particle diameter exceeded by 15% of the particles[m]
D_{85} = Particle diameter exceeded by 85% of the particles [m]
D_{n50} = Nominal diameter [m]
D_{n50S} = Nominal diameter of the secondary layer material [m]
D_{nA} = Nominal diameter of the armour unit [m]
E(f) = Frequency spectrum [m^2s]
f = Frequency [Hz]
F = $(h_c - h)/H'_0$ = dimensionless free-board [-]
F_0 = R/H'_0 = dimensionless crest height to avoid wave overtopping [-]
Fr = Froude number [-]
g = Gravitational acceleration [m/s^2]
h = water depth before the construction [m]
H = wave height [m]
H'_0 = wave height in deep water [m]
h_0 = Still water depth [m]
h_c = construction height [m]
h_{cr} = Height of the crest [m]
H_{m0} = significant wave height at toe of dike [m]
H_s = Significant wave height [m]
H_{si} = incident wave height near the toe [m]
H_{si0} = incident wave height in deep water [m]
H_{sr} = reflected wave height near the toe [m]
H_{sr0} = reflected wave height in deep water [m]
I = Hydraulic gradient [-]
K = Hydraulic conductivity [m/s]
K = Scale factor [-]
KC = Keulegan-Carpenter number [-]
K_R = Reflection coefficient near the toe [-]
K_{R0} = Reflection coefficient in deep water [-]
k_t = Layer thickness coefficient [-]
L = wave length [m]
L_o = deepwater wave length [m]
$L_{t,p}$ = local wave length at toe, based on T_p [m]
N = Number of waves [-]
N_a = Number of units per square meter [m^{-2}]

n_v = Packing density of the armour layer [-]
P = Permeability coefficient [-]
p = Pore pressure [N/m^2]
q = wave overtopping volume per m^1 crest length [$m^3/s/m^1$]
q* = wave overtopping volume [m^3/s]
Q = dimensionless overtopping volume [-]
Q* = dimensionless overtopping volume [-]
Q_0* = dimensionless overtopping volume when the free-board is zero [-]
R = wave run-up height in vertical surface [m]
R_c = freeboard [= crest level – still water level][m]
Re = Reynolds number [-]
s_{m0} = Deep water steepness based on the mean wave period [-]
s_{op} = wave steepness [-]
T_m = Mean wave period near the toe [s]
T_{m0} = Mean wave period in deep water [s]
$T_{m-1.0}$ = spectral wave period at toe of dike [s]
T_p = Peak wave period [s]
U = Characteristic pore velocity [m/s]
U_r = Ursell parameter [$U_r = H_s*L_t^2 / d^3$] [-]
V = volume of water in a wave above the still water level [m^3/m^1]
V = volume of overtopping water [m^3]
W_{50} = Weight of a unit/rock with a diameter D_{n50} [kg]
W_a = Weight of the armour units [kg]
W_c = Weight of the rock material in the core [kg]
W_s = Weight of the secondary rock material [kg]
α_1 = a parameter which determines the range of the tanh-curve [-]
δ = Damping coefficient [-]
η = the altering of the water surface [m]
ν = Kinematic viscosity [m^2/s]
ξ = Surf similarity parameter [-]
ρ_a = Density of the units [kg/m^3]
ρ_r = Density of the rocks [kg/m^3]
ρ_w = Density of water [kg/m^3]
α = slope angle [^{o}]
ξ_o = breaker parameter [-]

List of Tables

List of Figures

Appendix A Wave Overtopping Data

Test	Block	R_c [m]	Name	s_{m0} [-]	T_{m0} [s]	H_{si0} [m]	H_{sr0} [m]	K_{R0} [-]
1	Tetrapod	0,15	Jsh10s2	0,017	1,83	0,091	0,029	0,32
2	Tetrapod	0,15	Jsh10s4	0,033	1,28	0,084	0,018	0,21
3	Tetrapod	0,15	Jsh10s6	0,043	1,07	0,077	0,013	0,16
4	Tetrapod	0,15	Jsh12s2	0,021	1,83	0,110	0,034	0,31
5	Tetrapod	0,15	Jsh12s4	0,033	1,42	0,105	0,025	0,24
6	Tetrapod	0,15	Jsh12s6	0,046	1,16	0,096	0,016	0,17
7	Tetrapod	0,15	Jsh14s2	0,014	2,13	0,098	0,035	0,36
8	Tetrapod	0,15	Jsh14s4	0,040	1,42	0,125	0,034	0,27
9	Tetrapod	0,15	Jsh14s6	0,043	1,28	0,111	0,022	0,20
10	Tetrapod	0,15	Jsh16s6	0,050	1,28	0,129	0,028	0,22
11	Tetrapod	0,2	Jsh10s2	0,017	1,83	0,088	0,028	0,32
12	Tetrapod	0,2	Jsh10s4	0,034	1,28	0,086	0,021	0,25
13	Tetrapod	0,2	Jsh10s6	0,043	1,07	0,077	0,015	0,19
14	Tetrapod	0,2	Jsh12s2	0,022	1,83	0,116	0,038	0,33
15	Tetrapod	0,2	Jsh12s4	0,035	1,42	0,109	0,029	0,27
16	Tetrapod	0,2	Jsh12s6	0,046	1,16	0,096	0,020	0,21
17	Tetrapod	0,2	Jsh14s21	0,019	2,13	0,134	0,045	0,34
18	Tetrapod	0,2	Jsh14s22	0,019	2,13	0,137	0,046	0,34
19	Tetrapod	0,2	Jsh14s23	0,019	2,13	0,136	0,045	0,33
20	Tetrapod	0,2	Jsh14s41	0,039	1,42	0,122	0,034	0,28
21	Tetrapod	0,2	Jsh14s42	0,040	1,42	0,127	0,035	0,27
22	Tetrapod	0,2	Jsh14s43	0,041	1,42	0,128	0,035	0,27
23	Tetrapod	0,2	Jsh14s61	0,055	1,16	0,115	0,026	0,22
24	Tetrapod	0,2	Jsh14s62	0,055	1,16	0,116	0,026	0,22
25	Tetrapod	0,2	Jsh14s63	0,054	1,16	0,113	0,025	0,22
26	Tetrapod	0,2	Jsh16s2	0,022	2,13	0,153	0,052	0,34
27	Tetrapod	0,2	Jsh16s4	0,037	1,60	0,146	0,040	0,27
28	Tetrapod	0,2	Jsh16s6	0,051	1,28	0,130	0,028	0,21
29	Tetrapod	0,225	Jsh10s2	0,018	1,83	0,093	0,029	0,31
30	Tetrapod	0,225	Jsh10s4	0,034	1,28	0,086	0,022	0,25
31	Tetrapod	0,225	Jsh10s6	0,044	1,07	0,078	0,015	0,19
32	Tetrapod	0,225	Jsh12s2	0,021	1,83	0,111	0,036	0,32
33	Tetrapod	0,225	Jsh12s4	0,033	1,42	0,105	0,028	0,27
34	Tetrapod	0,225	Jsh12s6	0,044	1,16	0,093	0,019	0,21
35	Tetrapod	0,225	Jsh14s2	0,019	2,13	0,135	0,045	0,33
36	Tetrapod	0,225	Jsh14s4	0,039	1,42	0,122	0,033	0,27
37	Tetrapod	0,225	Jsh14s6	0,054	1,16	0,113	0,025	0,22

Test	Block	Rc [m]	Name	s_{m0} [-]	T_{m0} [s]	H_{si0} [m]	H_{sr0} [m]	K_{R0} [-]
38	Tetrapod	0,225	Jsh16s2	0,020	2,13	0,140	0,047	0,34
39	Tetrapod	0,225	Jsh16s4	0,035	1,60	0,139	0,037	0,26
40	Tetrapod	0,225	Jsh16s6	0,050	1,28	0,128	0,029	0,23
41	Tetrapod	0,25	Jsh10s2	0,018	1,83	0,092	0,030	0,32
42	Tetrapod	0,25	Jsh10s4	0,035	1,28	0,089	0,026	0,29
43	Tetrapod	0,25	Jsh10s6	0,043	1,07	0,077	0,019	0,25
44	Tetrapod	0,25	Jsh12s2	0,023	1,83	0,121	0,040	0,33
45	Tetrapod	0,25	Jsh12s4	0,036	1,42	0,112	0,034	0,30
46	Tetrapod	0,25	Jsh12s6	0,047	1,16	0,098	0,026	0,26
47	Tetrapod	0,25	Jsh14s2	0,019	2,13	0,137	0,046	0,33
48	Tetrapod	0,25	Jsh14s4	0,042	1,42	0,131	0,040	0,30
49	Tetrapod	0,25	Jsh14s6	0,045	1,28	0,114	0,031	0,27
50	Tetrapod	0,25	Jsh16s2	0,020	2,13	0,144	0,047	0,33
51	Tetrapod	0,25	Jsh16s4	0,035	1,60	0,138	0,036	0,26
52	Tetrapod	0,25	Jsh16s6	0,049	1,28	0,126	0,032	0,25
53	Xbloc	0,15	Jsh10s2	0,017	1,83	0,090	0,029	0,32
54	Xbloc	0,15	Jsh10s4	0,033	1,28	0,084	0,018	0,21
55	Xbloc	0,15	Jsh10s6	0,044	1,07	0,078	0,012	0,16
56	Xbloc	0,15	Jsh12s2	0,020	1,83	0,107	0,034	0,32
57	Xbloc	0,15	Jsh12s4	0,033	1,42	0,104	0,026	0,25
58	Xbloc	0,15	Jsh12s6	0,044	1,16	0,093	0,016	0,18
59	Xbloc	0,15	Jsh14s2	0,016	2,13	0,112	0,040	0,36
60	Xbloc	0,15	Jsh14s4	0,040	1,42	0,125	0,034	0,27
61	Xbloc	0,15	Jsh14s6	0,054	1,16	0,113	0,022	0,19
62	Xbloc	0,2	Jsh10s2	0,018	1,83	0,094	0,030	0,32
63	Xbloc	0,2	Jsh10s4	0,032	1,28	0,083	0,019	0,23
64	Xbloc	0,2	Jsh10s6	0,042	1,07	0,075	0,012	0,16
65	Xbloc	0,2	Jsh12s2	0,022	1,83	0,114	0,039	0,34
66	Xbloc	0,2	Jsh12s4	0,033	1,42	0,103	0,027	0,26
67	Xbloc	0,2	Jsh12s6	0,044	1,16	0,093	0,017	0,18
68	Xbloc	0,2	Jsh14s21	0,018	2,13	0,128	0,044	0,34
69	Xbloc	0,2	Jsh14s22	0,018	2,13	0,125	0,042	0,34
70	Xbloc	0,2	Jsh14s23	0,018	2,13	0,129	0,044	0,34
71	Xbloc	0,2	Jsh14s41	0,038	1,42	0,121	0,033	0,27
72	Xbloc	0,2	Jsh14s42	0,039	1,42	0,124	0,034	0,27
73	Xbloc	0,2	Jsh14s43	0,039	1,42	0,124	0,034	0,27
74	Xbloc	0,2	Jsh14s61	0,053	1,16	0,112	0,024	0,21
75	Xbloc	0,2	Jsh14s62	0,051	1,16	0,108	0,023	0,21
76	Xbloc	0,2	Jsh14s63	0,052	1,16	0,109	0,023	0,21

Test	Block	Rc [m]	Name	s_{m0} [-]	T_{m0} [s]	H_{si0} [m]	H_{sr0} [m]	K_{R0} [-]
77	Xbloc	0,2	Jsh16s6	0,049	1,28	0,126	0,030	0,24
78	Xbloc	0,225	Jsh10s2	0,017	1,83	0,088	0,027	0,31
79	Xbloc	0,225	Jsh10s4	0,032	1,28	0,081	0,019	0,24
80	Xbloc	0,225	Jsh10s6	0,041	1,07	0,074	0,012	0,17
81	Xbloc	0,225	Jsh12s2	0,021	1,83	0,110	0,036	0,32
82	Xbloc	0,225	Jsh12s4	0,031	1,42	0,099	0,026	0,26
83	Xbloc	0,225	Jsh12s6	0,042	1,16	0,088	0,017	0,19
84	Xbloc	0,225	Jsh14s2	0,018	2,13	0,129	0,043	0,33
85	Xbloc	0,225	Jsh14s4	0,038	1,42	0,119	0,032	0,27
86	Xbloc	0,225	Jsh14s6	0,050	1,16	0,105	0,023	0,22
87	Xbloc	0,25	Jsh10s2	0,017	1,83	0,087	0,025	0,29
88	Xbloc	0,25	Jsh10s4	0,030	1,28	0,076	0,019	0,25
89	Xbloc	0,25	Jsh10s6	0,030	1,28	0,076	0,019	0,25
90	Xbloc	0,25	Jsh12s2	0,020	1,83	0,106	0,031	0,30
91	Xbloc	0,25	Jsh12s4	0,032	1,42	0,101	0,026	0,26
92	Xbloc	0,25	Jsh12s6	0,041	1,16	0,086	0,018	0,21
93	Xbloc	0,25	Jsh14s2	0,018	2,13	0,125	0,038	0,31
94	Xbloc	0,25	Jsh14s4	0,038	1,42	0,119	0,032	0,27
95	Xbloc	0,25	Jsh14s6	0,050	1,16	0,106	0,024	0,23

Test	Block	Rc [m]	Name	T_m [s]	H_{si} [m]	H_{sr} [m]	K_R [-]	ξ_0 [-]
1	Tetrapod	0,15	Jsh10s2	1,83	0,088	0,035	0,40	5,05
2	Tetrapod	0,15	Jsh10s4	1,28	0,074	0,018	0,24	3,68
3	Tetrapod	0,15	Jsh10s6	1,07	0,066	0,013	0,19	3,21
4	Tetrapod	0,15	Jsh12s2	1,83	0,106	0,043	0,40	4,60
5	Tetrapod	0,15	Jsh12s4	1,42	0,095	0,029	0,30	3,65
6	Tetrapod	0,15	Jsh12s6	1,16	0,083	0,016	0,19	3,12
7	Tetrapod	0,15	Jsh14s2	2,13	0,092	0,031	0,34	5,67
8	Tetrapod	0,15	Jsh14s4	1,42	0,116	0,042	0,36	3,35
9	Tetrapod	0,15	Jsh14s6	1,28	0,098	0,021	0,21	3,20
10	Tetrapod	0,15	Jsh16s6	1,28	0,115	0,030	0,26	2,97
11	Tetrapod	0,2	Jsh10s2	1,83	0,087	0,033	0,37	5,14
12	Tetrapod	0,2	Jsh10s4	1,28	0,079	0,021	0,27	3,64
13	Tetrapod	0,2	Jsh10s6	1,07	0,068	0,014	0,21	3,21
14	Tetrapod	0,2	Jsh12s2	1,83	0,113	0,038	0,34	4,48
15	Tetrapod	0,2	Jsh12s4	1,42	0,101	0,033	0,33	3,58
16	Tetrapod	0,2	Jsh12s6	1,16	0,084	0,019	0,22	3,12
17	Tetrapod	0,2	Jsh14s21	2,13	0,130	0,042	0,32	4,85
18	Tetrapod	0,2	Jsh14s22	2,13	0,132	0,043	0,32	4,79
19	Tetrapod	0,2	Jsh14s23	2,13	0,132	0,043	0,32	4,81
20	Tetrapod	0,2	Jsh14s41	1,42	0,118	0,042	0,35	3,39
21	Tetrapod	0,2	Jsh14s42	1,60	0,122	0,044	0,36	3,32
22	Tetrapod	0,2	Jsh14s43	1,42	0,122	0,044	0,36	3,31
23	Tetrapod	0,2	Jsh14s61	1,16	0,103	0,025	0,25	2,85
24	Tetrapod	0,2	Jsh14s62	1,16	0,105	0,026	0,25	2,84
25	Tetrapod	0,2	Jsh14s63	1,16	0,102	0,025	0,24	2,88
26	Tetrapod	0,2	Jsh16s2	2,13	0,148	0,049	0,33	4,54
27	Tetrapod	0,2	Jsh16s4	1,60	0,141	0,052	0,37	3,49
28	Tetrapod	0,2	Jsh16s6	1,28	0,117	0,030	0,25	2,96
29	Tetrapod	0,225	Jsh10s2	1,83	0,093	0,035	0,38	5,00
30	Tetrapod	0,225	Jsh10s4	1,28	0,079	0,022	0,28	3,64
31	Tetrapod	0,225	Jsh10s6	1,07	0,068	0,013	0,20	3,19
32	Tetrapod	0,225	Jsh12s2	1,83	0,110	0,037	0,34	4,58
33	Tetrapod	0,225	Jsh12s4	1,42	0,098	0,032	0,33	3,65
34	Tetrapod	0,225	Jsh12s6	1,16	0,082	0,018	0,21	3,17
35	Tetrapod	0,225	Jsh14s2	2,13	0,133	0,045	0,34	4,83
36	Tetrapod	0,225	Jsh14s4	1,42	0,118	0,042	0,36	3,39
37	Tetrapod	0,225	Jsh14s6	1,16	0,101	0,025	0,25	2,88

Test	Block	Rc [m]	Name	T_m [s]	H_{si} [m]	H_{sr} [m]	K_R [-]	ξ_0 [-]
38	Tetrapod	0,225	Jsh16s2	2,13	0,139	0,051	0,37	4,74
39	Tetrapod	0,225	Jsh16s4	1,60	0,137	0,050	0,36	3,58
40	Tetrapod	0,225	Jsh16s6	1,28	0,117	0,032	0,27	2,98
41	Tetrapod	0,25	Jsh10s2	1,83	0,083	0,031	0,37	5,03
42	Tetrapod	0,25	Jsh10s4	1,28	0,077	0,022	0,29	3,58
43	Tetrapod	0,25	Jsh10s6	1,07	0,064	0,014	0,22	3,21
44	Tetrapod	0,25	Jsh12s2	1,83	0,108	0,036	0,34	4,38
45	Tetrapod	0,25	Jsh12s4	1,42	0,095	0,032	0,34	3,54
46	Tetrapod	0,25	Jsh12s6	1,16	0,081	0,019	0,23	3,09
47	Tetrapod	0,25	Jsh14s2	2,13	0,124	0,042	0,34	4,79
48	Tetrapod	0,25	Jsh14s4	1,42	0,116	0,042	0,36	3,27
49	Tetrapod	0,25	Jsh14s6	1,16	0,096	0,025	0,26	3,16
50	Tetrapod	0,25	Jsh16s2	2,13	0,144	0,050	0,35	4,68
51	Tetrapod	0,25	Jsh16s4	1,60	0,136	0,049	0,36	3,59
52	Tetrapod	0,25	Jsh16s6	1,28	0,116	0,035	0,30	3,00
53	Xbloc	0,15	Jsh10s2	1,83	0,087	0,036	0,42	5,08
54	Xbloc	0,15	Jsh10s4	1,28	0,074	0,018	0,25	3,68
55	Xbloc	0,15	Jsh10s6	1,06	0,066	0,013	0,19	3,19
56	Xbloc	0,15	Jsh12s2	1,83	0,102	0,042	0,41	4,66
57	Xbloc	0,15	Jsh12s4	1,42	0,095	0,029	0,30	3,67
58	Xbloc	0,15	Jsh12s6	1,16	0,082	0,016	0,19	3,17
59	Xbloc	0,15	Jsh14s2	2,13	0,107	0,037	0,35	5,30
60	Xbloc	0,15	Jsh14s4	1,42	0,117	0,042	0,36	3,35
61	Xbloc	0,15	Jsh14s6	1,16	0,099	0,021	0,21	2,88
62	Xbloc	0,2	Jsh10s2	1,83	0,093	0,038	0,41	4,97
63	Xbloc	0,2	Jsh10s4	1,28	0,075	0,019	0,25	3,70
64	Xbloc	0,2	Jsh10s6	1,07	0,066	0,012	0,18	3,26
65	Xbloc	0,2	Jsh12s2	1,83	0,114	0,042	0,36	4,52
66	Xbloc	0,2	Jsh12s4	1,42	0,096	0,031	0,32	3,69
67	Xbloc	0,2	Jsh12s6	1,16	0,082	0,016	0,20	3,17
68	Xbloc	0,2	Jsh14s21	2,13	0,125	0,042	0,34	4,96
69	Xbloc	0,2	Jsh14s22	2,13	0,123	0,041	0,33	5,02
70	Xbloc	0,2	Jsh14s23	2,13	0,126	0,042	0,33	4,94
71	Xbloc	0,2	Jsh14s41	1,42	0,117	0,044	0,38	3,40
72	Xbloc	0,2	Jsh14s42	1,42	0,120	0,045	0,38	3,36
73	Xbloc	0,2	Jsh14s43	1,42	0,120	0,045	0,37	3,36
74	Xbloc	0,2	Jsh14s61	1,16	0,102	0,024	0,23	2,89
75	Xbloc	0,2	Jsh14s62	1,16	0,098	0,023	0,23	2,94
76	Xbloc	0,2	Jsh14s63	1,16	0,098	0,023	0,23	2,93

Test	Block	Rc [m]	Name	T_m [s]	H_{si} [m]	H_{sr} [m]	K_R [-]	ξ_0 [-]
77	Xbloc	0,2	Jsh16s6	1,28	0,114	0,032	0,28	3,00
78	Xbloc	0,225	Jsh10s2	1,83	0,089	0,036	0,40	5,14
79	Xbloc	0,225	Jsh10s4	1,28	0,075	0,020	0,27	3,75
80	Xbloc	0,225	Jsh10s6	1,07	0,065	0,012	0,19	3,28
81	Xbloc	0,225	Jsh12s2	2,13	0,110	0,040	0,36	4,60
82	Xbloc	0,225	Jsh12s4	1,28	0,093	0,031	0,33	3,76
83	Xbloc	0,225	Jsh12s6	1,16	0,078	0,016	0,20	3,26
84	Xbloc	0,225	Jsh14s2	2,13	0,128	0,044	0,35	4,94
85	Xbloc	0,225	Jsh14s4	1,42	0,114	0,043	0,38	3,43
86	Xbloc	0,225	Jsh14s6	1,16	0,095	0,023	0,24	2,98
87	Xbloc	0,25	Jsh10s2	1,83	0,088	0,034	0,39	5,17
88	Xbloc	0,25	Jsh10s4	1,28	0,070	0,020	0,28	3,87
89	Xbloc	0,25	Jsh10s6	1,28	0,070	0,020	0,28	3,87
90	Xbloc	0,25	Jsh12s2	2,13	0,106	0,037	0,35	4,68
91	Xbloc	0,25	Jsh12s4	1,28	0,095	0,032	0,34	3,72
92	Xbloc	0,25	Jsh12s6	1,16	0,076	0,016	0,21	3,30
93	Xbloc	0,25	Jsh14s2	2,13	0,125	0,042	0,34	5,02
94	Xbloc	0,25	Jsh14s4	1,42	0,115	0,043	0,38	3,43
95	Xbloc	0,25	Jsh14s6	1,16	0,095	0,024	0,25	2,97

Test	Block	Rc [m]	Name	q* [m^3/s]	V [m^3]	q [m^3/s/m^1]
1	Tetrapod	0,15	Jsh10s2	2,05E-06	2,46E-03	2,57E-06
2	Tetrapod	0,15	Jsh10s4	2,13E-07	2,56E-04	2,67E-07
3	Tetrapod	0,15	Jsh10s6	8,53E-07	1,02E-03	1,07E-06
4	Tetrapod	0,15	Jsh12s2	1,89E-05	2,27E-02	2,36E-05
5	Tetrapod	0,15	Jsh12s4	2,80E-06	3,36E-03	3,50E-06
6	Tetrapod	0,15	Jsh12s6	5,33E-07	6,40E-04	6,67E-07
7	Tetrapod	0,15	Jsh14s2	1,29E-04	1,55E-01	1,61E-04
8	Tetrapod	0,15	Jsh14s4	2,81E-05	3,38E-02	3,52E-05
9	Tetrapod	0,15	Jsh14s6	3,49E-06	4,19E-03	4,37E-06
10	Tetrapod	0,15	Jsh16s6	1,77E-05	2,12E-02	2,21E-05
11	Tetrapod	0,2	Jsh10s2	4,53E-07	5,44E-04	5,67E-07
12	Tetrapod	0,2	Jsh10s4	1,07E-07	1,28E-04	1,33E-07
13	Tetrapod	0,2	Jsh10s6	8,00E-08	9,60E-05	1,00E-07
14	Tetrapod	0,2	Jsh12s2	2,03E-06	2,43E-03	2,53E-06
15	Tetrapod	0,2	Jsh12s4	6,40E-07	7,68E-04	8,00E-07
16	Tetrapod	0,2	Jsh12s6	1,44E-06	1,73E-03	1,80E-06
17	Tetrapod	0,2	Jsh14s21	3,29E-05	3,95E-02	4,11E-05
18	Tetrapod	0,2	Jsh14s22	3,97E-05	4,77E-02	4,97E-05
19	Tetrapod	0,2	Jsh14s23	3,79E-05	4,54E-02	4,73E-05
20	Tetrapod	0,2	Jsh14s41	8,00E-08	9,60E-05	1,00E-07
21	Tetrapod	0,2	Jsh14s42	1,95E-06	2,34E-03	2,43E-06
22	Tetrapod	0,2	Jsh14s43	1,73E-06	2,08E-03	2,17E-06
23	Tetrapod	0,2	Jsh14s61	4,80E-07	5,76E-04	6,00E-07
24	Tetrapod	0,2	Jsh14s62	1,01E-06	1,22E-03	1,27E-06
25	Tetrapod	0,2	Jsh14s63	6,40E-07	7,68E-04	8,00E-07
26	Tetrapod	0,2	Jsh16s2	1,53E-04	1,84E-01	1,91E-04
27	Tetrapod	0,2	Jsh16s4	9,23E-06	1,11E-02	1,15E-05
28	Tetrapod	0,2	Jsh16s6	1,44E-06	1,73E-03	1,80E-06
29	Tetrapod	0,225	Jsh10s2	2,67E-07	3,20E-04	3,33E-07
30	Tetrapod	0,225	Jsh10s4	2,13E-07	2,56E-04	2,67E-07
31	Tetrapod	0,225	Jsh10s6	1,60E-07	1,92E-04	2,00E-07
32	Tetrapod	0,225	Jsh12s2	4,00E-07	4,80E-04	5,00E-07
33	Tetrapod	0,225	Jsh12s4	8,00E-08	9,60E-05	1,00E-07
34	Tetrapod	0,225	Jsh12s6	8,00E-08	9,60E-05	1,00E-07
35	Tetrapod	0,225	Jsh14s2	1,71E-05	2,05E-02	2,13E-05
36	Tetrapod	0,225	Jsh14s4	7,20E-07	8,64E-04	9,00E-07
37	Tetrapod	0,225	Jsh14s6	2,13E-07	2,56E-04	2,67E-07

Test	Block	Rc [m]	Name	q* [m^3/s]	V [m^3]	q [m^3/s/m^1]
38	Tetrapod	0,225	Jsh16s2	8,65E-05	1,04E-01	1,08E-04
39	Tetrapod	0,225	Jsh16s4	1,39E-06	1,66E-03	1,73E-06
40	Tetrapod	0,225	Jsh16s6	7,47E-07	8,96E-04	9,33E-07
41	Tetrapod	0,25	Jsh10s2	8,00E-08	9,60E-05	1,00E-07
42	Tetrapod	0,25	Jsh10s4	1,60E-07	1,92E-04	2,00E-07
43	Tetrapod	0,25	Jsh10s6	1,07E-07	1,28E-04	1,33E-07
44	Tetrapod	0,25	Jsh12s2	2,67E-07	3,20E-04	3,33E-07
45	Tetrapod	0,25	Jsh12s4	2,13E-07	2,56E-04	2,67E-07
46	Tetrapod	0,25	Jsh12s6	8,00E-08	9,60E-05	1,00E-07
47	Tetrapod	0,25	Jsh14s2	1,92E-06	2,30E-03	2,40E-06
48	Tetrapod	0,25	Jsh14s4	1,87E-07	2,24E-04	2,33E-07
49	Tetrapod	0,25	Jsh14s6	5,33E-08	6,40E-05	6,67E-08
50	Tetrapod	0,25	Jsh16s2	2,07E-05	2,48E-02	2,59E-05
51	Tetrapod	0,25	Jsh16s4	2,67E-07	3,20E-04	3,33E-07
52	Tetrapod	0,25	Jsh16s6	5,07E-07	6,08E-04	6,33E-07
53	Xbloc	0,15	Jsh10s2	2,74E-06	3,28E-03	3,60E-06
54	Xbloc	0,15	Jsh10s4	1,28E-06	1,53E-03	1,68E-06
55	Xbloc	0,15	Jsh10s6	1,00E-06	1,20E-03	1,32E-06
56	Xbloc	0,15	Jsh12s2	1,87E-05	2,24E-02	2,46E-05
57	Xbloc	0,15	Jsh12s4	9,67E-06	1,16E-02	1,27E-05
58	Xbloc	0,15	Jsh12s6	3,47E-06	4,16E-03	4,56E-06
59	Xbloc	0,15	Jsh14s2	1,08E-04	1,29E-01	1,42E-04
60	Xbloc	0,15	Jsh14s4	5,96E-05	7,15E-02	7,85E-05
61	Xbloc	0,15	Jsh14s6	2,66E-05	3,19E-02	3,50E-05
62	Xbloc	0,2	Jsh10s2	1,32E-06	1,59E-03	1,74E-06
63	Xbloc	0,2	Jsh10s4	3,42E-07	4,10E-04	4,50E-07
64	Xbloc	0,2	Jsh10s6	4,56E-08	5,47E-05	6,00E-08
65	Xbloc	0,2	Jsh12s2	1,81E-05	2,17E-02	2,38E-05
66	Xbloc	0,2	Jsh12s4	3,35E-06	4,02E-03	4,41E-06
67	Xbloc	0,2	Jsh12s6	3,88E-07	4,65E-04	5,10E-07
68	Xbloc	0,2	Jsh14s21	1,07E-04	1,29E-01	1,41E-04
69	Xbloc	0,2	Jsh14s22	1,05E-04	1,25E-01	1,38E-04
70	Xbloc	0,2	Jsh14s23	1,06E-04	1,28E-01	1,40E-04
71	Xbloc	0,2	Jsh14s41	1,68E-05	2,02E-02	2,22E-05
72	Xbloc	0,2	Jsh14s42	1,64E-05	1,96E-02	2,15E-05
73	Xbloc	0,2	Jsh14s43	1,51E-05	1,81E-02	1,98E-05
74	Xbloc	0,2	Jsh14s61	2,17E-06	2,60E-03	2,85E-06
75	Xbloc	0,2	Jsh14s62	3,31E-06	3,97E-03	4,35E-06
76	Xbloc	0,2	Jsh14s63	2,51E-06	3,01E-03	3,30E-06

Test	Block	Rc [m]	Name	q* [m^3/s]	V [m^3]	q [m^3/s/m^1]
77	Xbloc	0,2	Jsh16s6	5,75E-06	6,89E-03	7,56E-06
78	Xbloc	0,225	Jsh10s2	4,10E-07	4,92E-04	5,40E-07
79	Xbloc	0,225	Jsh10s4	4,56E-08	5,47E-05	6,00E-08
80	Xbloc	0,225	Jsh10s6	0,00E+00	0,00E+00	0,00E+00
81	Xbloc	0,225	Jsh12s2	5,08E-06	6,10E-03	6,69E-06
82	Xbloc	0,225	Jsh12s4	6,38E-07	7,66E-04	8,40E-07
83	Xbloc	0,225	Jsh12s6	2,28E-08	2,74E-05	3,00E-08
84	Xbloc	0,225	Jsh14s2	3,34E-05	4,01E-02	4,39E-05
85	Xbloc	0,225	Jsh14s4	1,16E-06	1,40E-03	1,53E-06
86	Xbloc	0,225	Jsh14s6	3,42E-07	4,10E-04	4,50E-07
87	Xbloc	0,25	Jsh10s2	1,37E-07	1,64E-04	1,80E-07
88	Xbloc	0,25	Jsh10s4	0,00E+00	0,00E+00	0,00E+00
89	Xbloc	0,25	Jsh10s6	0,00E+00	0,00E+00	0,00E+00
90	Xbloc	0,25	Jsh12s2	8,89E-07	1,07E-03	1,17E-06
91	Xbloc	0,25	Jsh12s4	0,00E+00	0,00E+00	0,00E+00
92	Xbloc	0,25	Jsh12s6	0,00E+00	0,00E+00	0,00E+00
93	Xbloc	0,25	Jsh14s2	1,15E-05	1,38E-02	1,52E-05
94	Xbloc	0,25	Jsh14s4	2,05E-07	2,46E-04	2,70E-07
95	Xbloc	0,25	Jsh14s6	2,28E-07	2,74E-04	3,00E-07

Test	Block	Rc [m]	Name	Q [-]	R_c/H_{si} [-]
1	Tetrapod	0,15	Jsh10s2	3,14E-05	1,70E+00
2	Tetrapod	0,15	Jsh10s4	4,23E-06	2,03E+00
3	Tetrapod	0,15	Jsh10s6	2,01E-05	2,27E+00
4	Tetrapod	0,15	Jsh12s2	2,18E-04	1,42E+00
5	Tetrapod	0,15	Jsh12s4	3,82E-05	1,58E+00
6	Tetrapod	0,15	Jsh12s6	8,90E-06	1,81E+00
7	Tetrapod	0,15	Jsh14s2	1,85E-03	1,63E+00
8	Tetrapod	0,15	Jsh14s4	2,84E-04	1,29E+00
9	Tetrapod	0,15	Jsh14s6	4,54E-05	1,53E+00
10	Tetrapod	0,15	Jsh16s6	1,81E-04	1,30E+00
11	Tetrapod	0,2	Jsh10s2	7,05E-06	2,30E+00
12	Tetrapod	0,2	Jsh10s4	1,92E-06	2,53E+00
13	Tetrapod	0,2	Jsh10s6	1,80E-06	2,94E+00
14	Tetrapod	0,2	Jsh12s2	2,13E-05	1,77E+00
15	Tetrapod	0,2	Jsh12s4	7,96E-06	1,98E+00
16	Tetrapod	0,2	Jsh12s6	2,36E-05	2,38E+00
17	Tetrapod	0,2	Jsh14s21	2,80E-04	1,54E+00
18	Tetrapod	0,2	Jsh14s22	3,31E-04	1,52E+00
19	Tetrapod	0,2	Jsh14s23	3,15E-04	1,52E+00
20	Tetrapod	0,2	Jsh14s41	7,88E-07	1,69E+00
21	Tetrapod	0,2	Jsh14s42	1,82E-05	1,64E+00
22	Tetrapod	0,2	Jsh14s43	1,62E-05	1,64E+00
23	Tetrapod	0,2	Jsh14s61	5,80E-06	1,94E+00
24	Tetrapod	0,2	Jsh14s62	1,19E-05	1,90E+00
25	Tetrapod	0,2	Jsh14s63	7,84E-06	1,96E+00
26	Tetrapod	0,2	Jsh16s2	1,07E-03	1,35E+00
27	Tetrapod	0,2	Jsh16s4	6,95E-05	1,42E+00
28	Tetrapod	0,2	Jsh16s6	1,44E-05	1,71E+00
29	Tetrapod	0,225	Jsh10s2	3,75E-06	2,42E+00
30	Tetrapod	0,225	Jsh10s4	3,83E-06	2,85E+00
31	Tetrapod	0,225	Jsh10s6	3,60E-06	3,31E+00
32	Tetrapod	0,225	Jsh12s2	4,38E-06	2,05E+00
33	Tetrapod	0,225	Jsh12s4	1,04E-06	2,30E+00
34	Tetrapod	0,225	Jsh12s6	1,36E-06	2,74E+00
35	Tetrapod	0,225	Jsh14s2	1,40E-04	1,69E+00
36	Tetrapod	0,225	Jsh14s4	7,09E-06	1,91E+00
37	Tetrapod	0,225	Jsh14s6	2,65E-06	2,23E+00

Test	Block	Rc [m]	Name	Q [-]	R_c/H_{si} [-]
38	Tetrapod	0,225	Jsh16s2	6,66E-04	1,62E+00
39	Tetrapod	0,225	Jsh16s4	1,09E-05	1,64E+00
40	Tetrapod	0,225	Jsh16s6	7,45E-06	1,92E+00
41	Tetrapod	0,25	Jsh10s2	1,34E-06	3,01E+00
42	Tetrapod	0,25	Jsh10s4	2,99E-06	3,25E+00
43	Tetrapod	0,25	Jsh10s6	2,63E-06	3,91E+00
44	Tetrapod	0,25	Jsh12s2	3,00E-06	2,31E+00
45	Tetrapod	0,25	Jsh12s4	2,91E-06	2,63E+00
46	Tetrapod	0,25	Jsh12s6	1,38E-06	3,09E+00
47	Tetrapod	0,25	Jsh14s2	1,75E-05	2,02E+00
48	Tetrapod	0,25	Jsh14s4	1,89E-06	2,16E+00
49	Tetrapod	0,25	Jsh14s6	7,16E-07	2,60E+00
50	Tetrapod	0,25	Jsh16s2	1,51E-04	1,74E+00
51	Tetrapod	0,25	Jsh16s4	2,12E-06	1,84E+00
52	Tetrapod	0,25	Jsh16s6	5,12E-06	2,16E+00
53	Xbloc	0,15	Jsh10s2	4,48E-05	1,72E+00
54	Xbloc	0,15	Jsh10s4	2,66E-05	2,03E+00
55	Xbloc	0,15	Jsh10s6	2,49E-05	2,27E+00
56	Xbloc	0,15	Jsh12s2	2,41E-04	1,47E+00
57	Xbloc	0,15	Jsh12s4	1,39E-04	1,58E+00
58	Xbloc	0,15	Jsh12s6	6,20E-05	1,83E+00
59	Xbloc	0,15	Jsh14s2	1,29E-03	1,40E+00
60	Xbloc	0,15	Jsh14s4	6,26E-04	1,28E+00
61	Xbloc	0,15	Jsh14s6	3,58E-04	1,52E+00
62	Xbloc	0,2	Jsh10s2	1,96E-05	2,15E+00
63	Xbloc	0,2	Jsh10s4	6,99E-06	2,67E+00
64	Xbloc	0,2	Jsh10s6	1,13E-06	3,03E+00
65	Xbloc	0,2	Jsh12s2	1,97E-04	1,75E+00
66	Xbloc	0,2	Jsh12s4	4,73E-05	2,08E+00
67	Xbloc	0,2	Jsh12s6	6,93E-06	2,44E+00
68	Xbloc	0,2	Jsh14s21	1,02E-03	1,60E+00
69	Xbloc	0,2	Jsh14s22	1,02E-03	1,63E+00
70	Xbloc	0,2	Jsh14s23	9,98E-04	1,59E+00
71	Xbloc	0,2	Jsh14s41	1,77E-04	1,71E+00
72	Xbloc	0,2	Jsh14s42	1,65E-04	1,67E+00
73	Xbloc	0,2	Jsh14s43	1,52E-04	1,67E+00
74	Xbloc	0,2	Jsh14s61	2,79E-05	1,96E+00
75	Xbloc	0,2	Jsh14s62	4,53E-05	2,04E+00
76	Xbloc	0,2	Jsh14s63	3,43E-05	2,04E+00

Test	Block	Rc [m]	Name	Q [-]	R_c/H_{si} [-]
77	Xbloc	0,2	Jsh16s6	6,27E-05	1,75E+00
78	Xbloc	0,225	Jsh10s2	6,49E-06	2,53E+00
79	Xbloc	0,225	Jsh10s4	9,33E-07	3,00E+00
80	Xbloc	0,225	Jsh10s6	0,00E+00	3,46E+00
81	Xbloc	0,225	Jsh12s2	5,85E-05	2,05E+00
82	Xbloc	0,225	Jsh12s4	9,46E-06	2,42E+00
83	Xbloc	0,225	Jsh12s6	4,40E-07	2,88E+00
84	Xbloc	0,225	Jsh14s2	3,06E-04	1,76E+00
85	Xbloc	0,225	Jsh14s4	1,27E-05	1,97E+00
86	Xbloc	0,225	Jsh14s6	4,91E-06	2,37E+00
87	Xbloc	0,25	Jsh10s2	2,20E-06	2,84E+00
88	Xbloc	0,25	Jsh10s4	0,00E+00	3,57E+00
89	Xbloc	0,25	Jsh10s6	0,00E+00	3,57E+00
90	Xbloc	0,25	Jsh12s2	1,08E-05	2,36E+00
91	Xbloc	0,25	Jsh12s4	0,00E+00	2,63E+00
92	Xbloc	0,25	Jsh12s6	0,00E+00	3,29E+00
93	Xbloc	0,25	Jsh14s2	1,10E-04	2,00E+00
94	Xbloc	0,25	Jsh14s4	2,21E-06	2,17E+00
95	Xbloc	0,25	Jsh14s6	3,27E-06	2,63E+00